ÉCOLE DE TECHNOLOGIE SUPÉRIEURE
UNIVERSITÉ DU QUÉBEC

THESIS PRESENTED TO
ÉCOLE DE TECHNOLOGIE SUPÉRIEURE

IN PARTIAL FULFILLMENT OF THE REQUIREMENTS FOR
THE DEGREE OF DOCTOR OF PHILOSOPHY
Ph.D.

BY
Luana BEZERRA BATISTA

MULTI-CLASSIFIER SYSTEMS FOR OFF-LINE SIGNATURE VERIFICATION

MONTREAL, MARCH 30 2011

BOARD OF EXAMINERS

THIS THESIS HAS BEEN EVALUATED

BY THE FOLLOWING BOARD OF EXAMINERS

Mr. Robert Sabourin, thesis director
Département de génie de la production automatisée à l'École de technologie supérieure

Mr. Eric Granger, thesis co-director
Département de génie de la production automatisée à l'École de technologie supérieure

Mr. Bruno De Kelper, committee president
Département de génie électrique à l'École de technologie supérieure

Mr. Jean-Marc Robert, examiner
Département de génie logiciel et des technologies de l'information

Mrs. Nicole Vincent, external examiner
Université Paris Descartes

THIS THESIS HAS BEEN PRESENTED AND DEFENDED

BEFORE A BOARD OF EXAMINERS AND PUBLIC

MARCH 14 2011

AT ÉCOLE DE TECHNOLOGIE SUPÉRIEURE

ACKNOWLEDGMENTS

First of all, I would like to thank Dr. Robert Sabourin and Dr. Eric Granger, for supervising my work over these five years. Their expertise and guidance were fundamental for the accomplishment of this Thesis.

Thanks also to the members of my examining committee: Dr. Nicole Vincent, Dr. Jean-Marc Robert and Dr. Bruno De Kelper, for evaluating this Thesis and providing valuable comments.

I would like to thank all my colleagues in the LIVIA (Laboratoire d'imagerie, de vision et d'intelligence artificielle), for sharing so many ideas, and *Vins et Fromages*. Special thanks to Albert Ko, Bassem Guendy, Carlos Cadena, Clement Chion, César Alba, Cristophe Pagano, David Dubois, Dominique Rivard, Eduardo Vellasques, Éric Thibodeau, Eulanda dos Santos, Francis Quintal, George Eskander, Idrissa Coulibaly, Jean-François Connoly, Jonathan Bouchard, Jonathan Milgram, Luis da Costa, Marcelo Kapp, Mathias Adankon, Melyssa Ayala, Miguel de la Torre, Olaf Gagnon, Paulo Cavalin, Vincent Doré, and Wael Khreich.

Most of all, thanks to my boyfriend, Julien Lauzé, as well as to Ana Aguiar, Fernando Kajita, Jean-Pierre Caradant, Larissa Fernandes, Linda Henrichon, and Paulino Neto, for being my new family in Montreal.

I dedicate this Thesis to all my friends and family in Brazil, especially to my mother, Ligia Bezerra, my sister, Beatriz Bezerra, my aunt, Nina Bezerra, and my grandmother, Inah Bezerra. They have always supported and encouraged me.

This work was financially supported by the Defence Research and Development Canada, by the Fonds Québécois de la Recherche sur la Nature et les Technologies, and by the Natural Sciences and Engineering Research Council of Canada.

MULTI-CLASSIFIER SYSTEMS FOR OFF-LINE SIGNATURE VERIFICATION

Luana BEZERRA BATISTA

ABSTRACT

Handwritten signatures are behavioural biometric traits that are known to incorporate a considerable amount of intra-class variability. The Hidden Markov Model (HMM) has been successfully employed in many off-line signature verification (SV) systems due to the sequential nature and variable size of the signature data. In particular, the *left-to-right* topology of HMMs is well adapted to the dynamic characteristics of occidental handwriting, in which the hand movements are always from left to right. As with most generative classifiers, HMMs require a considerable amount of training data to achieve a high level of generalization performance. Unfortunately, the number of signature samples available to train an off-line SV system is very limited in practice. Moreover, only random forgeries are employed to train the system, which must in turn to discriminate between genuine samples and random, simple and skilled forgeries during operations. These last two forgery types are not available during the training phase.

The approaches proposed in this Thesis employ the concept of multi-classifier systems (MCS) based on HMMs to learn signatures at several levels of perception. By extracting a high number of features, a pool of diversified classifiers can be generated using random subspaces, which overcomes the problem of having a limited amount of training data.

Based on the multi-hypotheses principle, a new approach for combining classifiers in the ROC space is proposed. A technique to repair concavities in ROC curves allows for overcoming the problem of having a limited amount of genuine samples, and, especially, for evaluating performance of biometric systems more accurately. A second important contribution is the proposal of a hybrid generative-discriminative classification architecture. The use of HMMs as feature extractors in the generative stage followed by Support Vector Machines (SVMs) as classifiers in the discriminative stage allows for a better design not only of the genuine class, but also of the impostor class. Moreover, this approach provides a more robust learning than a traditional HMM-based approach when a limited amount of training data is available. The last contribution of this Thesis is the proposal of two new strategies for the dynamic selection (DS) of ensemble of classifiers. Experiments performed with the PUCPR and GPDS signature databases indicate that the proposed DS strategies achieve a higher level of performance in off-line SV than other reference DS and static selection (SS) strategies from literature.

Keywords : Dynamic Selection, Ensembles of Classifiers, Hidden Markov Models, Hybrid Generative-Discriminative Systems, Multi-Classifier Systems, Off-line Signature Verification, ROC Curves, Support Vector Machines.

SYSTÈMES DE CLASSIFICATEURS MULTIPLES POUR LA VÉRIFICATION HORS-LIGNE DE SIGNATURES MANUSCRITES

Luana BEZERRA BATISTA

RÉSUMÉ

Les signatures manuscrites sont des traits biométriques comportementaux caractérisés par une grande variabilité intra-classe. Les modèles de Markov cachés (MMCs) ont été utilisés avec succès en vérification hors-ligne des signatures manuscrites (VHS) en raison de la nature séquentielle et très variable de la signature. En particulier, la topologie *gauche-droite* des MMCs est très bien adaptée aux caractéristiques de l'écriture occidentale, dont les mouvements de la main sont principalement exécutés de la gauche vers la droite. Comme la plupart des classificateurs de type génératif, les MMCs requièrent une quantité importante de données d'entraînement pour atteindre un niveau de performance élevé en généralisation. Malheureusement, le nombre de signatures disponibles pour l'apprentissage des VHS est très limité en pratique. De plus, uniquement les faux aléatoires sont utilisés pour l'apprentissage des VHS qui doivent être en mesure de discriminer entre les signatures authentiques et les classes de faux aléatoires, les faux simples et les imitations. Ces deux dernières classes de faux ne sont pas disponibles lors de la phase d'apprentissage.

Les approches proposées dans cette thèse reposent sur le concept des classificateurs multiples basés sur des MMCs exploités pour l'extraction de plusieurs niveaux de perception des signatures. Cette stratégie basée sur la génération d'un nombre très important de caractéristiques permet la mise en œuvre de classificateurs dans les sous-espaces aléatoires, ce qui permet de s'affranchir du nombre limité de données disponibles pour l'entraînement.

Une nouvelle approche pour la combinaison des classificateurs basée sur le principe des hypothèses multiples dans l'espace ROC est proposée. Une technique de réparation des courbes ROC permet de s'affranchir du nombre limité de signatures disponibles et surtout pour l'évaluation de la performance des systèmes biométriques. Une deuxième contribution importante est la proposition d'une architecture de classification hybride de type génératif-discriminatif. L'utilisation conjointe des MMCs pour l'extraction des caractéristiques et des machines à vecteurs de support (MVSs) pour la classification permet une meilleure représentation non seulement de la classe des signatures authentiques, mais aussi de la classe des imposteurs. L'approche proposée permet un apprentissage plus robuste que les approches MMCs conventionnelles lorsque le nombre d'échantillons disponibles est limité. La dernière contribution de cette thèse est la proposition de deux nouvelles stratégies pour la sélection dynamique (SD) d'ensembles de classificateurs. Les résultats obtenus sur les bases de signatures manuscrites PUCPR et GPDS, montrent que les stratégies proposées sont plus performantes que celles publiées dans la littérature pour la sélection dynamique ou statique des ensembles de classificateurs.

Mots-clés : Courbes ROC, ensembles de classificateurs, machines à vecteurs de support, modèles de Markov cachés, sélection dynamique de classificateurs, systèmes hybrides génératifs-discriminatifs, systèmes à classificateurs multiples, vérification hors-ligne des signatures manuscrites.

TABLE OF CONTENT

Page

LIST OF TABLES

Page

LIST OF FIGURES

Page

LIST OF SYMBOLS

α	Number of genuine samples in the training set
$\mathcal{A}$	State transition probability distribution
β	Number of random forgery samples in the training set
$\mathcal{B}$	Observation symbol probability distribution
C	SVM cost parameter
$\mathcal{C}$	Pool of classifiers
C_1	Genuine class
C_2	Impostor class
c_r	Classifier trained with subspace r
CB_{35}	Codebook with 35 symbols
$cent$	Centroid in the vector quantization process
CI	Margin-based measure
$\mathcal{D}$	Number of input dimensions
$\mathbf{D}$	Vector of HMM likelihoods
$\mathbf{D}'$	Vector of HMM likelihoods in the random subspace
DB_{exp}	Exploitation database
DB_{dev}	Development database
DB_{ds}	Database used for dynamic selection
DB_{hmm}	Database used to train HMMs
DB_{roc}	Database used to generate ROC curves
DB_{svm}	Database used to train SVMs
DB_{tst}	Database used during operations
E	Ensemble of classifiers
$\mathcal{E}_t$	Error at time t
$\mathcal{F}$	Set of feature vectors
$\mathbf{F}$	Feature vector
$\mathcal{H}$	Bank of representative HMMs
$I(x, y)$	Signature image with coordinates (x, y)

$I'(x, y)$	Preprocesed signature image with coordinates (x, y)
I_{trn}	Training signature sample
I_{tst}	Test signature sample
I_{vld}	Validation signature sample
$\mathcal{L}$	Classification label
L	Number of observations in the sequence of observations
L_{min}	Number of observations in the smaller sequence of observations
$\mathcal{M}$	Bank of available HMMs
M	Size of the validation set
M	Alphabet size
$\mathcal{N}$	Number of clusters
N	Negative class
N	Size of the training set
O	Sequence of discrete observations
o	Discrete observation
O_{trn}	Set of observation sequences used for training
O_{tst}	Set of observation sequences used for test
O_{vld}	Set of observation sequences used for validation
P	Positive class
P	Probability
$P(\mathbf{O}\|\lambda)$	Probability of λ to have generated **O**
q	Codebook
Q	Number of codebooks
$\mathcal{Q}$	Size of the bank of HMMs
r	Random subspace
$\mathcal{R}$	Number of random subspaces
R	Number of HMMs in the genuine subspace
R'	Size of the genuine random subspace
S	Number of HMMs in the impostor subspace

S'	Size of the impostor random subspace
$\mathcal{S}$	Number of distinct states
$\mathbf{S}$	Set of states
s_t	State at time t
τ	Decision threshold
t	Time
$\mathcal{T}_{dev}$	Training set from the development database
$\mathcal{T}_{exp}$	Training set from the exploitation database
$\mathcal{T}'$	Random subspace training set
TST_{rand}	Test set containing random forgeries
TST_{simp}	Test set containing simple forgeries
TST_{skil}	Test set containing skilled forgeries
TST_{true}	Test set containing genuine samples
$\mathcal{U}$	Cluster in the vector quantization process
μ	Average
v	Observation symbol
$\mathbf{V}$	Set of symbols
V	Number of support vectors
$\mathcal{V}_{dev}$	Validation set from the development database
$\mathcal{V}_{exp}$	Validation set from the exploitation database
w_2	Set of HMMs of the impostor class
w_1	Set of HMMs of the genuine class
x_i	Input pattern
y_j	Output label
γ	Cumulative frequency of the impostors' scores
λ	Discrete HMM
π	Initial state distribution
σ	Variance
Φ_1	Set of available HMMs representing the genuine class

Φ_2	Set of available HMMs representing the impostor class
Ω	Set of margins
Δ	Limit of jumps in the left-to-right HMM topology

LIST OF ACRONYMS

AER	Average Error Rate
EER	Equal Error Rate
AUC	Area Under Curve
DS	Dynamic Selection
DR	Dissimilarity Representation
EoC	Ensemble of Classifiers
FNR	False Negative Rate
FPR	False Positive Rate
HMMs	Hidden Markov Models
K-NN	K-Nearest Neighbors
KNORA	K-Nearest Oracles
MCS	Multi-Classifier Systems
NC	Number of Clusters
OP	Output Profile
RBF	Radial Basis Function
RSM	Random Subspace Method
SV	Signature Verification
SS	Static Selection
TNR	True Negative Rate
2-CCs	2-Class Classifiers

INTRODUCTION

Biometrics refers to automated methods used to authenticate the identity of a person. In contrast to the conventional identification systems, whose features (such as ID cards or passwords) can be forgotten, lost or, either, stolen, biometric systems are based on physiological or behavioral features of the individual that are difficult for another individual to reproduce; thereby reducing the possibility of forgery (Kung et al., 2004). Fingerprints, voice, iris, retina, hand, face, handwriting, keystroke and finger shape are examples of popular features used in biometrics. The use of other biometric measures, such as gait, ear shape, head resonance, optical skin reflectance and body odor, is still in an initial research phase (Wayman et al., 2005).

The handwritten signature has always been one of the most simple and accepted biometric trait used to authenticate official documents. It is easy to obtain, results from a spontaneous gesture and it is unique to each individual. Automatic signature verification is, therefore, relevant in many situations where handwritten signatures are currently used, such as cashing checks, transactions with credit cards, and authenticating documents (Jain et al., 2002).

Signature Verification (SV) systems seek to authenticate the identity of an individual, based on the analysis of his/her signature, through a process that discriminates a genuine signature from a forgery (Plamondon, 1994). There are three main types of forgeries, namely, random, simple and skilled (see Figure 0.1). A random forgery is usually a genuine signature sample belonging to a different writer. It is produced when the forger has no access to the genuine samples, not even the writer's name. In the case of simple forgeries, only the writer's name is known. Thus, the forger reproduces the signature in his/her own style. Finally, a skilled forgery represents a reasonable imitation of a genuine signature. Generally, only genuine and random forgery samples are used to design a SV system. The reason is that, in practice, forged signatures samples are rarely available. On the other hand, different types of forgeries are used to evaluate the system performance.

Depending on the data acquisition mechanism, the process of SV can be classified as on-line or off-line. The on-line (or dynamic) approach employs specialized hardware (such as a digitizing

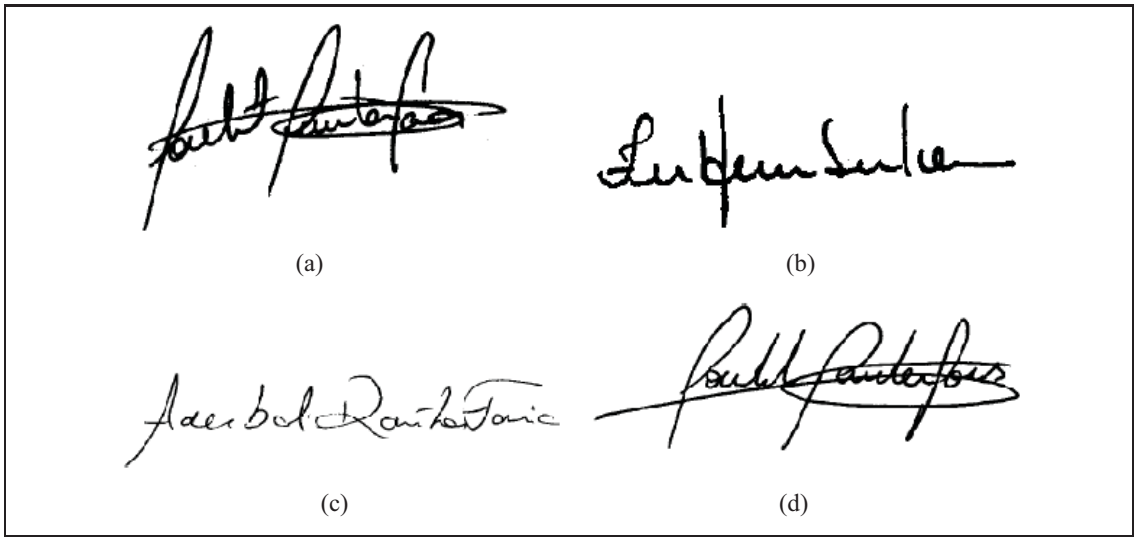

Figure 0.1 Examples of (a) genuine signature, (b) random forgery, (c) simple forgery and (d) skilled forgery.

tablet or a pressure sensitive pen) in order to capture the pen movements over the paper at the time of the writing. In this case, a signature can be viewed as a space-time variant curve that can be analyzed in terms of its curvilinear displacement, its angular displacement and the torsion of its trajectory (Plamondon and Lorette, 1989).

On the other hand, with the off-line (or static) approach, the signature is available on a sheet of paper, which is later scanned in order to obtain a digital representation composed of $m \times n$ pixels. Hence, the signature image is considered as a discrete 2-D function $I(x, y)$, where $x = 0, 1, 2, \ldots, m$ and $y = 0, 1, 2, \ldots, n$ denote the spatial coordinates, and the value of I in any (x, y) corresponds to the grey level (generally a value from 0 to 255) in that point (Gonzalez and Woods, 2002).

Figure 0.2 shows an example of a generic SV system, which follows the classical pattern recognition model steps, that is, image acquisition, preprocessing, feature extraction, and classification. After acquisition, some corrections – such as noise removal and centering – are applied to the raw signature image during the pre-processing step. Then, a set of representative features are extracted and assembled into a vector **F**. This feature vector should maximize the distance

between signature samples of different writers, while minimizing the distance between signature samples belonging to the same writer. Finally, a classification algorithm classifies the signature as genuine or forgery. Chapter 1 presents a survey of techniques employed by off-line SV systems in the steps of feature extraction and classification.

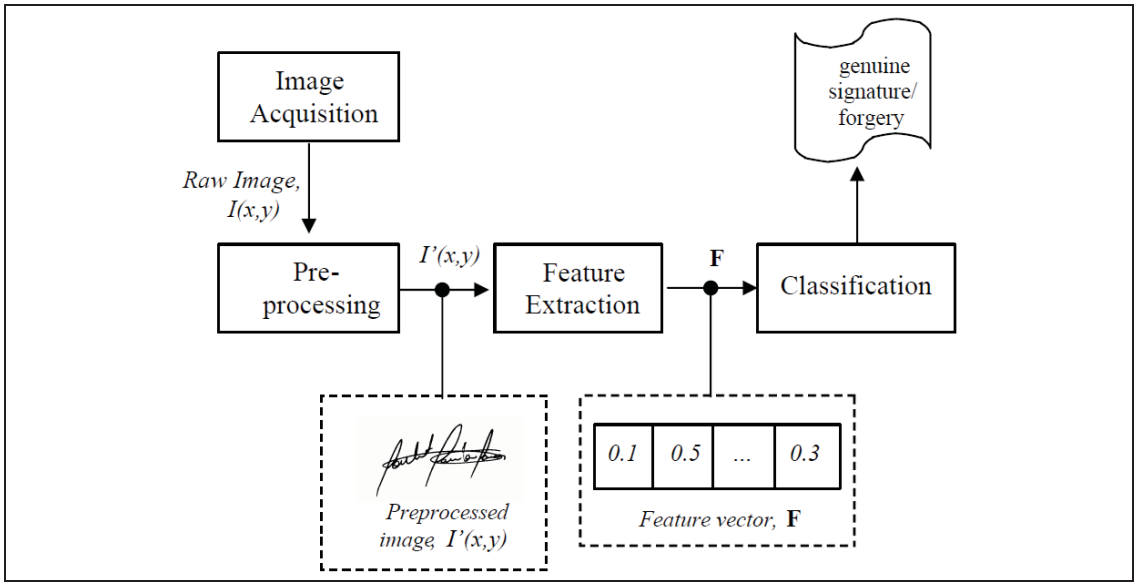

Figure 0.2 Block diagram of a generic SV system.

Problem Statement

Over the last two decades, and with the renewed interest in biometrics caused by the tragic events of 9/11, several innovative approaches for off-line SV have been introduced in the literature. Off-line SV research generally focuses on the phases of feature extraction and/or classification. In this Thesis, the main focus is on techniques and systems for the classification phase.

Among the well-known classifiers used in pattern recognition, the discrete Hidden Markov Model (HMM) (Rabiner, 1989) – a finite stochastic automata used to model sequences of observations – has been successfully employed in off-line SV due to the sequential nature and

variable size of the signature data (El-Yacoubi et al., 2000; Ferrer et al., 2005; Justino et al., 2000; Rigoll and Kosmala, 1998). In particular, the *left-to-right* topology of HMMs is well adapted to the dynamic characteristics of European and American handwriting, in which the hand movements are always from left to right.

Handwritten signatures are behavioural biometric traits that are known to incorporate a considerable amount of intra-class variability. Figure 0.3 presents the superimposition of several signature skeletons samples of the same writer. Note that the intrapersonal variability occurs mostly in the horizontal direction, since there is normally more space to sign in this direction. By using a grid segmentation scheme adapted to the signature size, Rigoll and Kosmala (1998), and later Justino et al. (2000), have shown that discrete HMMs are suitable for modeling the variabilities observed among signature samples of a same writer.

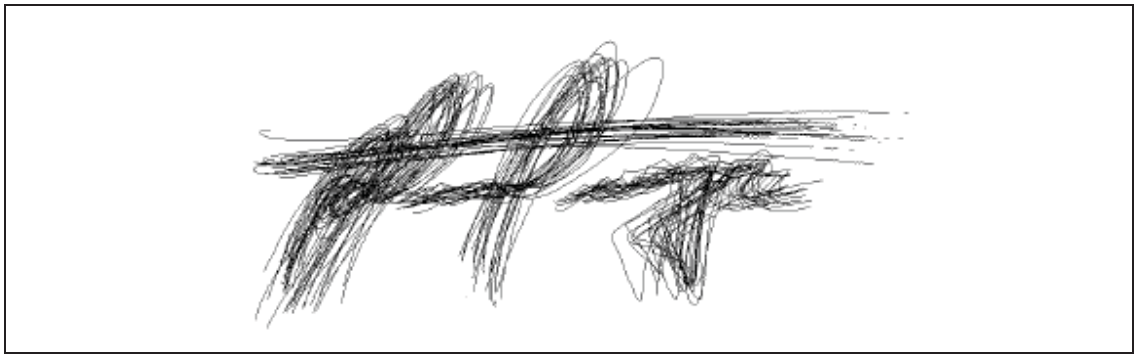

Figure 0.3 Example of several superimposed signature samples of the same writer.

As the HMM is a generative classifier (Drummond, 2006), it requires a considerable amount of training data to achieve a high level of performance. Unfortunately, acquiring signature samples for the design of off-line SV systems is a costly and time consuming process. For instance, in banking transactions, a client is asked to supply between 3 and 5 signatures samples at the time of his/her subscription.

Another issue with the use of discrete HMMs regards the design of codebooks[1]. Typically, the data used to generate codebooks are the same data that are employed to train the HMMs (Ferrer et al., 2005; Rigoll and Kosmala, 1998). In the work of Ferrer et al. (2005), all writers share a global codebook generated with their training data. The main drawback of this strategy is the need to reconstruct the codebook and retrain the HMMs, whenever a new writer is added to the system. According to Rigoll and Kosmala (1998), the utilization of user-specific codebooks, generated by using only the training signatures of a particular writer, adds one more personal characteristic to the verification process. However, this strategy has been shown to yield poor system performance when few signature samples are available (El-Yacoubi et al., 2000).

Regardless the type of classifier chosen to perform off-line SV, the availability of a limited amount of signature samples per writer is a fundamental problem in this field. By using a small training set, the class statistics estimation errors may be significant, resulting in unsatisfactory classification performance (Fang and Tang, 2005). Moreover, a high number of features is generally extracted from a handwritten signature image, which increases the difficulty of the problem. These crucial issues have received little attention in the literature. Proposed solutions from literature are:

1) *The generation of synthetic samples*, by adding noise or applying transformations to the available genuine signature samples (Fang et al., 2002; Fang and Tang, 2005; Huang and Yan, 1997; Vélez et al., 2003);

2) *The selection of the most discriminative features*, by using feature selection algorithms such as Genetic Algorithms (Xuhua et al., 1996) or Adaboost (Rivard, 2010);

3) *The use of a dichotomic approach based on dissimilarity representation*. This approach allows to reduce the SV problem into two classes (i.e., genuine and impostor classes), regardless the number of writers enrolled to the system, while increasing the quantity of training

[1] A codebook contains a set of symbols, each one associated with a cluster of feature vectors, used to generate sequences of discrete observations in discrete HMM-based systems.

vectors. In this case, the population of writers shares a same global classifier (Bertolini et al., 2010; Rivard, 2010; Santos et al., 2004).

Objectives and Contributions

The main objective of this Thesis is to design accurate and adaptive off-line SV systems, based on multiple *left-to-right* HMMs, with a reduced number of genuine signatures per writer. For this purpose, this Thesis contains the following contributions to the advancement of knowledge in off-line SV and pattern recognition in general:

1) **Use of the concept of Multi-Classifier Systems (**MCS**) in off-line SV.** A promising way to improve off-line SV performance is through MCS (Bajaj and Chaudhury, 1997; Bertolini et al., 2010; Blatzakis and Papamarkos, 2001; Huang and Yan, 2002; Sabourin and Genest, 1995; Sansone and Vento, 2000). The motivation of using MCS stems from the fact that different classifiers usually make different errors on different samples. Indeed, it has been shown that, when the response of a set of $\mathcal{C}$ classifiers is averaged, the variance contribution in the bias-variance decomposition decreases by $1/\mathcal{C}$, resulting in a smaller expected classification error (Tax, 2001; Tumer and Ghosh, 1996). Instead of trying to increase the number of training samples or to select the most discriminative features to overcome the problem of having a limited amount of training data, the off-line SV approaches proposed in this Thesis take advantage of the high number of features typically extracted from handwritten signatures to produce multiple classifiers that work together in order to reduce error rates.

2) **Proposal of a multi-hypothesis approach.** Off-line SV systems based on HMMs generally employs a single HMM per writer. By using a single codebook, different number of states are tried in order to select that one providing the highest training probability (Justino et al., 2001; El-Yacoubi et al., 2000). In an attempt to reduce error rates and to take advantage of the sub-optimal HMMs often discarded by the traditional systems, a multi-hypothesis approach is proposed in this Thesis. Multiple discrete *left-to-right* HMMs are trained per writer by using different number of states and codebook sizes, allowing the system to learn

a signature at different levels of perception. The codebooks are generated using signature samples of an independent database, supplied by writers not enrolled to the SV system. This *prior* knowledge ensures that system design can be triggered even with a single user. This contribution has been published as a journal article in (Batista et al., 2010a) and as a conference article in (Batista et al., 2009).

3) **Proposal of a hybrid generative-discriminative architecture.** Despite the success of HMMs in SV, several important systems have been developed with discriminative classifiers (Impedovo and Pirlo, 2008). In this Thesis, a hybrid architecture composed of a generative stage followed by discriminative stage is proposed. In the generative stage, multiple discrete *left-to-right* HMMs – some representing the genuine class, some representing the impostor class – are used as feature extractors for the discriminative stage. In other words, HMM likelihoods are measured for each training signature, resulting in feature vectors used to train a pool of two-class classifiers (2-CCs) in the discriminative stage. The 2-CCs are trained through a specialized Random Subspace Method (RSM), which takes advantage of the high number of features produced by the generative stage. The main advantage of this hybrid architecture is that it allows to model not only the genuine class, but also the impostor class. Traditional SV approches based on HMMs generally use only genuine signatures as training set. Then, a decision threshold is defined by using a validation set composed of genuine and random forgery samples. This contribution has been published as conference articles in (Batista et al., 2010b) and (Batista et al., 2010c), and submitted as a journal article to Pattern Recognition (december, 2010).

4) **Proposal of new dynamic selection strategies.** Given a pool of classifiers, an important issue is the selection of a diversified subset of classifiers to form an ensemble, such that the recognition rates are maximized during operations (Ko et al., 2008). In this work, this task is performed dynamically, with two new strategies based on K-nearest-oracles (KNORA) (Ko et al., 2008) and on output profiles (OP) (Cavalin et al., 2010). As opposed to static selection (SS), where a single ensemble of classifiers (EoC) is selected before operations and used for all input samples, dynamic selection (DS) allows the selection of a different

EoC for each input sample during the operational phase. Moreover, when signature samples become available overtime, they can be incrementally incorporated to the system and used to improve the selection of the most adequate EoC. This is an important challenge in SV, since it is very difficult to get all possible signature variations – due to the age, psychological and physical state of an individual – during the training phase. This contribution has been published as conference articles in (Batista et al., 2010b) and (Batista et al., 2010c), accepted for publication in (Batista et al., 2011), and submitted as a journal article to Pattern Recognition (december, 2010).

5) **Use of ROC curves as performance evaluation tool**. Generally, SV systems have been evaluated through error rates calculated from a single threshold, assuming that the classification costs are always the same. Though not fully explored in the literature, it has recently been shown that the Receiver Operating Characteristic (ROC) curve provides a powerful tool for evaluating, combining and comparing off-line SV systems (Coetzer and Sabourin, 2007; Oliveira et al., 2007). In this work, the overall system performance is measured by an averaged ROC curve that takes into account all the writers enrolled to the system. Each writer has his/her own set of thresholds, and the decision of using a specific operating point may be made dynamically according to the risk associated with the amount of a bank check.

6) **Proposal of an approach to repair ROC curves**. As the dataset used to model the signatures of a writer generally contains a reduced number of genuine samples against several random forgeries, it is common to obtain ROC curves with concave areas. In general, a concave area indicates that the ranking provided by the classifier in this region is worse than random (Flach and Wu, 2003). Based on the combination of multiple discrete *left-to-right* HMMs, this Thesis proposes an approach to repair concavities of individual ROC curves while generating a high quality averaged ROC curve. This contribution has been published as a journal article in (Batista et al., 2010a) and as a conference article in (Batista et al., 2009).

Organization of the Thesis

This Thesis is composed of three main chapters. In Chapter 1, the state-of-the-art in off-line SV over the last two decades is presented. It includes the most important techniques used for feature extraction and classification, the strategies proposed to face the problem of limited amount of data, as well as the research directions in this field.

In Chapter 2, an approach based on the combination of multiple discrete *left-to-right* HMMs in the ROC space is proposed to improve performance of off-line SV systems designed from limited and unbalanced data. By selecting the most accurate HMM(s) for each operating point, we show that it is possible to construct a composite ROC curve that provides a more accurate estimation of system performance during training (i.e., without concavities) and significantly reduces the error rates during operations. Experiments performed with a real-world signature database (comprised of random, simple and skilled forgeries) are presented and analysed.

In Chapter 3, the problem of having a limited amount of genuine signature samples is addressed by designing a hybrid system based on the dynamic selection of generative-discriminative ensembles. By using multiple discrete *left-to-right* HMMs as feature extractors in the generative stage and an ensemble of two-class classifiers in the discriminative stage, we demonstrate the advantages of using a hybrid approach. This chapter also proposes two dynamic selection (DS) strategies – to select the most accurate EoC for each input signature – suitable for incremental learning. Experiments performed with two different real-world signature databases are presented and analysed.

Finally, the conclusions and proposals for further work are presented.

CHAPTER 1

THE STATE-OF-THE-ART IN OFF-LINE SIGNATURE VERIFICATION

The goal of a Signature Verification (SV) system is to authenticate the identity of an individual, based on the analysis of his/her signature, through a process that discriminates a genuine signature from a forgery (Plamondon, 1994). Such as described in the previous chapter, random, simple and skilled are the three main types of forgeries.

SV is directly related to the alphabet (Roman, Chinese, Arabic, etc.) and the form of writing of each region (Justino, 2001). Figure 1.1 presents examples of signatures proceeding from the Roman (occidental) and Japanese alphabets.

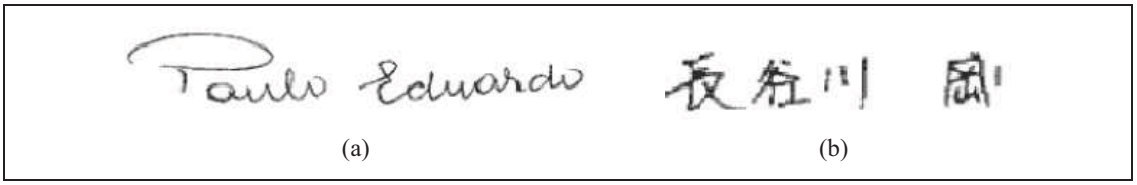

Figure 1.1 Examples of (a) Occidental and (b) Japanese signatures.
Adapted from Justino (2001)

The occidental signatures can be classified in two main styles: cursive or graphical, as shown in Figure 1.2. With cursive signatures, the author writes his or her name in a legible way, while the graphical signatures contain complex patterns which are very difficult to interpret as a set of characters.

Off-line SV systems deal with signature samples originally available on sheets of paper, which are later scanned in order to obtain a digital representation. Given a digitized signature image, an off-line SV system will perform preprocessing, feature extraction, and classification (also called “verification” in the SV field).

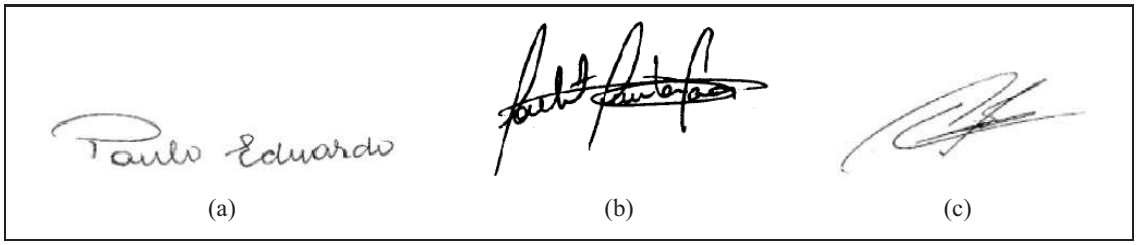

Figure 1.2 Examples of (a) (b) cursive and (c) graphical signatures.

The rest of this chapter is organized as follows. Sections 1.1 and 1.2 present, respectively, a literature review on feature extraction techniques and verification strategies proposed for off-line SV. Then, Section 1.3 describes some strategies used to face the problem of having a limited amount of data. Finally, Section 1.4 concludes the chapter with a general discussion. The contents of this chapter have been published as a book chapter in (Batista et al., 2007).

1.1 Feature Extraction Techniques

Feature extraction is essential to the success of a SV system. In an off-line environment, the signatures are usually acquired from a paper document, and preprocessed before the feature extraction begins. Feature extraction is a fundamental task because of the handwritten signatures variability and the lack of dynamic information about the signing process. An ideal feature extraction technique extracts a minimal feature set that maximizes the interpersonal distance between signature examples of different writers, while minimizing the intrapersonal distance for those belonging to the same writer. There are two classes of features used in off-line SV, namely, (i) *Static*, related to the signature shape, and (ii) *Pseudo-dynamic*, related to the dynamics of the handwriting.

These features can be extracted locally, if the signature is viewed as a set of segmented regions, or globally, if the signature is viewed as a whole. It is important to note that techniques used to extract global features can also be applied to specific regions of the signature in order to produce local features. In the same way, a local technique can be applied to the whole image

to produce global features. Figure 1.3 presents a taxonomy of the categories of features used SV.

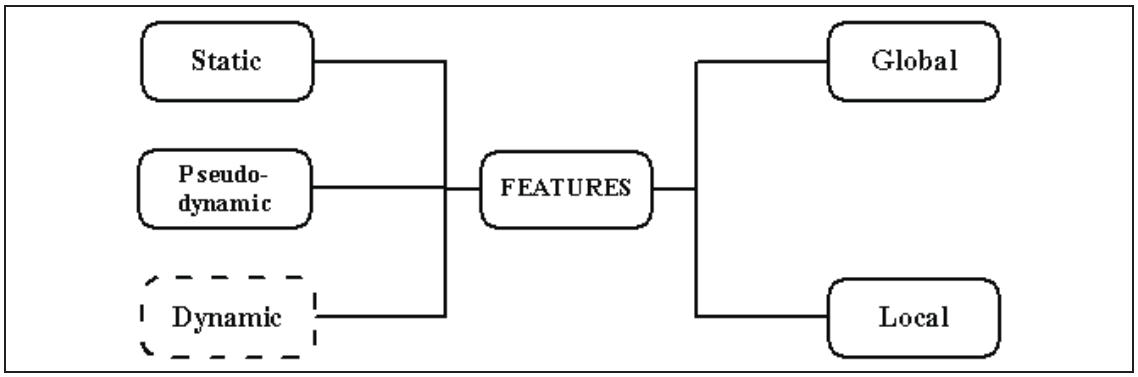

Figure 1.3 A taxonomy of feature types used in SV.

Local features can be categorized as contextual and non-contextual. If the signature segmentation is performed in order to interpret the text (for example, bars of "t" and dots of "i"), the analysis is considered contextual (Chuang, 1977). This type of analysis is not popular for two reasons: (i) it requires a complex segmentation process and (ii) it is not suitable to deal with graphical signatures. On the other hand, if the signature is viewed as a drawing composed of line segments (as it occurs in the majority of the literature), the analysis is considered non-contextual.

Before describing the most important feature extraction techniques in the field of off-line SV, the main types of signature representations are discussed.

1.1.1 Signature Representations

Some techniques transform the signature image into another representation before extracting the features. Off-line SV literature is quite extensive about signature representations.

The box representation (Frias-Martinez et al., 2006) is composed of the smallest rectangle fitting the signature. Its perimeter, area and perimeter/area ratio are generally employed as fea-

tures. The convex hull representation (Frias-Martinez et al., 2006) is composed of the smallest convex hull fitting the signature. The area, roundness, compactness, length and orientation are examples of features extracted from this representation.

The skeleton of the signature, its outline, directional frontiers and ink distributions have also been used as signature representations (Huang and Yan, 1997). The skeleton (or core) representation is the pixel wide strokes resulting from the application of a thinning algorithm to a signature image. The skeleton can be used to identify the signature edge points (1-neighbor pixels) that mark the beginning and ending of strokes (Ozgunduz et al., 2005). Pseudo-Zernike moments have also been extracted from this kind of representation (Wen-Ming et al., 2004).

The outline representation is composed of every black pixel adjacent to at least one white pixel. Huang and Yan (1997) consider as belonging to the signature outline, the pixels whose grey-level values are above the threshold of 25% and whose 8-neighbor count is below 8 (see Figure 1.4). Whereas Ferrer et al. (2005) obtained the signature outline by applying morphological operations (see Figure 1.5). First, a dilatation is applied in order to reduce the signature variability. After that, a filling operation is used to simplify the outline extraction process. Finally, the extracted outline is represented in terms of its Cartesian and Polar coordinates.

(a) (b)

Figure 1.4 Examples of (a) handwritten signature and (b) its outline.
Adapted from Huang and Yan (1997)

Directional frontiers (also called shadow images) are obtained when keeping only the black pixels touching a white pixel in a given direction (and there are 8 possible directions). To perform ink distribution representations, a virtual grid is superposed over the signature image. The cells containing more than 50% of black pixels are completely filled, while the others are

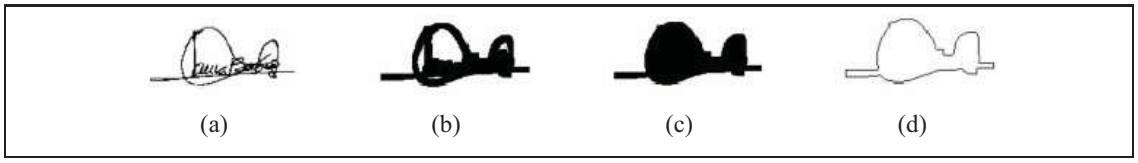

Figure 1.5 Signature outline extraction using morphological operations: (a) original signature, (b) dilated signature, (c) filled signature and (d) signature outline. Adapted from Ferrer et al. (2005)

emptied. Depending on the grid scale, the ink distributions can be coarser or more detailed. The number of filled cells can also be used as a global feature.

Upper and lower envelopes (or profiles) are also found in the literature. The upper envelope is obtained by selecting column-wise the upper pixels of a signature image, while the lower envelope is achieved by selecting the lower pixels, as illustrated by Figure 1.6. The numbers of turns and gaps in these representations have been used as global features (Ramesh and Murty, 1999).

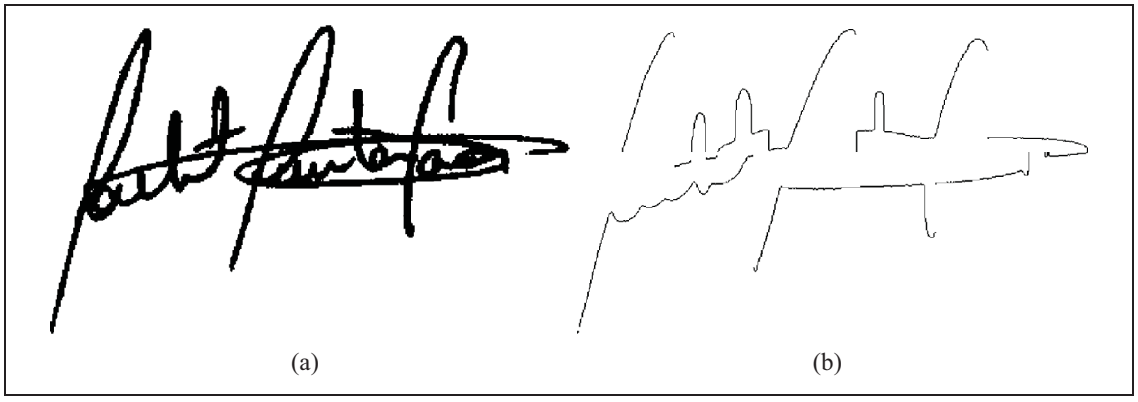

Figure 1.6 Examples of (a) handwritten signature and (b) its upper and lower envelopes. Adapted from Bertolini et al. (2010)

Regarding the Mathematic transforms, Nemcek and Lin (1974) employed the fast Hadamard transform in their feature extraction process as a trade-off between computational complexity and representation accuracy, when compared to other transforms. Whereas Coetzer et al.

(2004) employed the Discrete Radon transform to extract observation sequences of signatures, which was used to train a Hidden Markov Model.

Finally, signature images can also undergo a series of transformations before feature extraction. For example, Tang et al. (2002) used a central projection to reduce the signature image to a 1-D signal that was, in turn, transformed by a wavelet before fractal features were extracted.

1.1.2 Geometrical Features

Global geometric features measure the shape of a signature. The height, the width (Armand et al., 2006a) and the area (or pixel density) (El-Yacoubi et al., 2000) of the signature are basic features belonging to this category. The height and width can be combined to form the aspect ratio (or caliber) (Oliveira et al., 2005), as depicted in Figure 1.7.

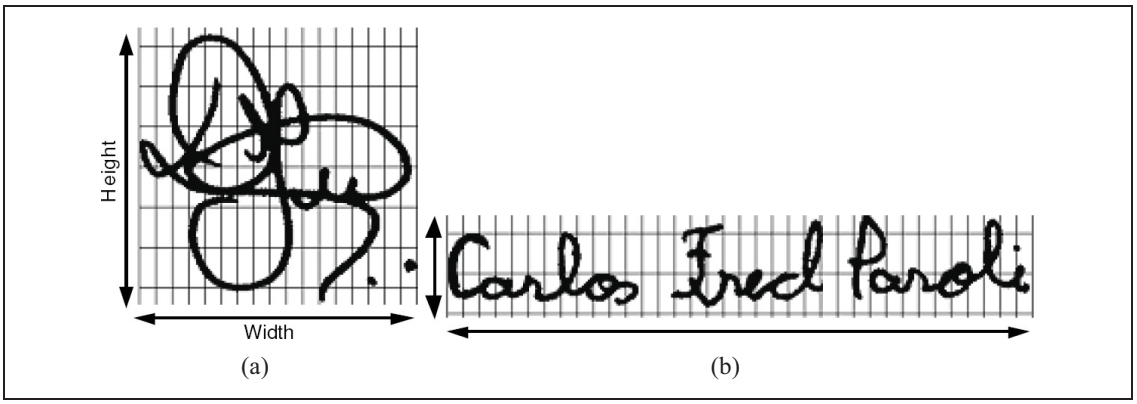

Figure 1.7 Examples of signatures with two different calibers: (a) large, and (b) medium. Adapted from Oliveira et al. (2005)

More elaborated geometric features consist of proportion, spacing and alignment to baseline. Proportion, as depicted in Figure 1.8, measures the height variations of the signature; while spacing, depicted in Figure 1.9, describes the gaps in the signature (Oliveira et al., 2005). Alignment to baseline extracts the general orientation of the signature according to a baseline reference (Armand et al., 2006a; Frias-Martinez et al., 2006; Oliveira et al., 2005; Senol and

Yildirim, 2005) (see Figure 1.10). Finally, connected components can also be employed as global features, such as the number of 4-neighbors and 8-neighbors pixels in the signature image (Frias-Martinez et al., 2006).

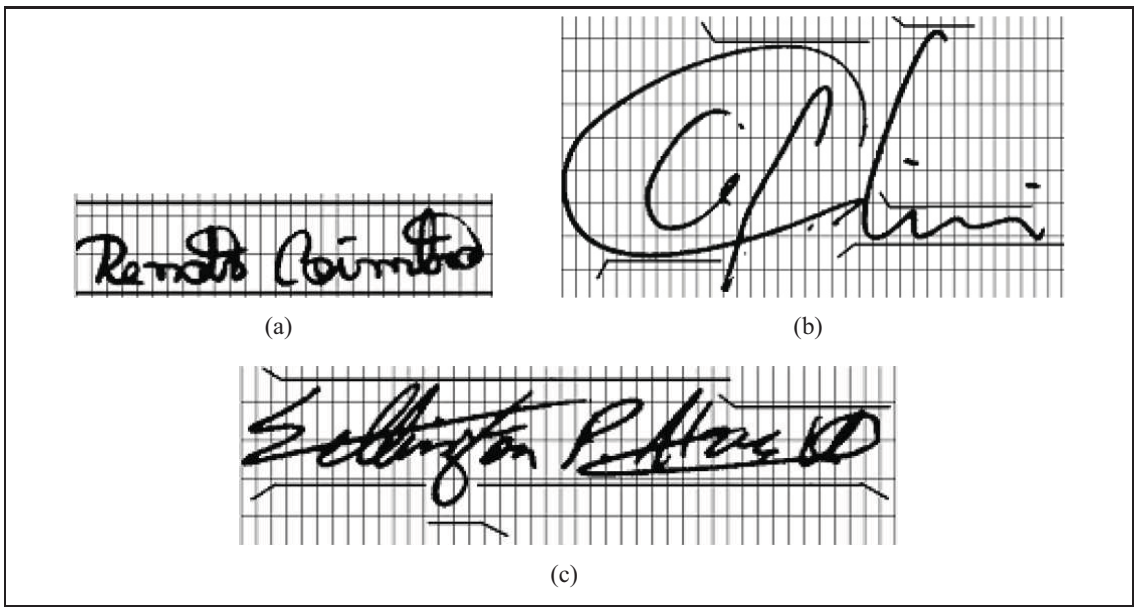

Figure 1.8 Examples of (a) proportional, (b) disproportionate, and (c) mixed signatures. Adapted from Oliveira et al. (2005)

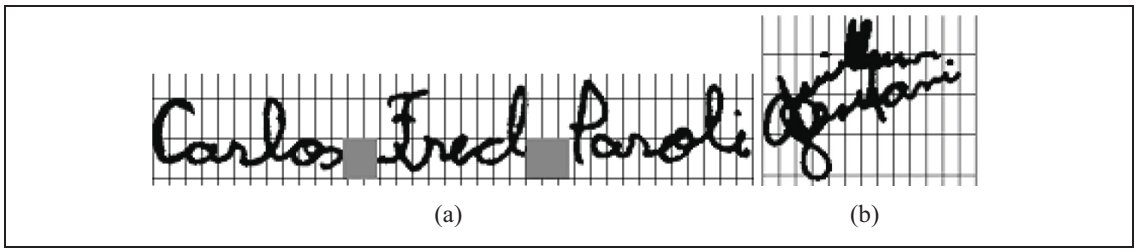

Figure 1.9 Examples of signatures (a) with spaces and (b) no space. Adapted from Oliveira et al. (2005)

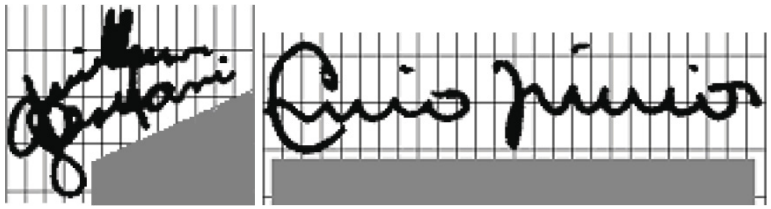

(a) (b)

Figure 1.10 Examples of signatures with an alignment to baseline of (a) 22°, and (b) 0°. Adapted from Oliveira et al. (2005)

1.1.3 Statistical Features

Many authors use projection representation. It consists of projecting every pixel on a given axis (usually horizontal or vertical), resulting in a pixel density distribution. Statistical features, such as the mean (or center of gravity), global and local maximums are generally extracted from this distribution (Frias-Martinez et al., 2006; Ozgunduz et al., 2005; Senol and Yildirim, 2005). Moments - which can include central moments (i.e. skewness and kurtosis) (Bajaj and Chaudhury, 1997; Frias-Martinez et al., 2006) and moment invariants (Al-Shoshan, 2006; Lv et al., 2005; Oz, 2005) - have also been extracted from a pixel density distribution.

Several other types of distributions can be extracted from an off-line signature. Drouhard et al. (1996) extracted directional PDF (Probability Density Function) from the gradient intensity representation of the silhouette of a signature. Stroke direction distributions have been extracted using structural elements and morphologic operators (Frias-Martinez et al., 2006; Lv et al., 2005; Madasu, 2004; Ozgunduz et al., 2005). A similar technique is used to extract edge-hinge (strokes changing direction) distributions (Madasu, 2004) and slope distributions, from signature envelopes (Fierrez-Aguilar et al., 2004; Lee and Lizarraga, 1996). Finally, Madasu et al. (2003) extracted distributions of angles with respect to a reference point from a skeleton representation.

1.1.4 Similarity Features

Similarity features differ from other types of features in the sense that they are extracted from a set of signatures. Thus, in order to extract these features, one signature is the questioned signature while the others are used as references.

In literature, Dynamic Time Warping seems to be the matching algorithm of choice. However, since it works with 1-D signals, the 2-D signature image must be reduced to one dimension. To that effect, projection and envelope representations have been used (Fang et al., 2003; Kholmatov, 2003). A weakness of the Dynamic Time Warping is that it cumulates errors and, for this reason, the sequences to match must be the shortest as possible. To solve this problem, a wavelet transform can be used to extract inflection points from the 1-D signal. Then, Dynamic Time Warping matches this shorter sequence of points (Deng et al., 2003). The inflection points can also be used to segment the wavelet signal into shorter sequences to be matched by the Dynamic Time Warping algorithm (Ye et al., 2005).

Among other methods, a local elastic algorithm was used by Fang et al. (2003) and You et al. (2005) to match the skeleton representations of two signatures, and cross-correlation was used by Fasquel and Bruynooghe (2004) to extract correlation peak features from multiple signature representations obtained from identity filters and Gabor filters.

1.1.5 Fixed Zoning

Several fixed zoning methods are described in the literature. Usually, the signature is divided into strips (vertical or horizontal) or using a layout like a grid (see Figure 1.11) or angular partitioning. Then, geometric features (Armand et al., 2006b; Ferrer et al., 2005; Huang and Yan, 1997; Justino et al., 2005; Martinez et al., 2004; Ozgunduz et al., 2005; Qi and Hunt, 1994; Santos et al., 2004; Senol and Yildirim, 2005), wavelet transform features and statistical features (Fierrez-Aguilar et al., 2004; Frias-Martinez et al., 2006; Hanmandlu et al., 2005; Justino et al., 2005; Madasu, 2004) can be extracted.

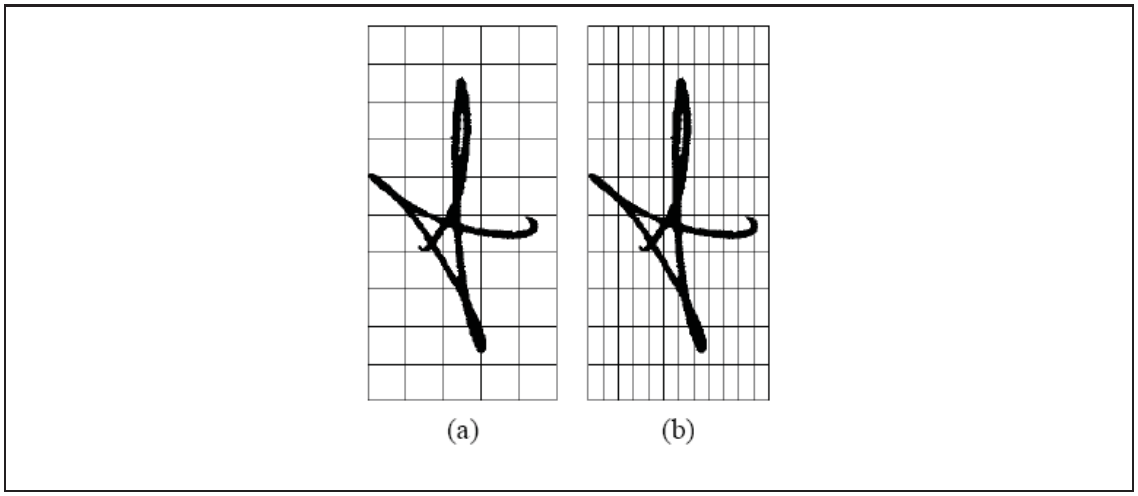

Figure 1.11 Grid segmentation using (a) square cells and (b) rectangular cells.
Adapted from Justino et al. (2000)

Strips based methods include peripheral features extraction from horizontal and vertical strips of a signature edge representation. Peripheral features measure the distance between two edges and the area between the virtual frame of the strip and the first edge of the signature (Fang et al., 2002; Fang and Tang, 2005).

The Modified Direction Feature (MDF) technique (Armand et al., 2006b) extracts the location of the transitions from the background to the signature and their corresponding direction values for each cell of a grid superposing the signature image. The Gradient, Structural and Concavity (GSC) technique (Kalera et al., 2004; Srihari et al., 2004) extracts gradient features from edge curvature, structural features from short strokes and concavity features from certain hole types independently for each grid cell covering the signature image.

The Extended Shadow Code (ESC) technique, proposed by Sabourin and colleagues (Sabourin et al., 1993; Sabourin and Genest, 1994, 1995), centers the signature image on a grid layout where each rectangular cell of the grid is composed of six bars: one bar for each side of the cell plus two diagonal bars stretching from a corner of the cell to the other in an ‘X’ fashion. The pixels of the signature are projected perpendicularly on the nearest horizontal bar, the nearest

vertical bar, and also on both diagonal bars (see Figure 1.14). The features are extracted from the normalized area of each bar that is covered by the projected pixels.

The envelope-based technique (Bajaj and Chaudhury, 1997; Ramesh and Murty, 1999) describes, for each grid cell, the comportment of the upper and lower envelope of the signature. In the approach of Bajaj and Chaudhury (1997), a grid 4X3 is superimposed on the upper and lower envelopes, as shown in the Figure 1.12. After that, a numerical value is assigned for each grid element. The following values are possible (Bajaj and Chaudhury, 1997; Ramesh and Murty, 1999) :

- 0, if the envelope does not pass through the cell;
- 1, if the envelope passes through the cell, but no prominent peak/valley lies inside the cell (or both prominent peak and valley lies in the cell);
- 2, if a prominent peak (maximal curvature) lies inside the cell;
- 3, if a prominent valley (minimum curvature) lies inside the cell;
- 4, if a prominent upslope lies inside the cell;
- 5, if a prominent downslope lies inside the cell.

While the pecstrum technique (Sabourin et al., 1996, 1997b) centers the signature image on a grid of overlapping retinas and then uses successive morphological openings to extract local Granulometric Size Distributions. The *positive pattern spectrum* is computed by measuring the result of successive morphological openings of the object, as the size of the structuring element increases. In a similar way, the *negative pattern spectrum* is obtained from the sequence of closings of the object. Figure 1.13 shows a retina example.

1.1.6 Signal Dependent Zoning

Signal dependent zoning generates different regions adapted to individual signatures. Martinez et al. (2004), followed by Ferrer et al. (2005) and Vargas et al. (2008), extracted position

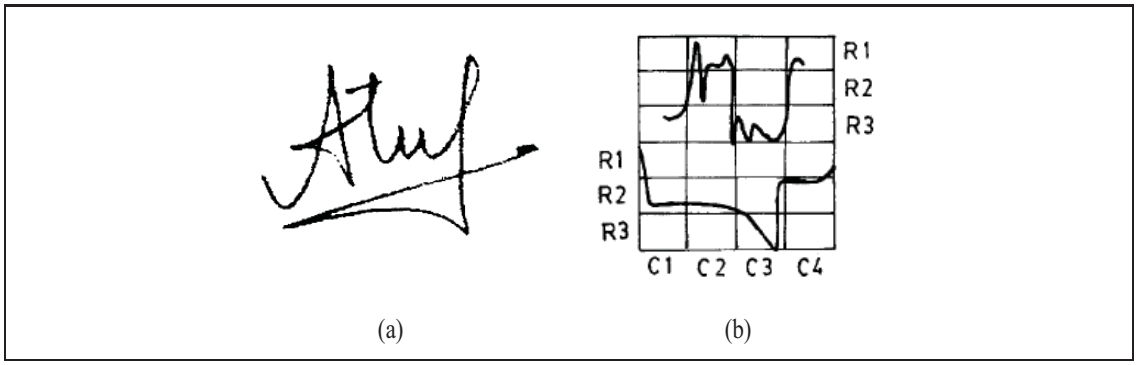

Figure 1.12 Examples of (a) handwritten signature and (b) its envelopes.
Adapted from Bajaj and Chaudhury (1997)

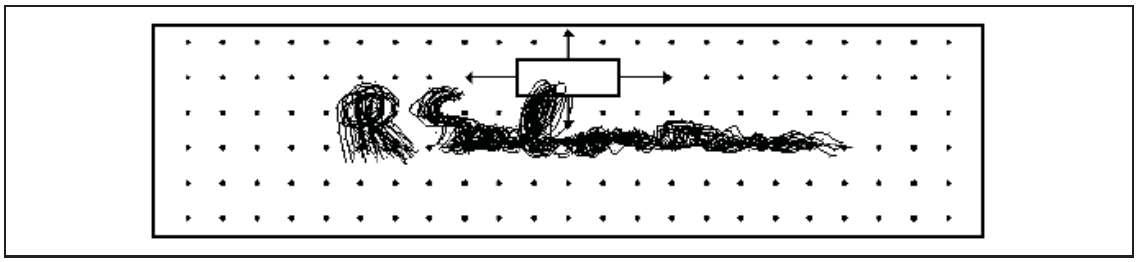

Figure 1.13 Retina used to extract local Granulometric Size Distributions.
Adapted from Sabourin et al. (1997b)

features from a contour representation in polar coordinates. Still using the polar coordinate system, signal dependent angular-radial partitioning techniques have been developed. These techniques adjust themselves to the circumscribing circle of the signature to achieve scale invariance. Rotation invariance is achieved by synchronizing the sampling with the baseline of the signature. Shape matrices have been defined in this way to sample the silhouette of two signatures and extract similarity features (Sabourin et al., 1997a) (see Figure 1.15). A similar method is used by Chalechale et al. (2004), though edge pixel area features are extracted from each sector and rotation invariance is obtained by applying a 1-D discrete Fourier transform to the extracted feature vector.

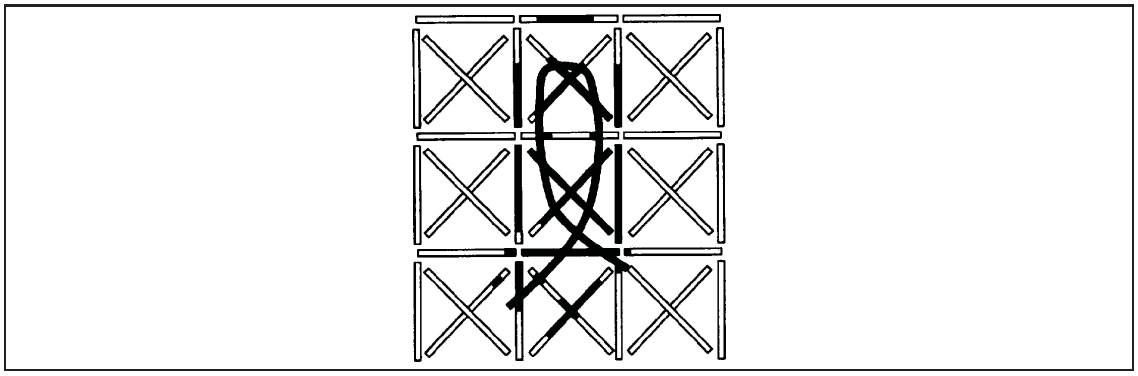

Figure 1.14 Example of feature extraction on a looping stroke by the Extended Shadow Code technique. Pixel projections on the bars are shown in black.
Adapted from Sabourin et al. (1993)

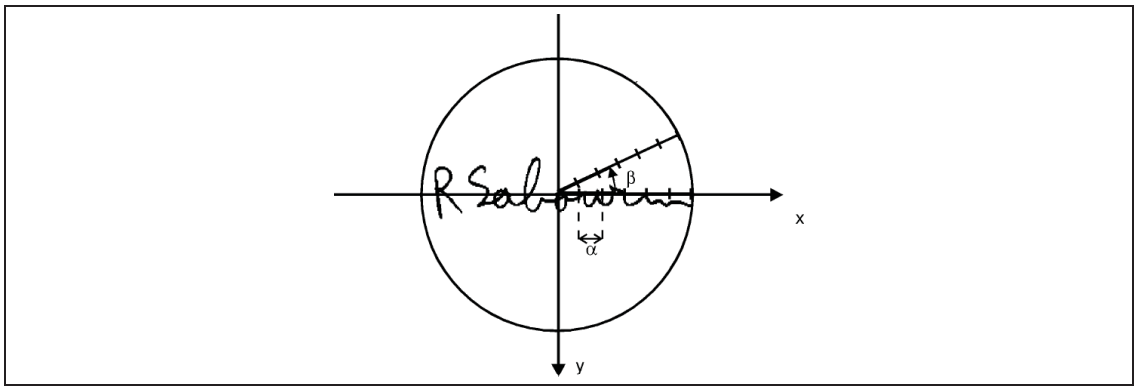

Figure 1.15 Example of polar sampling on an handwritten signature. The coordinate system is centered on the centroid of the signature to achieve translation invariance and the signature is sampled using a sampling length α and an angular step β.
Adapted from Sabourin et al. (1997a)

By using a Cartesian coordinate system, signal dependent retinas were employed by Ando and Nakajima (2003) to define the best local regions capturing the intrapersonal similarities from the reference signatures of individual writers. The location and size of the retinas were optimized through a genetic algorithm. Then, similarity features could be extracted from the questioned signature and its reference set.

In the work of Igarza et al. (2005), a connectivity analysis was performed on the signature images in order to obtain local regions from which geometric and position features were extracted. A more detailed analysis was performed by Perez-Hernandez et al. (2004), where stroke segments were obtained by first finding the direction of each pixel of the skeleton of the signature and then using a pixel tracking process. Then, the orientation and endpoints of the strokes were employed as features. Another technique consists of eroding the stroke segments into bloated regions before extracting similarity features (Franke et al., 2002).

Instead of using strokes, Xiao and Leedham (2002) segmented upper and lower envelopes whose orientation changed sharply. After that, length, orientation, position and pointers to the left and right neighbors of each segment were extracted. Finally, Chen and Srihari matched two signature contours using Dynamic Time Warping before segmenting and extracting Zernike moments.

1.1.7 Pseudo-dynamic Features

The lack of dynamic information is a serious constraint in off-line SV. The knowledge of the pen trajectory, along with speed and pressure, gives an edge to on-line systems. To overcome this difficulty, some approaches use dynamic signature references to develop individual stroke models that can be applied to off-line questioned signatures. For instance, Guo et al. (1997, 2000) used stroke-level models and heuristic methods to locally compare dynamic and static pen positions and stroke directions. Lau et al. (2005) developed the Universal Writing Model (UWM), which consists of a set of distribution functions constructed using the attributes extracted from on-line signature samples. Whereas Nel et al. (2005) used a probabilistic model of the static signatures based on Hidden Markov Models, where the models restricted the choice of possible pen trajectories describing the signature morphology. Then, the optimal pen trajectory was calculated by using a dynamic sample of the signature.

Without resorting to on-line examples, it is possible to extract pseudo-dynamic features from static signature images. Pressure features can be extracted from pixel intensity (i.e. grey levels) (Huang and Yan, 1997; Lv et al., 2005; Santos et al., 2004; Wen-Ming et al., 2004) and stroke

width (Lv et al., 2005; Oliveira et al., 2005). In the approach of Huang and Yan (1997), pixels whose grey-level values are above the threshold of 75% are considered as belonging to high pressure regions (see Figure 1.16).

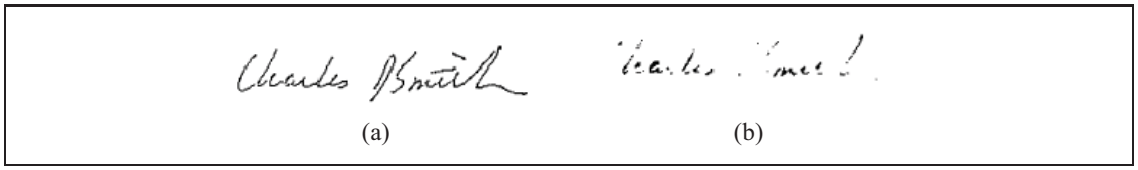

Figure 1.16 Examples of (a) signature and (b) its high pressure regions.
Adapted from Huang and Yan (1997)

Finally, speed information can be extrapolated from stroke curvature (Justino et al., 2005; Santos et al., 2004), stroke slant (Justino et al., 2005; Oliveira et al., 2005; Senol and Yildirim, 2005), progression (Oliveira et al., 2005; Santos et al., 2004) and form (Oliveira et al., 2005). Figure 1.17 illustrates two stroke progressions.

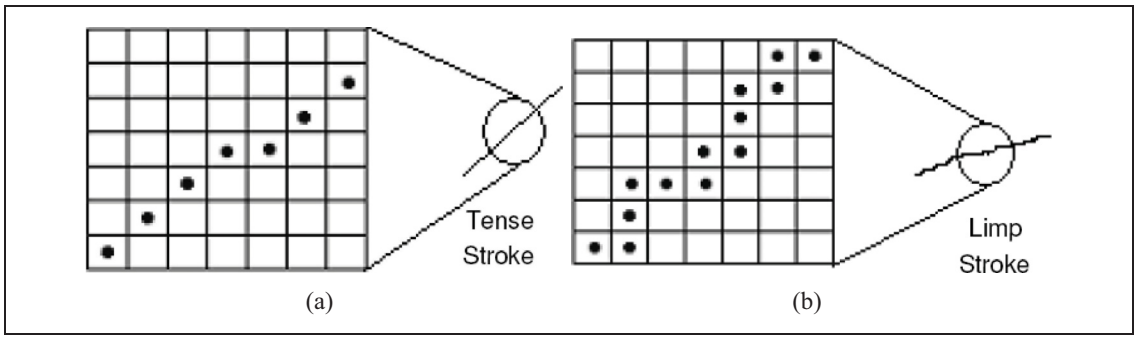

Figure 1.17 Examples of stroke progression: (a) few changes in direction indicates a tense stroke, and (b) a limp stroke changes direction many times.
Adapted from Oliveira et al. (2005)

1.2 Verification Strategies and Experimental Results

This section categorizes some research in off-line SV according to the technique used to perform verification, that is, Distance Classifiers, Artificial Neural Networks, Hidden Markov Models, Dynamic Time Warping, Support Vector Machines and Multi-Classifier Systems.

In SV, the verification strategy can be categorized either as writer-independent or as writer-dependent (Srihari et al., 2004). With writer-independent verification, a single classifier deals with the whole population of writers. In contrast, writer-dependent verification needs a different classifier for each writer. As the majority of the research presented in literature is designed to perform writer-dependent verification, this aspect is mentioned only when writer-independent verification is considered.

Before describing the verification strategies, the measures used to evaluate the performance of SV systems are presented.

1.2.1 Performance Evaluation Measures

The simplest way to report the performance of SV systems is in terms of error rates. The False Negative Rate (FNR) is related to the number of genuine signatures erroneously classified by the system as forgeries. Whereas the False Positive Rate (FPR) is related to the number of forgeries misclassified as genuine signatures. FNR and FPR are also known as type 1 and type 2 errors, respectively. Finally, the Average Error Rate (AER) is related to the total error of the system, where type 1 and type 2 errors are averaged by taking into account the *a priori* probabilities.

On the other hand, if the decision threshold of a system is set to have the FNR approximately equal to the FPR, the Equal Error Rate (EER) is calculated. Finally, a few works in the literature measure their system performances in terms of classication rate, which corresponds to the ratio of samples correctly classified to the total of samples.

1.2.2 Distance Classifiers

A simple Distance Classifier is a statistical technique which usually represents a pattern class with a Gaussian probability density function (PDF). Each PDF is uniquely defined by the mean vector and covariance matrix of the feature vectors belonging to a particular class. When the full covariance matrix is estimated for each class, the classification is based on Mahalanobis distance. On the other hand, when only the mean vector is estimated, classification is based on Euclidean distance (Coetzer, 2005).

Approaches based on Distance Classifiers are traditionally writer-dependent. The reference samples of a given author are used to compose the class of genuine signatures and a subset of samples from each other writer is chosen randomly to compose the class of (random) forgeries. The questioned signature is classified according to the label of its nearest reference signature in the feature space. Further, if the classifier is designed to find a number of K-nearest reference signatures, a voting scheme is used to take the final decision.

Distance Classifiers were one of the first classification techniques to be used in off-line SV. One of the earliest reported research was by Nemcek and Lin (1974). By using a fast Hadamard transform as feature extraction technique on genuine signatures and simple forgeries, and Maximum Likelihood Classifiers, they obtained an FNR of 11% and an FPR of 41%.

Then, Nagel and Rosenfeld (1977) proposed a system to discriminate between genuine signatures and simple forgeries using images obtained from real bank checks. A number of global and local features were extracted considering only the North American's signature style. Using Weighted Distance Classifiers, they obtained $FNRs$ ranging from 8% to 12% and an FPR of 0%.

It is only years later that skilled forgeries began to be considered in off-line SV. Besides proposing a method to separate the signatures from noisy backgrounds and to extract pseudo-dynamic features from static images, Ammar and colleagues (Ammar, 1991; Ammar et al., 1985, 1988) were the first to try to detect skilled forgeries using an off-line SV system. In their research,

distance classifiers were used together with the leave-one-out cross validation method, since the number of signatures samples was small.

Qi and Hunt (1994) presented a SV system based on global geometric features and local grid-based features. Different types of similarity measures, such as Euclidean distance, were used to discriminate between genuine signatures and forgeries (including simple and skilled). They achieved an FNR ranging from 3% to 11.3% and an FPR ranging from 0% to 15%.

Sabourin and colleagues have done extensive research in off-line SV since middle 80's. In one of their research (Sabourin et al., 1993), the Extended Shadow Code was used in order to extract local features from genuine signatures and random forgeries. The first experiment used a K-Nearest Neighbors (K-NN) classifier with a voting scheme, obtaining an AER of 0.01% when $K = 1$. The second experiment used a Minimum Distance Classifier, obtaining an AER of 0.77% when 10 training signatures were used for each writer. In another relevant research (Sabourin et al., 1997b), they used granulometric size distributions as local features, also in order to eliminate random forgeries. By using K-NN and Threshold Classifiers, they obtained an AER around 0.02% and 1.0%, respectively.

Fang et al. (2001) developed a system based on the assumption that the cursive segments of skilled forgeries are generally less smooth than those of genuine signatures. Besides the utilization of global shape features, a crossing and a fractal dimension methods were proposed to extract the smoothness features from the signature segments. Using a simple Distance Classifier and the leave-one-out cross-validation method, an FNR of 18.1% and an FPR of 16.4% were obtained. Later, Fang et al. (2002) extracted a set of peripheral features in order to describe internal and external structures of the signatures. To discriminate between genuine signatures and skilled forgeries, they used a Mahalanobis distance classifier together with the leave-one-out cross-validation method. The obtained $AERs$ were in the range of 15.6% (without artificially generated samples) and 11.4% (with artificially generated samples).

1.2.3 Artificial Neural Networks

An Artificial Neural Network (ANN) is a massively parallel distributed system composed of processing units capable of storing knowledge learned from experience (samples) and using it to solve complex problems (Haykin, 1998). Multi-Layer Perceptrons (MLPs) trained with the error Back Propagation (BP) algorithm (Rumelhart et al., 1986) have been so far the most frequently ANN architecture used in pattern recognition.

Mighell et al. (1989) were the first to apply ANNs to off-line SV. In order to eliminate simple forgeries, they used the raw images as input to a MLP. In the experiments, by using a training set composed of genuine signatures and forgeries, they achieved an EER of 2%.

Sabourin and Drouhard (1992) used directional PDFs as global feature vectors and MLP as classifier in order to eliminate random forgeries. Since their database was composed of few data, some signature samples were artificially generated by rotating the directional PDFs. In the experiments, they obtained an FNR of 1.75% and an FPR of 9%.

Murshed et al. (1995) proposed a verification strategy based on Fuzzy ARTMAPs in the context of random forgeries. Differently from other neural networks types, the Fuzzy ARTMAPs allows training by using examples of only one class. Therefore, in this approach, the genuine signatures are used for training and the random forgeries (as well as some unseen genuine signatures samples), for testing. In order to simulate different experts examining different regions of the signature, the image is divided in a number of overlapping squares, according to the writer signature shape. Then, each signature region is verified by a specialized Fuzzy ARTMAP. In the experiments, they obtained an AER of 9.14%.

Fadhel and Bhattacharyya (1999) proposed a SV system based on Steerable Wavelets as feature extraction technique and MLP as classifier. In the first experiment, by selecting only the first 2 of the 16 coefficients which represent each signature image, they obtained a classification rate of 85.4%. Whereas in a second experiment, by using all the 16 coefficients, the classification rate was improved to 93.8%.

Quek and Zhou (2002) proposed a system based on Fuzzy Neural Networks, in order to eliminate skilled forgeries. To represent the signatures, they used reference pattern-based features, global baseline features, pressure features and slant features. In the first set of experiments, using both genuine signatures and skilled forgeries to train the network, an average EER of 22.4% was obtained. Comparable results were obtained in the second set of experiments, in which only genuine signatures were used as training data.

Vélez et al. (2003) performed SV by comparing sub-images or positional cuttings of a test signature to the representations stored in Compression Neural Networks. In this approach, neither image preprocessing nor feature extraction is performed. By using one signature per writer, together with a set of artificially generated samples, they obtained a classification rate of 97.8%.

Armand et al. (2006b) proposed the combination of the Modified Direction Feature (MDF) extracted from the signature's contour with a set of geometric features. In the experiments, they compared Radial Basis Function (RBF) and Resilient Backpropagation (RBP) neural network performances. Both networks performed writer identification and contained 40 classes: 39 corresponding to each writer and one corresponding to the forgeries. In this case, skilled forgeries were used in the training phase. The best classification rates obtained were 91.21% and 88.0%, using RBF and RBP, respectively.

1.2.4 Hidden Markov Models

Hidden Markov Models (HMMs) (Rabiner, 1989) are finite stochastic automata used to model sequences of observations. They are widely applied in time-dependent problems - such as speech recognition and on-line signature verification - where the number of observations is unknown or difficult to define *a priori*. In off-line SV, discrete HMMs have been used to perform writer-dependent verification, where only the genuine signatures are modeled. In this case, the decision threshold is generally defined by using an independent set composed of genuine and random forgery samples. Another particularity of systems based on discrete HMMs is the use of a codebook to extract discrete observation sequences from the signature images.

Rigoll and Kosmala (1998) presented a comparison between on-line and off-line SV using HMMs. To represent the signatures in the on-line model, they used both static and dynamic features. In the first set of experiments, in which each feature was investigated separately, surprising results were obtained. The bitmap feature was the most important one, achieving a classification rate of 92.2%. The Fourier feature also supplied a high classification rate. Finally, another surprise was the low importance of the acceleration. As expected, good results were obtained using the velocity feature. Other experiments, using several features together, were performed in order to obtain high classification rates. The best result (99%) was obtained when only 4 features (bitmap, velocity, pressure and Fourier feature) where combined. To represent the signatures in the off-line model, they subdivided the signature image into several squares of 10×10 pixels. After that, the grey value of each square was computed and used as feature. In the experiments, a classification rate of 98.1% was achieved. The small difference between the on-line and off-line classification rates is an important practical result, since off-line verification is simpler to implement.

El-Yacoubi et al. (2000) proposed an approach based on HMM and pixel density feature in order to eliminate random forgeries. To perform training while choosing the optimal HMM parameters, the Baum-Welch algorithm and the cross-validation method were used. Each signature was analyzed under three resolutions (100×100, 40×40 and 16×16 pixels). Then, a majority-vote rule took the final decision. An AER of 0.46% was obtained when both genuine and impostor spaces were modeled, and AER of 0.91% was obtained when only the genuine signatures were modeled.

Justino (2001) used HMMs to detect random, simple and skilled forgeries. Also using a grid-segmentation scheme, three features were extracted from the signatures: pixel density feature, Extended Shadow Code and axial slant feature. They applied the cross-validation method in order to define the number of states for each HMM writer model. Using the Bakis model topology and the Forward algorithm, they obtained an FNR of 2.83% and FPRs of 1.44%, 2.50% and 22.67%, for random, simple and skilled forgeries, respectively.

Ferrer et al. (2005) used two *left-to-right* HMMs per writer in order to model features (i.e., signature envelope and interior stroke distribution) extracted from polar and Cartesian coordinates. Each HMM was trained with the Baum-Welch algorithm, using 35 states. By using the GPDS-160 database, and 12 genuine samples per writer during training, they obtained a FNR of 14.1% and a FPR of 12.6%, with respect to skilled forgeries.

1.2.5 Dynamic Time Warping

Widely applied in Speech Recognition, Dynamic Time Warping (DTW) is a Template Matching technique used for measuring similarity between two sequences of observations. The primary objective of DTW is to non-linearly align the sequences before they are compared (or matched) (Coetzer, 2005).

Wilkinson and Goodman (1990) used DTW to discriminate between genuine signatures and simple forgeries. Assuming that curvature, total length and slant angle are constant among different signatures of a same writer, they used a slope histogram to represent each sample. In the experiments, they obtained an EER of 7%. Increases in the error rates were observed when the forgers had some *a priori* knowledge about the signatures.

Deng et al. (1999) proposed a Wavelet-based approach to eliminate simple and skilled forgeries. After applying a Closed-Contour Tracing algorithm to the signatures, the obtained curvature data were decomposed into multi-resolution signals using Wavelets. Then, DTW were used to match the corresponding zero-crossings. Experiments were performed using English and Chinese signature datasets. For the English dataset, an FNR of 5.6% and FPRs of 21.2% on skilled forgeries and 0% on simple forgeries were obtained. Whereas using the Chinese dataset, an FNR of 6.0% and FPRs of 13.5% and 0% were achieved on skilled and simple forgeries, respectively.

Fang et al. (2003) proposed a method based on DTW and one-dimensional projection profiles in order to deal with intra-personal signature variations. To achieve discrimination between genuine signatures and skilled forgeries, a non-linear DTW was used in a different way. Instead

of using the distance between a test signature and a reference sample to take a decision, the positional distortion at each point of the projection profile was incorporated into a distance measure. Using the leave-one-out cross-validation method and the Mahalanobis distance, they obtained $AERs$ of 20.8% and 18.1%, when binary and grey level signatures were considered, respectively.

1.2.6 Support Vector Machines

SVM (Vapnik, 1999) use a kernel-based learning technique which has shown successful results in various domains, such as pattern recognition, regression estimation, density estimation, novelty detection and others.

Signature verification systems that use SVM as classifier are designed in a similar way to those that use neural networks. That is, in a writer-dependent approach, there is one class for the genuine signatures and other class for the forgeries. In addition, by using one-class SVMs (Scholkopf et al., 2001), it is possible to perform training by using only genuine signatures. In the research of Srihari et al. (2004) they tried to use it in the context of skilled forgeries. However, by using the traditional two-class approach, the AER decreased from 46.0% to 9.3%.

Martinez et al. (2004) used SVM with RBF kernel in order to detect skilled forgeries. In the experiments, different types of geometrical features, as well as raw signatures were tested. The best result, an FPR of 18.85%, was obtained when raw images with a scale of 0.4 were used.

Justino et al. (2005) performed a comparison between SVM and HMM classifiers in the detection of random, simple and skilled forgeries. By using a grid-segmentation scheme, they extracted a set of static and pseudo-dynamic features. Under different experimental conditions, that is, varying the size of the training set and the types of forgeries, the SVM with a linear kernel outperformed the HMM.

Ozgunduz et al. (2005) used Support Vector Machines in order to detect random and skilled forgeries. To represent the signatures, they extracted global geometric features, direction features and grid features. In the experiments, a comparison between SVM and ANN was per-

formed. Using a SVM with RBF kernel, an FNR of 0.02% and an FPR of 0.11% were obtained. Whereas the ANN, trained with the Backpropagation algorithm, provided an FNR of 0.22% and an FPR of 0.16%. In both experiments, skilled forgeries were used to train the classifier.

In order to detect skilled forgeries, Vargas et al. (2011) proposed a SV system based on SVMs and grey level information. After removing the signature background and reducing the influence of different ink pens, the grey level variations were measured globally using statistical texture features (i.e., the co-occurence matrix and local binary pattern). By using two different databases, that is, GPDS-100 and MCYT-75, and 5 genuine samples *vs.* 5 random forgeries per writer to train the SVMs, they obtained, respectivelly, $EERs$ of 13.38% and 12.92%, regarding genuine and skilled forgery samples.

1.2.7 Multi-Classifier Systems

Multi-Classifier Systems (MCS) have been used to reduce error rates of many challenging pattern recognition problems, including SV. In a Multi-Classifier System (MCS), classifiers may be combined in parallel by changing (i) the training set (e.g., bagging (Breiman, 1996) and boosting (Freund, 1990)), (ii) the input features (e.g., random subspaces (Ho, 1998)) and (iii) the parameters/architecture of the classifier. Another way to use multiple classifiers is through multi-stage approaches, where each classification level receives the results of the previous one.

The first multi-classifier off-line SV systems were designed (from the 90's) to detect random forgeries. Cardot et al. (1994) proposed a multi-stage neural network architecture based on Kohonen maps and MLPs. They used the outline of the signature images and geometric features to compose two types of feature vectors. The first level was composed of two Kohonen maps (one for each set of features), in order to perform an initial classification and to choose the random forgeries to train the networks of the second level. As the number of writers was very large (over 300), they had to limit the number of classes to less than 50. In the second level, two MLPs per writer were used to perform writer-dependent verification. Finally, in the last

level, an MLP accepted or rejected the signature. By using 6000 signature images extracted from real postal checks, they achieved an FNR of 4% and an FPR of 2%.

Sabourin and Genest (1995) used the Extended Shadow Code (ESC) to extract 15 different signature representations from 800 genuine signatures of 20 writers. The authors showed that the cooperation of 15 classifiers (either K-NN or Minimum Distance classifiers) provides a mean performance as good as or better than the mean performance provided by the best individual classifier. In another work, Sabourin et al. (1997b) used Granulometric Size Distributions to obtain four different signature representations. By using an ensemble of four K-NN classifiers (one for each signature representation), they obtained an AER below 0.02%. When using an ensemble of four Minimum Distance classifiers, they obtained an AER below 1%.

Bajaj and Chaudhury (1997) proposed a system based on the combination of three writer-independent MLPs, each one representing a different feature vector: moments, upper envelope and lower envelop. During experiments, a substantial reduction on the error rates was obtained when using the three classifiers together (FNR = 1%; FPR = 3%).

Blatzakis and Papamarkos (2001) proposed a two-stage system based on global geometric features, grid features and texture features. In the first stage, three MLPs (one for each feature set) performed a coarse classification. After that, a RBF neural network - trained with samples which were not used in the first stage - took the final decision. By using a set of 2000 signatures from 115 writers, a FNR of 3% and a FPR of 9.8% were obtained.

In the 2000's, other forgery types started to be handled by the multi-classifier off-line SV systems. Sansone and Vento (2000) proposed a multi-stage system for dealing with three types of forgeries. The first stage used signature's outline in order to eliminate random and simple forgeries. Then, the signatures accepted by the first stage (i.e., classified as genuine) were sent to the second stage, where they could be classified as genuine or as skilled forgery by using high pressure regions as features. Finally, a third stage took the final decision. By using MLP as classifiers, and a set of 980 genuine signatures and 980 forgeries from 49 writers, they

obtained a FNR of 2.04% and FPRs of 0.01%, 4.29% and 19.80% - with respect to random, simple and skilled forgeries, respectively.

Huang and Yan (2002) proposed a two-stage system based on ANN and a structural approach. To represent the signatures, they used geometric and directional frontier features. In the first stage of the system, a neural network attributes to the signature three possible labels: pass (genuine signature), fail (random or less skilled forgery) and questionable (skilled forgery). For the questionable signatures, the second stage uses a Structural Feature Verification algorithm to compare the detailed structural correlation between the test signature and the reference samples. In the experiments, the first classifier rejected 2.2% of the genuine signatures, accepted 3.6% of the forgeries and was undecided on 32.7% of the signatures. The second classifier rejected 31.2% of the questionable genuine signatures and accepted 23.2% of the questionable forgeries. Finally, the combined classifier provided a FNR of 6.3% and a FPR of 8.2%.

Bertolini et al. (2010) employed a dichotomic approach based on dissimilarity representation (Cha, 2001) to design writer-independent classifiers that deals with a population of 100 writers. They represented the signatures by means of Bezier curves using different grid sizes in order to extract a set of graphometric features (i.e., pixel distribution, curvature, density and slant). By using an ensemble of SVMs built with a standard genetic algorithm and 15 reference signatures per writer, they obtained a FNR of 11.32% and $FPRs$ of 4.32% (random), 3.00% (simple) and 6.48% (skilled).

1.3 Dealing with a limited amount of data

Mainly for practical reasons, a limited number of signatures per writer is available to train a classifier for SV. However, by using a small training set, the class statistics estimation errors may be significant, resulting in unsatisfactory verification performance (Fang and Tang, 2005).

In order to generate additional training samples, Huang and Yan (1997) applied slight transformations to the genuine signatures; and heavy transformations, also to the genuine signatures,

in order to generate forgeries. In the two cases, the transformations were: slant distortions, scalings in horizontal and vertical directions, rotations and perspective view distortions.

Vélez et al. (2003) tried to reproduce intrapersonal variability using only one signature per writer. To generate additional training samples, they applied rotations (in the range of $\pm 15°$), scalings (in the range of $\pm 20\%$), horizontal and vertical displacements (in the range of $\pm 20\%$) and different types of noise for each original signature.

By using a different approach, Fang and Tang (2005) proposed the generation of additional samples in the following way:

1) At first, two samples are selected from the set of genuine signatures;
2) Then, an Elastic Matching Algorithm is applied to the pair of signatures in order to establish the correspondences between individual strokes;
3) Next, the corresponding stroke segments are linked up by displacement vectors;
4) Finally, the displacement vectors are used to perform an interpolation between the two signatures and, thus, to produce a new training sample.

Figure 1.18 presents the process explained above and Figure 1.19 shows examples of generated signatures.

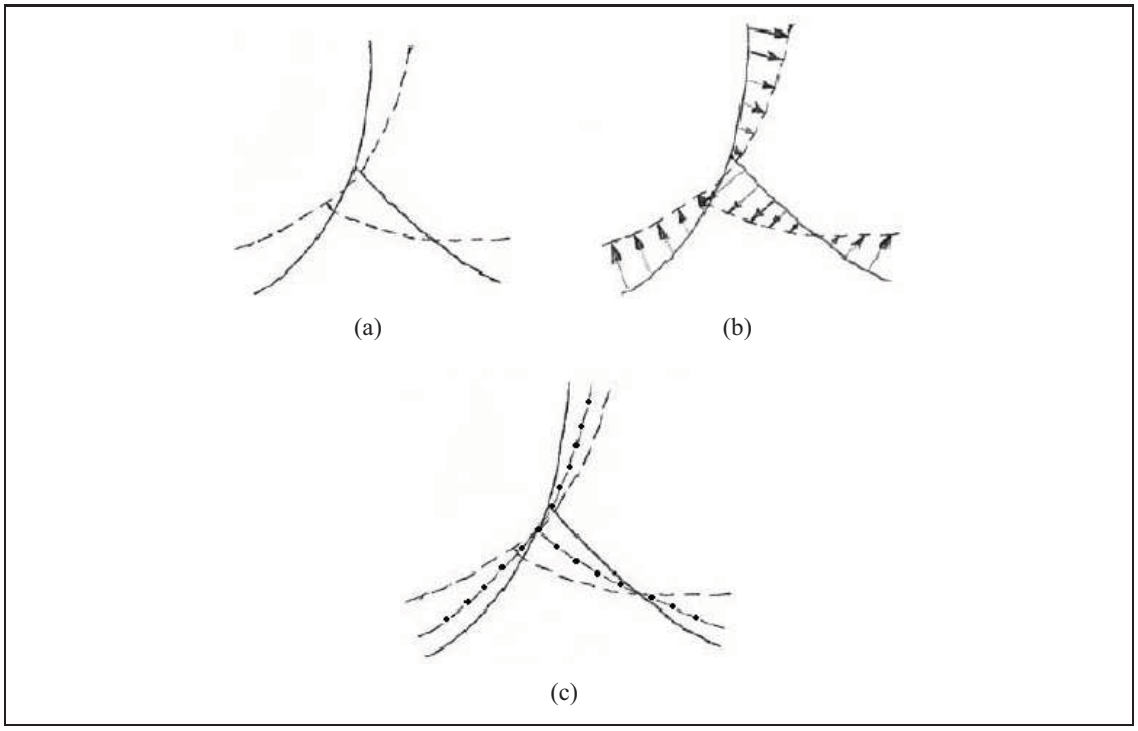

Figure 1.18 Additional Sample Generation: (a) Pair of genuine samples overlapped, (b) The corresponding strokes identified and linked up by displacement vectors, (c) New sample generated by interpolation (dashed lines with dots).
Adapted from Fang and Tang (2005)

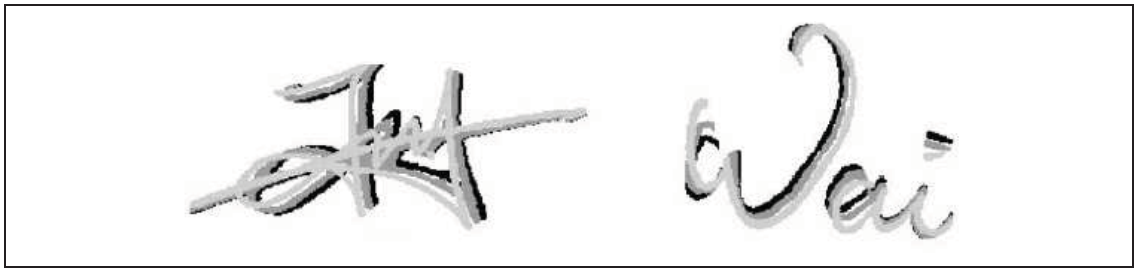

Figure 1.19 Examples of computer generated signatures (in grey), obtained using an strategy based on elastic matching, and the original signatures (in black).
Adapted from Fang and Tang (2005)

By using a dichotomic approach based on Dissimilarity Representation (DR) (Cha, 2001), Santos et al. (2004), followed by Bertolini et al. (2010) and Rivard (2010), solved the problem

of having a limited number of samples to perform SV. Instead of using one class per writer to train a global classifier, only two classes are used: genuine and forgery. After the usual feature extraction phase, new feature vectors are generated in the following way:

1) Compute the Euclidean distance vector between each pair of signatures;

2) If the pair of signatures belongs to the same writer, label the distance vector as 1. Otherwise, label the distance vector as 0;

3) Use the distance vectors to train a two-class classifier.

In the verification phase, distance vectors are computed between the input signature and a set of reference signatures of a specific writer, and sent as input to the classifier. The final decision is taken by combining all classifier outputs in a voting schema. Similar SV approaches have also been developed by Shihari and his team (Kalera et al., 2004; Srihari et al., 2004).

1.4 Discussion

This chapter presented a survey of techniques developed in the field of off-line SV over the last twenty years. Even if error rates are reported, it is very difficult to compare performances between verification strategies since each research uses a different experimentation protocol, and a different signature database. For security reasons, it is not easy to make a signature dataset available to the SV community, especially if the signatures come from a real application, as banking documents, for example. Table 1.1 presents a summary of some signature databases reported in the off-line SV literature.

In off-line SV, a significant level of uncertainty resides due to the availability of partial knowledge during system design. Generaly, only genuine and random forgery samples are available to design a SV system. This system, in turn, must detect other forgery types during operations. Thus, the choice of using global or local features depends on the types of forgeries to be detected by the system. The global features are extracted at a low computational cost and

have good noise resilience. However, they have less capacity to discriminate between genuine signatures and skilled forgeries. On the other hand, local features are more suitable to identify skilled forgeries, despite their dependence on a zoning process. Thus, a verification system designed to eliminate random, simple and skilled forgeries could benefit from using both global and local features. With respect to the classification techniques, writer-independent classifiers are more useful to eliminate rough forgery samples (i.e., random and simple), since a single classifier deals with all population of writers; while writer-dependent classifiers can deal with more skilled forgeries. A drawback with the use of writer-dependent approaches is the high number of classifiers generated, since at least one classifier per writer is employed.

Another important issue is the large number of samples required to ensure that the classifier will be able to generalize on unseen data (Leclerc and Plamondon, 1994). Classifiers without explicit training phase, such as Distance Classifiers and Dynamic Time Warping, despite not requiring many reference samples, they tend to have a low generalization capability. In addition to genuine signature samples, discriminative classifiers such as MLPs and SVMs need forgery samples in the training set in order to allow class separation. Most researchers have been dealing with this problem by using a subset of genuine signatures taken from other writers (i.e., random forgeries). Other solutions have been the use of one-class classifiers (Murshed et al., 1995; Srihari et al., 2004) and computer generated forgeries (Mighell et al., 1989). Although only genuine signature samples are used during the training phase of generative classifiers such as Hidden Markov Models, random forgery samples are subsequently needed to define the decision thresholds.

The generation of synthetic samples (Fang et al., 2002; Fang and Tang, 2005; Huang and Yan, 1997; Vélez et al., 2003) and the use of dichotomic approaches (Bertolini et al., 2010; Rivard, 2010; Kalera et al., 2004; Santos et al., 2004; Srihari et al., 2004) are examples of strategies used to increase the number of training data from the available genuine signature samples. The disadvantage of using synthetic samples is that they may increase the confusion between genuine samples and skilled forgeries. With respect to dichotomic approaches, since writer-independent classifiers are employed, they are less suitable for detecting skilled forgeries.

Finally, the use of multiple classifiers seems to be a promising solution to reduce error rates of off-line SV systems. In the next chapter, the problem of having a limited amount of training data is dealt through a writer-dependent multi-hypothesis approach. Instead of trying to increase the training set size, the available signature samples are learned at different levels of perception. This is acomplished by using multiple discrete *left-to-right* HMMs trained with different number of states and codebook sizes. The codebooks are designed using signature samples of an independent database, supplied by writers not enrolled to the SV system. This *prior* knowledge ensures that system design can be triggered even with a single user.

Table 1.1 Signature verification databases

(I = Individual; G = Genuine; F = Forgeries; S = Samples)

References	Images	Signatures	Forgery Types
Nemcek and Lin (1974)	128x256 pixels binary	600G / 15I 120F / 4I	Simple
Nagel and Rosenfeld (1977)	500 ppi 64 grey levels	11G / 2I 14F / 2I	Simple
Ammar et al. (1985)	256x1024 pixels 256 grey levels	200G / 10I 200F / 10I	Simple
Qi and Hunt (1994)	300 dpi 256 grey levels	300G / 15I 150F / 10I	Simple Skilled
Sabourin and Drouhard (1992) Sabourin et al. (1993) Sabourin and Genest (1994) Sabourin et al. (1997b)	128x512 pixels 256 grey levels	800G / 20I	Random
Fang et al. (2002) Fang et al. (2003)	300 dpi 256 grey levels	1320G / 55I 1320F / 12I	Skilled
Mighell et al. (1989)	128x64 pixels binary	80G / 1I 66F	Skilled
Cardot et al. (1994)	1024x512 pixels 256 grey levels	6000G/ 300I	Random
Murshed et al. (1995)	128x512 pixels 256 grey levels	200G / 5I	Random
Bajaj and Chaudhury (1997)	200 dpi binary	150G / 10I	Random
Fadhel and Bhattacharyya (1999)	340 dpi 256 grey levels	300S / 30I	Skilled

Continued on Next Page. . .

References	Images	Signatures	Forgery Types
Sansone and Vento (2000)	300 dpi 256 grey levels	980G / 49I 980F / 49I	Simple Skilled
Blatzakis and Papamarkos (2001)	binary	2000G / 115I	Random
Quek and Zhou (2002)	516x184 pixels 256 grey levels	535G / 24I 15-20F / 5I	Skilled
Vélez et al. (2003)	300 dpi 256 grey levels	112S / 28I	not specified
Armand et al. (2006b)	not specified	936G / 39I 1170F / 39I	Skilled
Rigoll and Kosmala (1998)	not specified	280G / 14I 60F	Simple Skilled
Justino (2001) Justino et al. (2005) Bertolini et al. (2010)	300 dpi 256 grey levels	4000G / 100I 1200F / 10I	Simple Skilled
Coetzer (2005)	300 dpi binary	660G / 22I 264F / 6I	Simple Skilled
Deng et al. (1999)	600 ppi 256 grey levels	1000G / 50I 2500G / 50I	Simple Skilled
Srihari et al. (2004)	300 dpi 256 grey levels	1320G/ 55I 1320F / 55I	Skilled
Martinez et al. (2004) Ferrer et al. (2005)	300dpi 256 grey levels	3840G / 160I 4800F / 160I	Skilled
Ozgunduz et al. (2005)	256 grey levels	1320S / 70I	Skilled
Bastos et al. (1997)	not specified	120G / 6I	Random
Huang and Yan (2002)	100 dpi 256 grey levels	1272G / 53I 7632F / 53I	Skilled

CHAPTER 2

A MULTI-HYPOTHESIS APPROACH

Though not fully explored in literature, it has recently been shown that the Receiver Operating Characteristic (ROC) curve – where the True Positive Rates are plotted as function of the False Positive Rates – provides a powerful tool for evaluating, combining and comparing off-line SV systems (Coetzer and Sabourin, 2007; Oliveira et al., 2007). Several interesting properties can be observed from ROC curves. First, Area Under Curve (AUC) is equivalent to the probability that the classifier will rank a randomly chosen positive sample higher than a randomly chosen negative sample (Fawcett, 2006). This measure is useful to characterize the system performance by using a single scalar value. In addition, the optimal threshold for a given class distribution lies on the ROC convex hull, which is defined as being the smallest convex set containing the points of the ROC curve. Finally, by taking into account several operating points (thresholds), the ROC curve allows to analyze these systems under different classification costs (Fawcett, 2006). This property is useful, for instance, for off-line SV systems where the operating points are selected dynamically according to the risk associated with the amount of a bank check.

In this chapter, an approach based on the combination of classifiers in the ROC space is proposed to improve performance of off-line SV systems designed from limited and unbalanced data. By training a set of classifiers with different parameters, and then selecting the best classifier(s) for each operating point, it is possible to construct a composite ROC curve that provides a more accurate estimation of system performance during training and significantly reduces the error rates during operations. This approach is based on the multiple-hypothesis principle (Fujisawa, 2007), which request the system to propagate several hypothesis throughout the recognition steps, generating a hierarchical tree of possible solutions.

Although the proposed approach may be applied to any type of statistical or neural 2-class classifier, this work involves HMMs trained by using different number of states and different

codebooks. In order to avoid the problems caused by the use of limited codebooks, and ensure that the system can be designed even with a single user, two databases are employed by the proposed approach: the development database (DB_{dev}), which contains the signatures of writers (not enrolled to the SV system) used to generate the candidate codebooks; and the exploitation database (DB_{exp}), which contains the signatures of the final users. The latter contains samples used to train, validate and test HMMs.

The rest of this chapter is organized as follows. The next section presents a brief survey of off-line SV systems based on discrete HMMs. Section 2.2 describes some key issues that affect the performance of off-line SV systems. Then, Section 2.4 describes the proposed approach and its advantages. In Section 2.5, the experimental results are shown and discussed. Finally, Section 2.6 concludes the chapter with a general discussion. The contents of this chapter have been published as a journal article in (Batista et al., 2010a) and as a conference article in (Batista et al., 2009).

2.1 Off-line SV systems based on discrete HMMs

A traditional off-line SV system based on discrete HMMs follows the steps shown by Figure 2.1. At first, the signature is scanned in order to obtain a digital representation $I(x, y)$. After applying some corrections to the signature image during the pre-processing step (such as noise removal and centering), a set of feature vectors $\mathcal{F} = \{\mathbf{F}_1, \mathbf{F}_2, ..., \mathbf{F}_L\}$ are extracted and quantized in a sequence of discrete observations $\mathbf{O} = \{o_1, o_2, ..., o_L\}$, where each observation o_i is a symbol provided by the codebook and L is the sequence size. Finally, the signature is classified as genuine or forgery by using the corresponding writer-dependent HMM λ.

Note that Figure 2.1 illustrates a writer-dependent system, where each writer is associated to a specific HMM trained with his/her corresponding genuine signature samples. Since each writer is associated with a single HMM, this system is also referred as a single-hypothesis system. Multi-hypothesis systems, on the other hand, allow a same writer to employ different classifiers depending on the input samples.

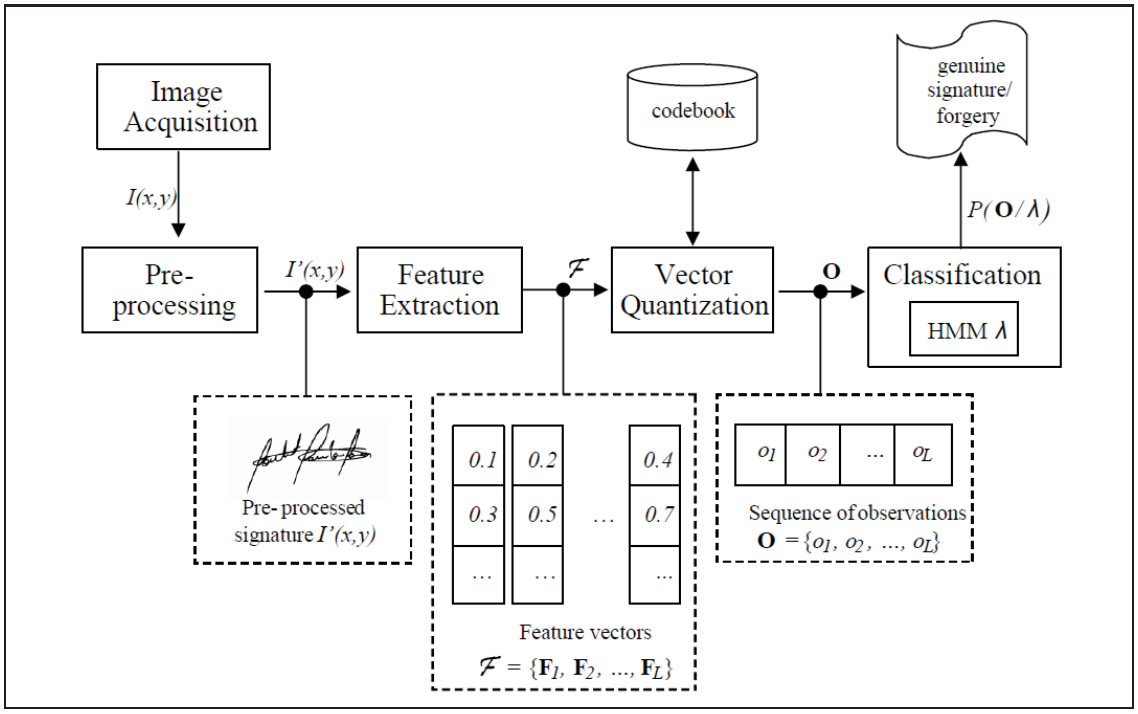

Figure 2.1 Block diagram of a traditional off-line SV system based on discrete HMMs.

The rest of this section provides additional details on the feature extraction, vector quantization and classification sub-systems considered in this work.

2.1.1 Feature Extraction

As described in Chapter 1, two classes of features are used in off-line SV: (i) static, related to the signature shape and (ii) pseudo-dynamic, related to the dynamics of the writing. These features can be extracted locally, if the signature is viewed as a set of segmented regions, or globally, if the signature is viewed as a whole. Since the HMMs are used to model sequence of observations, the local approach is typically employed (El-Yacoubi et al., 2000; Justino, 2001; Justino et al., 2000; Rigoll and Kosmala, 1998).

In the grid segmentation scheme of Justino (2001), for instance, the signature images (composed of 400x1000 pixels) are divided in 62 horizontal cells, where each cell is a rectangle

composed of 40x16 pixels. To absorb the horizontal variability of the signatures, the blank cells in the end of the images are discarded. Therefore, the images may have a variable number of horizontal cells, while the number of vertical cells is always 10. Figure 2.2 shows an example of a signature image with its final width. Note that the segmentation can be performed both in horizontal and vertical directions.

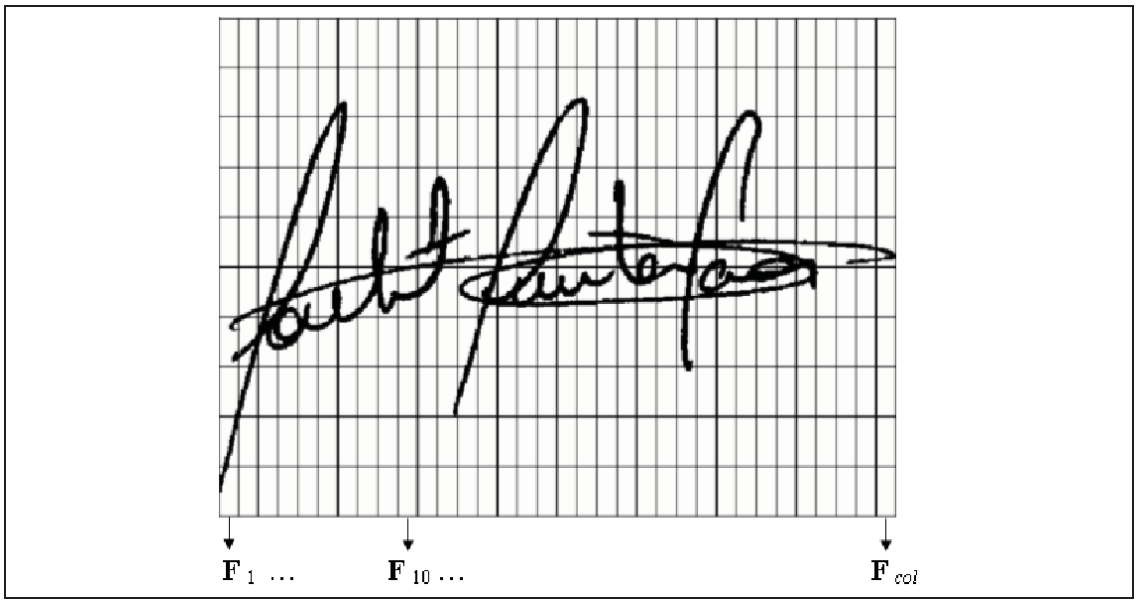

Figure 2.2 Example of grid segmentation scheme.

Each column of cells is then converted into a feature vector, where each vector element contains the density of pixels in its respective cell. In other words, each vector element is a value between 0 and 1 which corresponds to the number of black pixels in a cell divided by the total number of pixels of this cell. Therefore, the preprocessed signature $I'(x, y)$ is represented by a set of feature vectors $\mathcal{F} = \{\mathbf{F}_j\}, 1 \leq j \leq col$, where col is the number of columns in the grid. Other static features, such as pixel distribution and gravity center, as well as pseudo-dynamic features, such as axial slant and stroke curvature, have been extracted through this segmentation scheme (Justino, 2001; Justino et al., 2005).

2.1.2 Vector Quantization

In order to generate a sequence of discrete observations, each extracted feature vector is quantized as one of the previously-computed symbols of the codebook. The codebook may be generated through an iterative clustering algorithm called *K-means* (Makhoul et al., 1985). As explained by Algorithm 2.1, the feature vectors $\mathcal{F} = \{\mathbf{F}_j\}, 1 \leq j \leq col$, are separated into $\mathcal{N}$ clusters $\mathcal{U}_i$, $1 \leq i \leq \mathcal{N}$, where each cluster $\mathcal{U}_i$ represents a symbol in the the codebook.

Inputs:
– the set of feature vectors, $\mathcal{F} = \{\mathbf{F}_j\}, 1 \leq j \leq col$
– the number of centroids/clusters, $\mathcal{N}$
Outputs: the set of updated centroids, $cent_i$, $1 \leq i \leq \mathcal{N}$,

1: from the set of feature vectors $\mathcal{F}$, choose an initial set of $\mathcal{N}$ centroids $cent_i$
2: classify the feature vectors into the clusters $\mathcal{U}_i$ by using the nearest neighbor rule:

$$\mathbf{F}_j \in \mathcal{U}_i, \ iff \ dist(\mathbf{F}_j, cent_i) \leq dist(\mathbf{F}_j, cent_k), \ k \neq j, 1 \leq k \leq \mathcal{N}$$

3: update the centroid of each cluster by averaging its corresponding feature vectors
4: **if** the centroids have changed **then**
5: go to step 2
6: **end if**

Algorithm 2.1 *K-means* algorithm, where $\mathcal{U}_i$ is the i^{th} cluster with centroid $cent_i$.

2.1.3 Classification

Once the sequences of discrete observations are obtained, they are used to train and test the HMMs. A discrete HMM λ can be defined as $\lambda = (\mathbf{S}, \mathbf{M}, \mathcal{A}, \mathcal{B}, \pi)$, where (Rabiner, 1989):

1) $\mathcal{S}$ is the number of distinct states in the model. The set of states is denoted by $\mathbf{S} = \{\mathbf{S}_1, \mathbf{S}_2, ..., \mathbf{S_S}\}$, and s_t is the state at time t;

2) $\mathbf{M}$ is the alphabet size, that is, the number of distinct observation symbols per state. The set of symbols is denoted by $\mathbf{V} = \{v_1, v_2, ..., v_{\mathbf{M}}\}$;

3) $\mathcal{A}$ is the state transition probability distribution, denoted by $\mathcal{A} = \{a_{ij}\}$, where $a_{ij} = P\left[s_{t+1} = \mathbf{S}_j | s_t = \mathbf{S}_i\right]$, and $1 \leq i, j \leq \mathbf{S}$;

4) $\mathcal{B}$ is the observation symbol probability distribution, denoted by $\mathcal{B} = \{b_j(k)\}$, where $b_j(k) = P\left[v_k \; at \; t | s_t = \mathbf{S}_j\right]$, and $1 \leq k \leq \mathbf{M}, 1 \leq j \leq \mathbf{S}$;

5) and π is the initial state distribution, denoted by $\pi = \{\pi_i\}$, where $\pi_i = P\left[s_1 = S_i\right]$, and $1 \leq i \leq \mathbf{S}$.

HMMs can be classified in two main types of topologies (Rabiner, 1989): the *ergotic* and the *left-to-right* topologies, as depicted by Figure 2.3. The *ergotic* topology is a specific case of a fully-connected model in which every state can be reached from any other state in a finite number of steps. With the *left-to-right* topology, the state indices increase from left to right (that is, $a_{ij} = 0, j < i$), and no transitions are allowed to states whose indices are lower than the current state. As consequence, the sequence of observations must begin in $\mathbf{S}_1$ (that is, $\pi_i = 0$ when $i \neq 1$, and $\pi_i = 1$ when $i = 1$) and must end in $\mathbf{S}_N$. Often, the additional constraint $a_{ij} = 0, j > i + \Delta$ is used, where Δ is a value used as the limit of jumps. For instance, the *left-to-right* model illustrated in Figure 2.3 (b) has Δ = 2, which forbids jumps with more than 2 states.

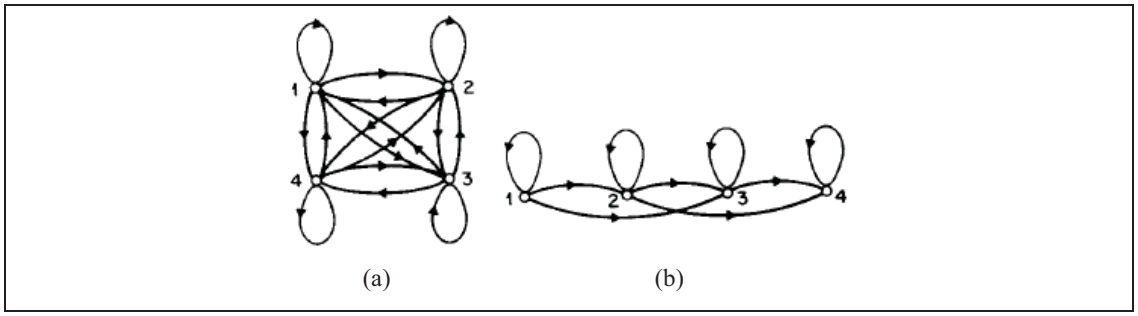

Figure 2.3 Examples of (a) 4-state *ergodic* model and (b) 4-state *left-to-right* model. Adapted from Rabiner (1989)

Given a model initialized according to the constraints described so far, there are three tasks of interest (Huang et al., 2001):

1) *The Evaluation Problem*. Given a model λ and a sequence of observations $\mathbf{O} = \{o_1, o_2, ..., o_L\}$, what is the probability of the model λ has generated the observation $\mathbf{O}$, that is, $P(\mathbf{O}|\lambda)$;

2) *The Decoding Problem*. Given a model λ, what is the most likely sequence of states $\mathbf{S} = \{\mathbf{S}_1, \mathbf{S}_2, ..., \mathbf{S_S}\}$ in the model that produces the sequence of observations $\mathbf{O} = \{o_1, o_2, ..., o_L\}$;

3) *The Learning Problem*. Given a model λ and a sequence of observations $\mathbf{O}$, how the model parameters can be adjusted so as to maximize the probability $P(\mathbf{O}|\lambda)$.

An advantage of the discrete HMMs is that it is not necessary to have *a priori* knowledge about the probability distributions to model a signal (Britto, 2001). With enough representative training data, it is possible to adjust the parameters for the HMM. Algorithms based on the expectation-maximization (E-M) technique (e.g., the Baum-Welch algorithm) are generally used to perform this task (Gotoh et al., 1998).

Typically, only genuine signatures are used for training an user-specific HMM for SV. In this case, the decision boundary between impostor and genuine spaces is defined by using a validation set that contains samples of both classes. Another particularity of HMM-based SV systems is the use of the *left-to-right* topology. Indeed, this topology is perfectly adapted to the dynamic characteristics of the occidental handwritten, in which the hand movements are always from left to right.

2.2 Challenges with the Single-Hypothesis Approach

In this work, it is assumed that the performance of the whole SV system is measured by an overall ROC curve obtained from a set of user-specific ROC curves. Averaging methods have been used to group ROC curves produced from different user-specific classifiers in single-hypothesis systems (Fawcett, 2006; Jain and Ross, 2002).

Jain and Ross (2002), for instance, proposed a method to generate an averaged ROC curve taking into account user-specific thresholds[1]. For each user i, the cumulative histogram of his/her random forgery scores (taken from a validation dataset) is computed. Then, the scores providing a same value of cumulative frequency, γ, are used as thresholds to compute the operating points $\{TPR_i(\gamma), FPR_i(\gamma)\}$. Finally, the operating points associated with a same γ (and related to different users) are averaged. Note that γ can be viewed as the True Negative Rate (TNR) (i.e., ratio of random forgeries correctly classified to the total of random forgeries) and that it may be associated with different thresholds. Fig. 2.4 shows an example where the thresholds associated with $\gamma = 0.3$ are different for users 1 and 2, that is $\tau_{user1}(0.3) \cong -5.6$ and $\tau_{user2}(0.3) \cong -6.4$.

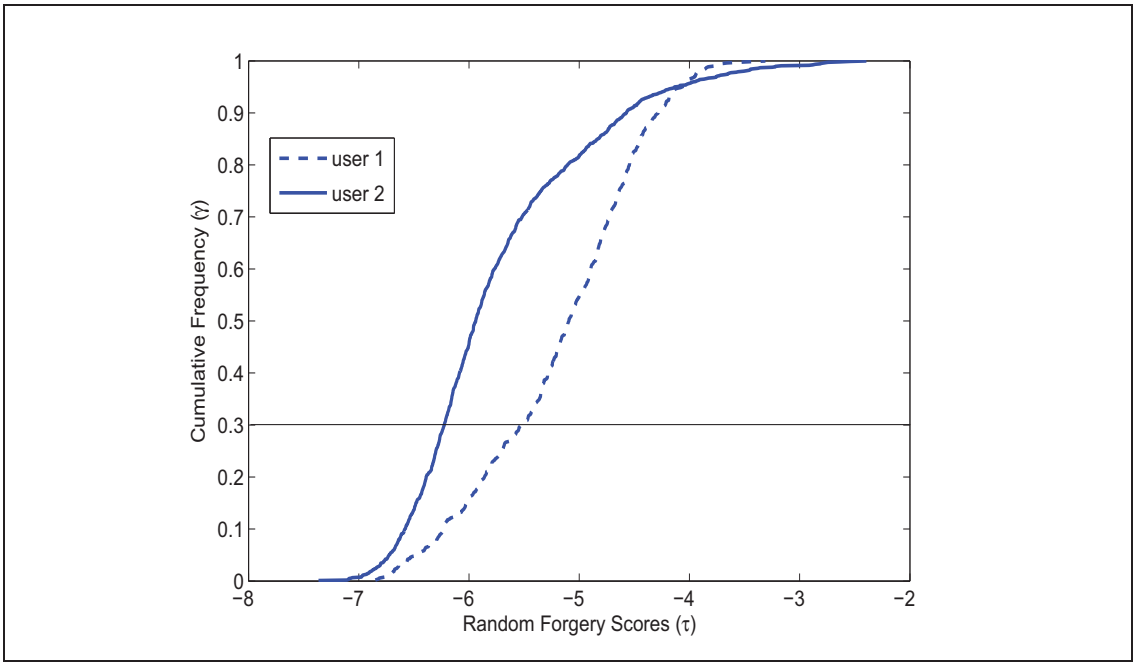

Figure 2.4 Cumulative histogram of random forgery scores regarding two different users in a single-hypothesis system. The horizontal line indicates that $\gamma = 0.3$ is associated to two different thresholds, that is, $\tau_{user1}(0.3) \cong -5.6$ and $\tau_{user2}(0.3) \cong -6.4$.

[1]Since biometric systems typically use a common threshold across users, Jain and Ross (Jain and Ross, 2002) have shown that it is possible to improve system performance by setting user-specific thresholds.

In off-line SV, where the dataset used to model a writer generally contains a reduced number of genuine samples against several random forgeries, it is common to obtain ROC curves with concave areas. In general, a concave area indicates that the ranking provided by the classifier in this region is worse than random (Flach and Wu, 2003). Figure 2.5 shows an example of score distribution in an off-line SV system. The positive class, P, contains only 10 genuine samples of a given writer, while the negative class, N, contains 100 samples of forgeries.

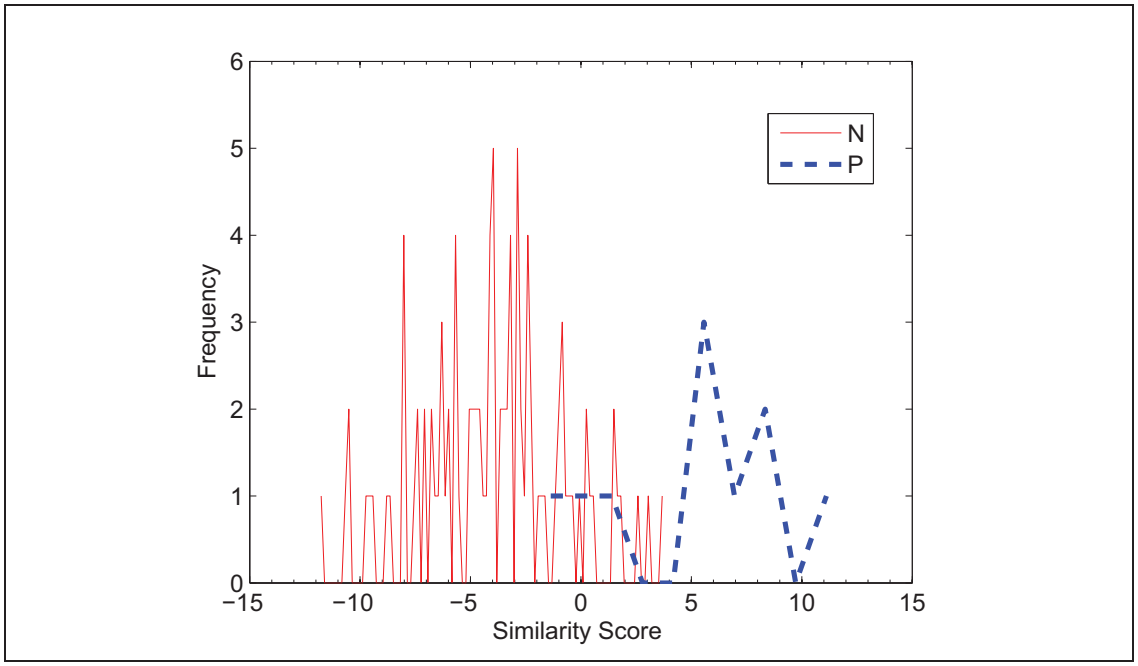

Figure 2.5 Typical score distribution of a writer, composed of 10 positive samples (genuine signatures) *vs.* 100 negative samples (forgeries).

Due to the limited amount of samples in the positive class, the resulting ROC curve (see Figure 2.6) presents three concave areas, which correspond to low-quality predictions (Flach and Wu, 2003). For example, the similarity scores between -1.2 and 0 provide $TPRs$ of 90%. The result of averaging the ROC curves related to the models of 100 different writers, by using the Ross's method, is illustrated by Figure 2.7. Note that the imperfections of individual

ROC curves are hidden within the average points, which can be observed with any averaging algorithm.

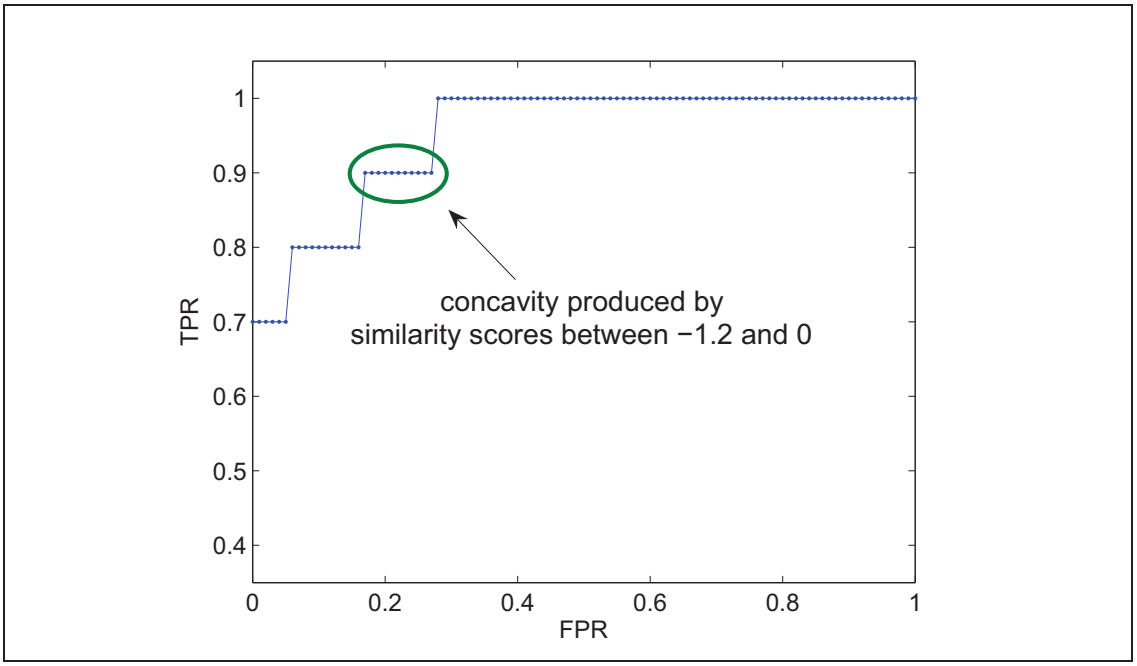

Figure 2.6 ROC curve with three concavities.

The drawback of using an averaged ROC curve can be observed during the selection of optimal thresholds in the respective convex hull. Given two γ in the convex hull, γ_1 and γ_2, where each one minimizes a different set of costs (Tortorella, 2005), γ_2 should provide a TPR higher than γ_1 whenever $\gamma_1 > \gamma_2$. However, regarding a user-specific ROC curve, γ_1 and γ_2 may fall in a same concave area, providing identical $TPRs$. An example is illustrated by Figure 2.7, where $TPR(\gamma = 0.86)$ is higher than $TPR(\gamma = 0.91)$ in the global convex hull, but, in the user-specific ROC curve, $TPR(\gamma = 0.86)$ is equal to $TPR(\gamma = 0.91)$.

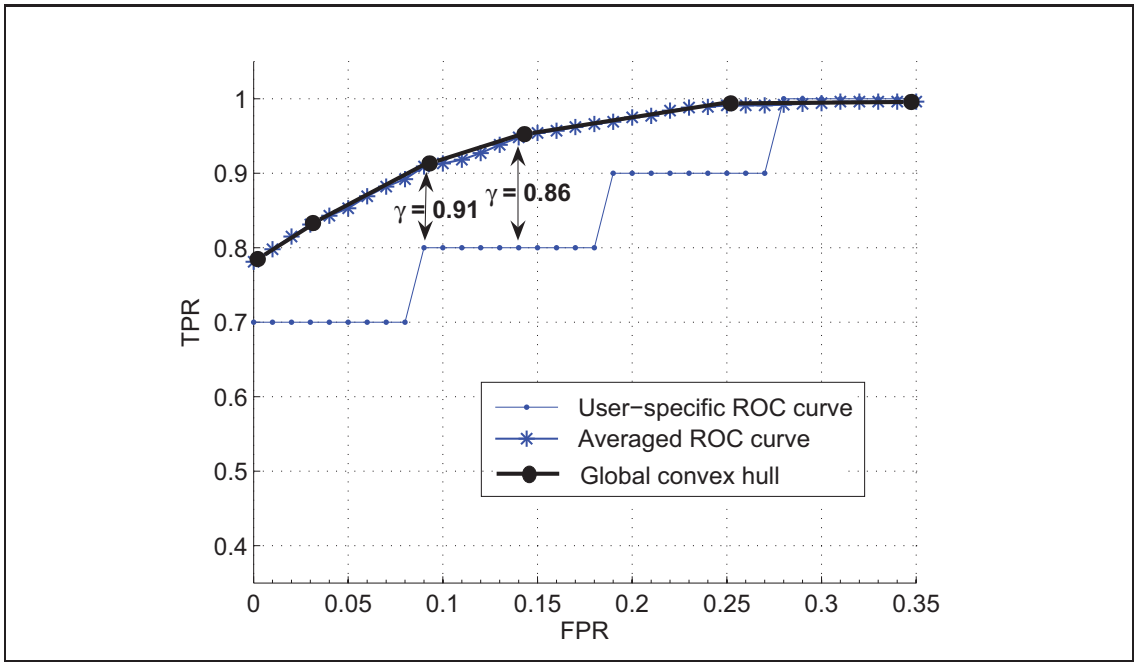

Figure 2.7 Averaged ROC curve obtained by applying the Ross's method to 100 different user-specific ROC curves.The global convex hull is composed of a set of optimal thresholds that minimize different classification costs. However, these thresholds may fall in concave areas of the user-specific ROC curves, as indicated by $\gamma = 0.91$ and $\gamma = 0.86$.

2.3 The Multi-Hypothesis Approach

Based on the combination of HMMs trained with different number of states, the approach proposed in this section provides a solution to repair concavities of user-specific ROC curves while generating a high quality averaged ROC curve. The utilization of different HMMs is motivated by the fact that the superiority of a classifier over another may not occur on the whole ROC space (Fawcett, 2006). Indeed, in off-line SV systems where the optimal number of states for a HMM is found empirically by a cross-validation process[2], it is often observed that the best HMM is not superior than the other intermediate/ sub-optimal HMMs in all operating points of the ROC space. Three steps are involved in the proposed multi- hypothesis approach: model selection, combination and averaging.

[2]Given a set of HMMs trained with different number of states, the cross-validation process selects the HMM providing the highest training probability (Justino et al., 2001; El-Yacoubi et al., 2000).

2.3.1 Model Selection

This step allows to select the best classifier for each operating point such that every writer's performance is optimized. In this work, a ROC outer boundary is constructed for each writer in order to encapsulate the best operating points provided by multiple HMMs, each one trained by using a different number of states. Given a set of ROC curves generated from different classifiers associated with a same writer, the process consists in splitting the *x axis* $\in [0, 1]$ into a number of bins, and within each bin finding the pair (FPR, TPR) having the largest value of TPR. While the ROC outer boundary is being generated, the best model HMM_j, where j is the number of states, is automatically chosen for each operating point. Figure 2.8 shows an example of a user-specific ROC outer boundary constructed from ROC curves of two different classifiers, HMM_7 and HMM_9. The corresponding convex hull is composed of three vertices, p, q and r, where p and q are associated with HMM_9, and r is associated with HMM_7.

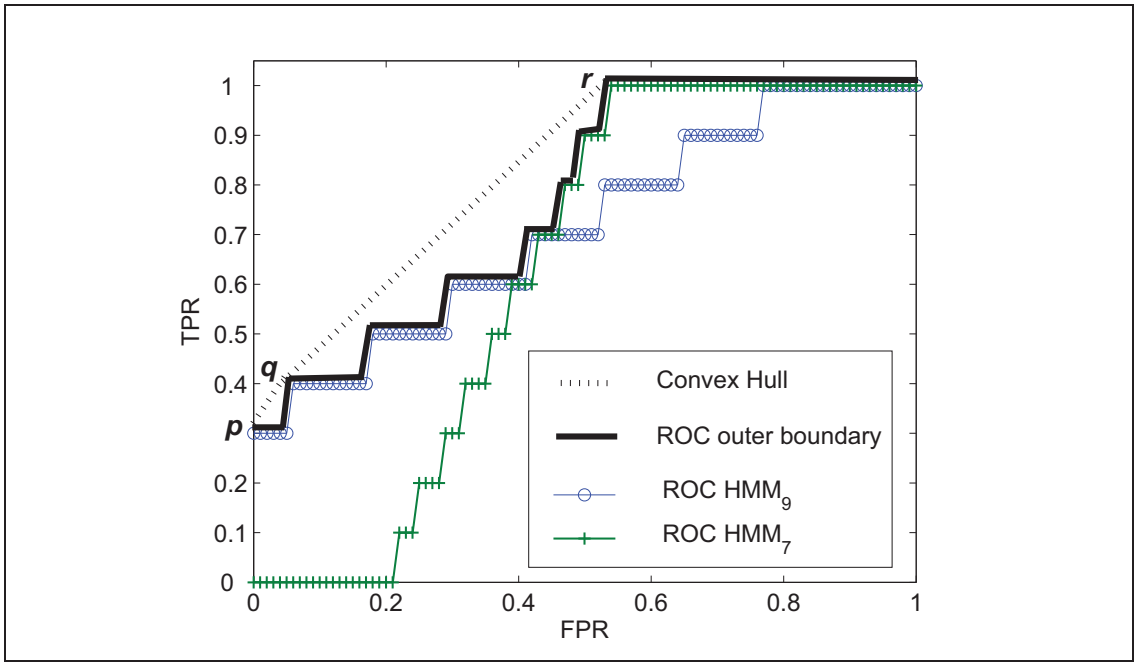

Figure 2.8 ROC outer boundary constructed from ROC curves of two different HMMs. Above $TPR = 0.7$, the operating points are taken from HMM_7, while below $TPR = 0.7$, the operating points correspond to HMM_9.

Algorithm 2.2 presents the approach for generating the outer boundary of ROC curves produced by training L_{min} HMMs on a same dataset but with different number of states; where L_{min} is the number of observations in the shorter training sequence.

Inputs: the training and validation sets
Outputs: the set of ROC outer boundaries

for each writer $i = 1, 2, ..., M$ **do**
  for each number of states $j = 2, 3, ..., L_{min}$ **do**
    train an HMM with j states
    calculate the ROC curve j by using the validation set
  end for
  for each bin $k \in [0, 1]$ **do**
    let $\lambda(k)$ be the classifier associated to the current bin
    set $TPR(k) \leftarrow 0$
    for each ROC curve j **do**
      if $TPR_j(k) > TPR(k)$ **then**
        $TPR(k) \leftarrow TPR_j(k)$
        $FPR(k) \leftarrow FPR_j(k)$
        $\lambda(k) \leftarrow HMM_j(k)$
      end if
    end for
  end for
  use the pairs $\{FPR(k), TPR(k)\}$ to generate the ROC outer boundary i
end for

Algorithm 2.2 Generating ROC outer boundaries from different HMMs.

Note that this process can also be extended for multiple codebooks. In other words, by training an ensemble of HMMs with different codebook sizes and different number of states, each bin can be associated with the pair {codebook, state} providing the highest TPR. Therefore, depending on the operating point, a same individual may use a different model, denoted as $HMM_j^{\mathcal{N}}$, trained with j states and with a codebook of $\mathcal{N}$ clusters.

2.3.2 Combination

This step allows to interpolate between two consecutive classifiers on the ROC curve in order to obtain not yet reached operating points. In this work, the method proposed by Scott et. al (Scott et al., 1998) is applied to the ROC outer boundaries in order to repair concavities. Given two vertices A and B on the convex hull, it is possible to realize a point C, located between A and B, by randomly choosing A or B. The probability of selecting one of the two operating points is determined by the distance of C regarding A and B (see Equations 2.1 and 2.2). The expected operating point (FPR_C, TPR_C) is given by Equations 2.3 and 2.4 (Scott et al., 1998).

$$\mathcal{P}(C = A) = (FPR_C - FPR_B)/(FPR_A - FPR_B) \tag{2.1}$$

$$\mathcal{P}(C = B) = 1 - \mathcal{P}(C = A) \tag{2.2}$$

$$FPR_C = (\mathcal{P}(C = A) \cdot FPR_A) + (\mathcal{P}(C = B) \cdot FPR_B) \tag{2.3}$$

$$TPR_C = (\mathcal{P}(C = A) \cdot TPR_A) + (\mathcal{P}(C = B) \cdot TPR_B) \tag{2.4}$$

By using the Equations 2.1 to 2.4, Algorithm 2.3 can realize any FPR_C located between two consecutive classifiers, A and B, where each classifier corresponds to a hull vertex of a user-specific ROC outer boundary. Figure 2.9 presents an example of a maximum realizable ROC (MRROC) curve.

2.3.3 Averaging

Finally, a process based on the Jain and Ross's method (Jain and Ross, 2002) is used to group the operating points already computed during the combination step. Given a γ, the Algorithm 2.4 searches the pairs $\{TPR_i(\gamma), FPR_i(\gamma)\}$ where $FPR_i(\gamma) = 1 - \gamma$ (recalling that γ can be

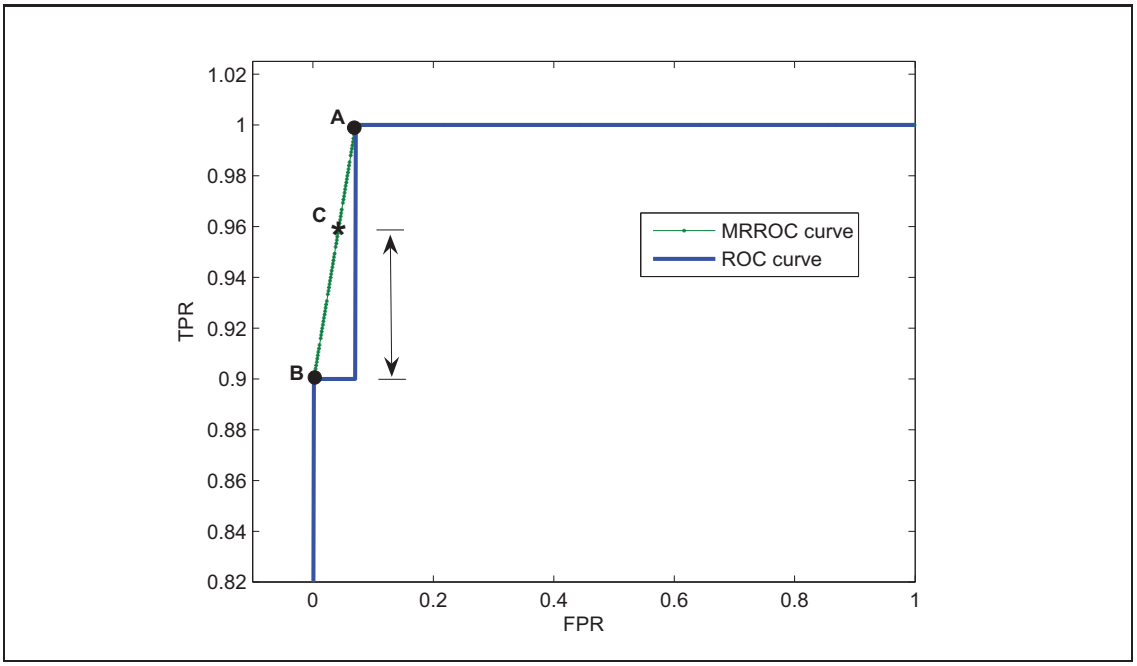

Figure 2.9 Example of MRROC curve. By using combination, any operating point C between A and B is realizable. In this example, for a same FPR, the TPR associated with C could be improved from 90% to 96%.

viewed as the TNR). Then, the operating points corresponding to a same γ are averaged and used to generate the averaged ROC curve.

2.3.4 Testing

During operations, γ is used to retrieve the set of user-specific HMMs/thresholds which will be applied on input samples. Figure 2.10 illustrates two possible situations linking the averaged ROC curve and a user-specific MRROC curve. In the first case, γ falls directly on HMM_7. Thus, the user-specific threshold associated to this γ will be used to classify the input samples. In the second case, the requested γ is obtained by combining classifiers HMM_7 and HMM_9. That is, each test sample must be randomly assigned to either HMM_7 or to HMM_9, according to the probabilities given by Equations 2.1 and 2.2. Note that a test sample is not assigned to both classifiers at the same time. However, if a fusion strategy is incorporated to the process,

Inputs: the set of ROC outer boundaries
Outputs: the set of MRROC curves

1: **for** each writer $i = 1, 2, ..., M$ **do**
2: **for** each $FPR_C \in [0, 1]$ **do**
3: find, in the convex hull of his/her ROC outer boundary, the pair of classifiers (A, B) able to realize FPR_C
4: calculate:
5: //the probability of A to be chosen (Eq. 2.1):

$$\mathcal{P}(A) \leftarrow \frac{(FPR_C - FPR_i(B))}{(FPR_i(A) - FPR_i(B))}$$

6: //the probability of B to be chosen (Eq. 2.2):

$$\mathcal{P}(B) \leftarrow 1 - \mathcal{P}(A)$$

7: //the expected operating points (Eqs. 2.3 and 2.4):

$$FPR_C \leftarrow (\mathcal{P}(A) \cdot FPR_i(A)) + (\mathcal{P}(B) \cdot FPR_i(B))$$

$$TPR_C \leftarrow (\mathcal{P}(A) \cdot TPR_i(A)) + (\mathcal{P}(B) \cdot TPR_i(B))$$

8: **end for**
9: use the pairs $\{FPR_C, TPR_C\}$ to generate the MRROC curve i
10: **end for**

Algorithm 2.3 Generating MRROC curves.

there are no restrictions to combine the decisions of both classifiers.

2.4 Experimental Methodology

Two types of codebook have been employed in off-line SV systems based on discrete HMMs: the *universal* codebook, shared by all writers enrolled to the system, and the *user-specific* codebook, adapted to a particular writer. However, as discussed before, these codebooks have typically been constructed by using the same data that are used to train the HMMs (Ferrer et al., 2005; Rigoll and Kosmala, 1998). Instead, this section investigates the use of an independent SV database to generate *universal* and *user-specific* codebooks. In both cases, the impact of applying the multi-hypothesis approach to improve the system performance is analysed.

Inputs: the set of MRROC curves
Outputs: the averaged ROC curve

1: **for** each value of $\gamma \in [0, 1]$ **do**
2: set $\{FPR(\gamma), TPR(\gamma)\} \leftarrow 0$
3: **for** each writer $i = 1, 2, ..., M$ **do**
4: find, in his/her MRROC curve, the operating point associated with γ, that is:

$$\{FPR_i(\gamma), TPR_i(\gamma)\} \,|FPR_i(\gamma) = 1 - \gamma$$

5: update $FPR(\gamma)$ and $TPR(\gamma)$ as:

$$FPR(\gamma) \leftarrow FPR(\gamma) + FPR_i(\gamma)$$

$$TPR(\gamma) \leftarrow TPR(\gamma) + TPR_i(\gamma)$$

6: **end for**
7: divide $FPR(\gamma)$ and $TPR(\gamma)$ by the number of writers M:

$$FPR(\gamma) \leftarrow FPR(\gamma)/M$$

$$TPR(\gamma) \leftarrow TPR(\gamma)/M$$

8: **end for**
9: use the pairs $\{FPR(\gamma), TPR(\gamma)\}$ to generate the averaged ROC curve

Algorithm 2.4 Generating the averaged ROC curve.

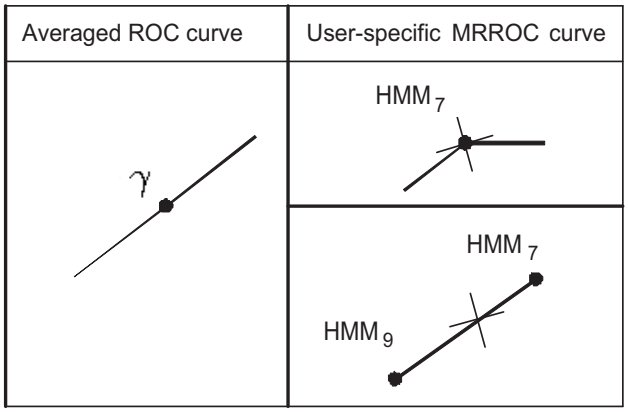

Figure 2.10 Retrieving user-specific HMMs from an averaged ROC curve.

The Brazilian signature database from PUCPR (Pontifícia Universidade Católica do Paraná) (Batista et al., 2010a, 2009; Bertolini et al., 2010; Justino et al., 2000), is used for proof-of-concept computer simulations. It contains 7920 samples of signatures that were digitized as 8-bit greyscale images over 400x1000 pixels, at resolution of 300 dpi. The signatures were provided by 168 writers and are organized as follows:

1) **The development database (DB_{dev}).** DB_{dev} is composed of 4320 genuine samples supplied by 108 writers, and is mostly used to construct *universal* codebooks. For each writer, there are 20 genuine samples for training, 10 genuine samples for validation and 10 genuine samples for test.

2) **The exploitation database (DB_{exp}).** DB_{exp} contains 60 writers, each one with 40 samples of genuine signatures, 10 samples of simple forgery and 10 samples of skilled forgery. For each writer, 20 genuine samples are used for training, 10 genuine samples for validation, and 30 samples for test (10 genuine samples, 10 simple forgeries and 10 skilled forgeries). Moreover, 10 genuine samples are randomly selected from the other 59 writers and used as random forgeries to test the current model. For ROC analysis, we use 10 genuine samples (from validation) *versus* 1080 random forgeries taken from DB_{dev} (i.e., 10 validation samples from 108 writers).

Given DB_{dev} and DB_{exp}, two experiments are performed:

1) *Off-line SV based on an universal codebook.* As proposed by Justino et al. (2000), an evaluation system is generated with DB_{dev} by trying different candidate codebooks obtained from this same dataset. Then, the codebook which performs the best in DB_{dev} is selected to develop the final system, that is, a system for the writers in DB_{exp}. This strategy assumes that if DB_{dev} is representative of the whole population, the codebook selected to represent this database will also work well for DB_{exp}.

2) *Off-line SV based on user-specific codebooks.* By using the same candidate codebooks of the previous experiment, the idea is to find, for each writer in DB_{exp}, the codebook which

the best adapts to his/ her individual characteristics. Thus, a same off-line SV system may work with multiple codebooks.

Therefore, while DB_{dev} is used to construct codebooks, as well as to develop evaluation SV systems, a DB_{exp} is employed for training, testing and validation of the final SV system. As mentioned, the use of DB_{dev} allows to construct codebooks earlier, with enough data, independently of the writers in DB_{exp}.

The greyscale signature images are converted to black and white using the Otsu's binarization method (Gonzalez and Woods, 2002). Then, they are represented by means of density of pixels, extracted through the same grid resolution described in Section 2.1. By trying different resolutions, Justino (2001) showed that the grid with 10 vertical cells (where each cell is a rectangle composed of 40x16 pixels) is the most suitable for the Brazilian SV database. This analysis was performed with DB_{dev}, that is, using signature samples from writers not enrolled to the system.

By varying the number of clusters from 10 to 150, in steps of 5, 29 candidate codebooks are obtained; where each one is constructed by using the first 30 signatures (training set + validation set) of each writer in DB_{dev}. In the first experiment, in order to select the universal codebook, an averaged ROC curve is produced for each different version of the evaluation system. Then, the codebook providing the averaged ROC curve with highest AUC is chosen. In the second experiment, the user-specific codebooks are selected before the averaging step; that is, by choosing the codebook providing the MRROC curve with highest AUC for each writer. Then, the individual MRROC curves are averaged. Since high values of FPR are rarely useful in real situations, the AUC may be calculated regarding a specific region of interest of the ROC space.

After codebook selection, an off-line SV system is designed for each writer enrolled to the system (i.e., using DB_{exp}). In the first experiment, a ROC outer boundary is obtained for each writer by using the same universal codebook and a set of HMMs trained with a different number of states. In the second experiment, a ROC outer boundary is obtained for each writer

by using his/her own codebook and a set of HMMs trained with a different number of states. Note that, in both experiments, the ROC curves are generated by using a validation set which contains only genuine samples and random forgeries.

Each HMM is trained by using the Baum-Welch forward-backward algorithm (Rabiner, 1989), and at each iteration t, a error measure $\mathcal{E}_t$ is calculated as:

$$\mathcal{E}_t = \frac{\mathcal{P}(\mathbf{O}/\lambda^{(t)}) - \mathcal{P}(\mathbf{O}/\lambda^{(t-1)})}{\mathcal{P}(\mathbf{O}/\lambda^{(t)}) + \mathcal{P}(\mathbf{O}/\lambda^{(t-1)})} \tag{2.5}$$

where $\mathcal{P}(\mathbf{O}/\lambda^{(t)})$ and $\mathcal{P}(\mathbf{O}/\lambda^{(t-1)})$ represent the joint probabilities of the training sequences $\mathbf{O}$ have been generated by the HMM λ in the instants t and $t-1$, respectively. The goal is to reach an error of 10^{-5} or smaller (Justino, 2001). Besides this stop criteria, the validation set is used in order to select the optimal training point before overfitting.

2.5 Simulation Results and Discussions

2.5.1 Off-line SV based on an universal codebook

In a first step, the multi-hypothesis approach (Algorithms 2.2 to 2.4) was applied for each one of the candidate codebooks by using the whole validation set. Among the 29 averaged ROC curves, the codebook of 35 clusters (CB_{35}) provided the highest AUC (i.e., 0.997). Figure 2.11 shows the averaged ROC curve and AUC associated with CB_{35}. Then, in order to confirm this result, 10 different averaged ROC curves were generated for each codebook by randomly selecting a subset of signatures in the validation set. Since there are much more random forgeries than genuine samples, only the forgery space was changed for each averaged ROC curve.

Figure 2.12 presents the relation between the Number of Clusters (NC) used in each codebook and the corresponding AUC, calculated on the entire averaged ROC space. This graphic confirms that the codebook with 35 clusters provides the highest $AUCs$ for this population. Moreover, the Kruskal-Wallis test (Gibbons, 1985) indicates that the AUC values corresponding to CB_{35} are significantly different to the data regarding any other codebook in the graphic.

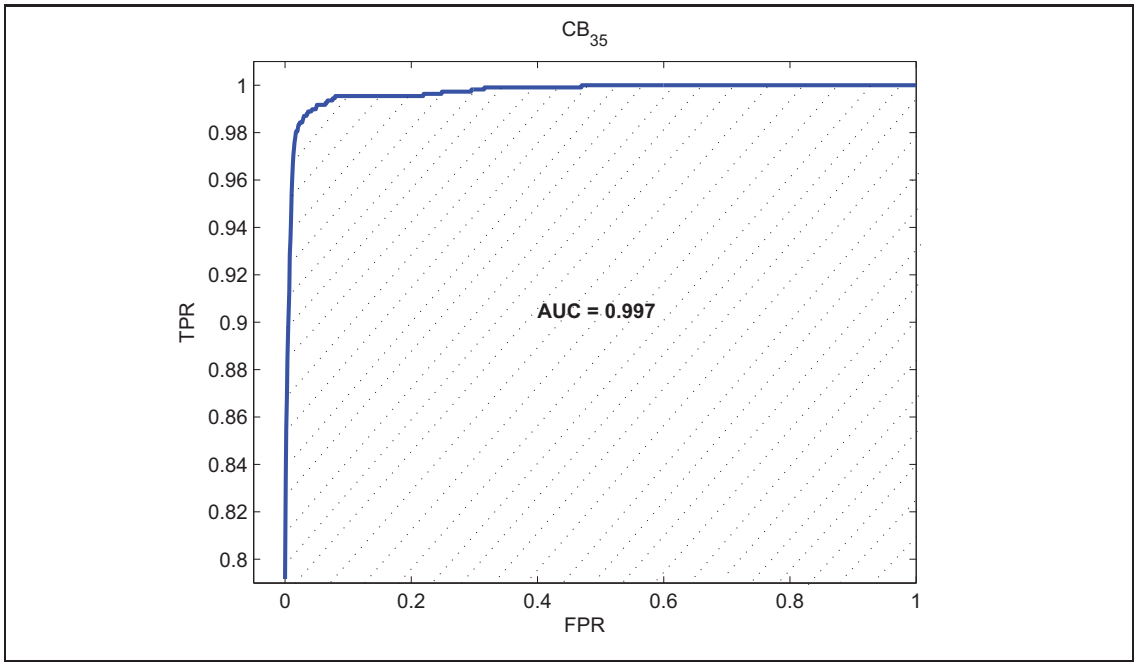

Figure 2.11 Composite ROC curve, with $AUC = 0.997$, provided by CB_{35} on the whole validation set of DB_{dev}.

The next step consisted of applying the codebook CB_{35} to DB_{exp}, which is composed of 60 writers. As expected, CB_{35} also performed well for this population, providing an AUC of 0.998 in the region of interest (i.e., between $FPR = 0$ and $FPR = 0.1$) of the averaged ROC space. The ROC curve of the multi-hypothesis system is indicated by the star-dashed line in Figure 2.13. Whereas the circle-dashed line represents the baseline or single-hypothesis system used for comparisons. In this system, only the HMM which performs the best in the cross-validation process (Justino et al., 2001; El-Yacoubi et al., 2000) is considered for generating a user-specific ROC curve. This means that all operating points of an individual ROC curve are associated with a same HMM. Moreover, the user-specific ROC curves are directly averaged, without repairing, by using the standard Ross's method (Jain and Ross, 2002) (see the inner graphic in Figure 2.13). As expected, the multi-hypothesis system provided a higher ROC curve, and, due to the Scott's method (Scott et al., 1998), a superior number of operating points was obtained.

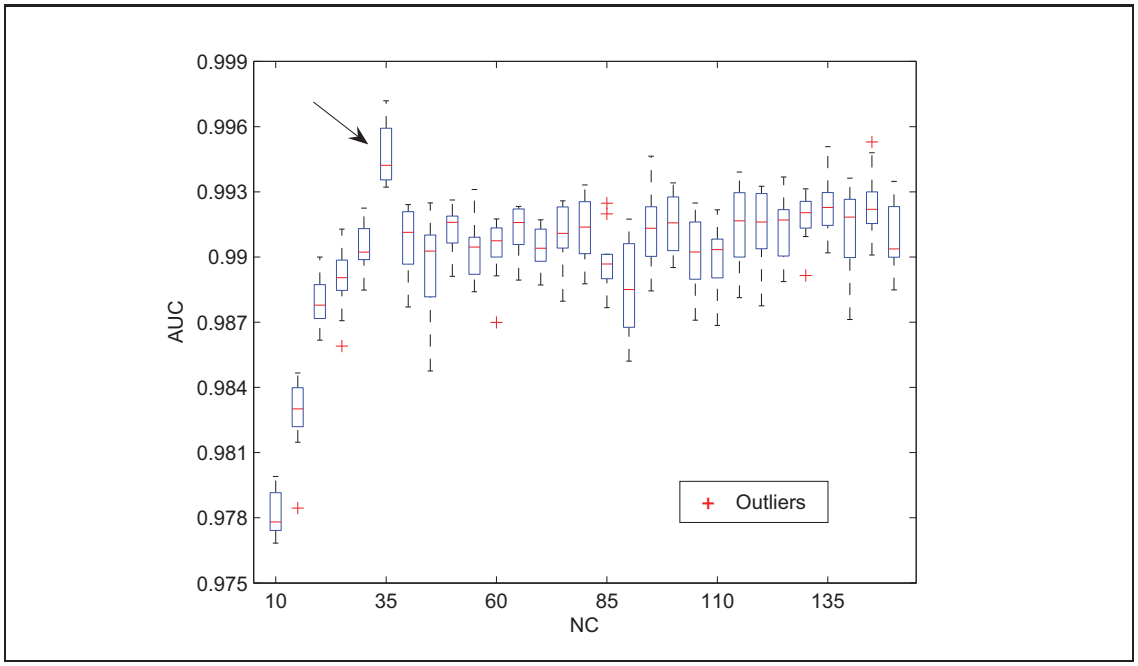

Figure 2.12 AUC (area under curve) *vs* NC (number of clusters). As indicated by the arrow, CB_{35} represents the best codebook for DB_{dev} over 10 averaged ROC curves generated with different validation subsets of DB_{dev}.

Depending on the operating point, a same writer could employ a different HMM, as shows Figure 2.14. It is worth noting that the complexity of the HMMs increases with the value of γ; which indicates that the operating points in the best region of the ROC space (i.e., the upper-left part) are achieved with a greater number of states.

Figure 2.15 shows the user-specific MRROC curves of two writers. While writer 1 employs different HMMs in the MRROC space, writer 3 uses the same HMM in all operating points. The fact that writer 3 obtained AUC=1 by using an HMM with only 2 states (i.e., HMM_2) indicates that his/her corresponding genuine and forgery spaces in the validation set are easily separable. In other words, high inter-class variability demands less complex models.

In the following phase, the operating points of the averaged ROC space (given by γ) were used to retrieve the user-specific HMMs/thresholds, and apply them to the test set. Table 2.1 presents the test set error rates for some γ values in both baseline and proposed systems. In order to ob-

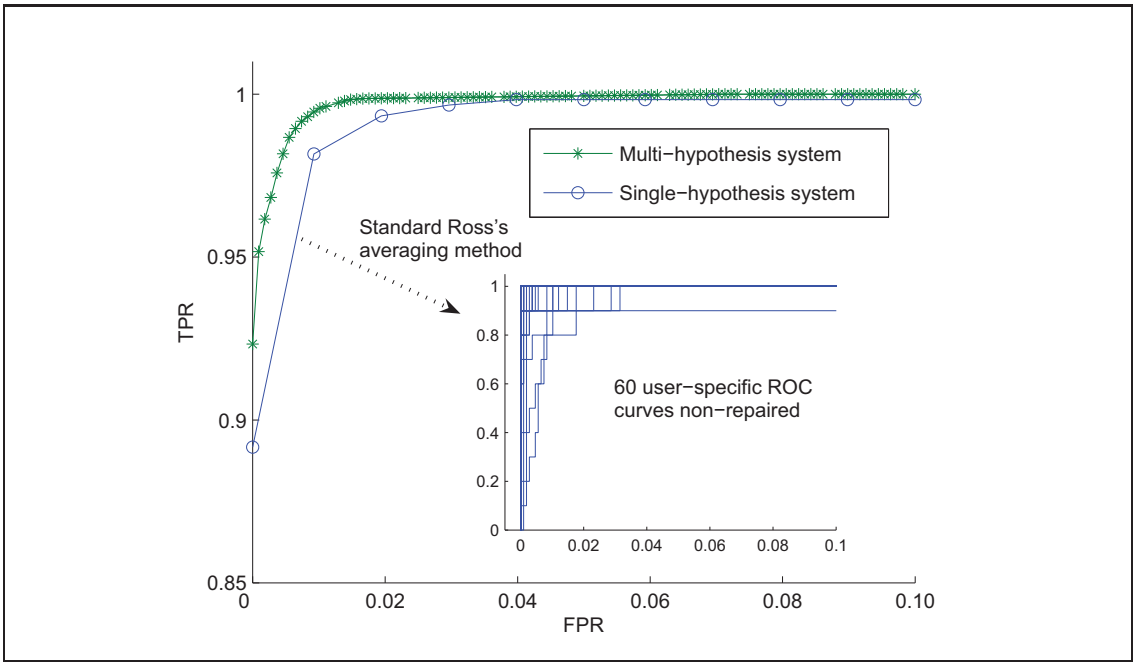

Figure 2.13 Averaged ROC curves when applying CB_{35} to DB_{exp}. Before using the Ross's averaging method, the proposed system used the steps of model selection and combination in order to obtain smoother user-specific ROC curves; while the baseline system directly averaged the 60 user-specific ROC curves, as shows the inner figure.

serve the impact on system performance at each step of the multi-hypothesis approach, results are first shown without the combination step (that is, by performing model selection followed by averaging), while the last results correspond to the whole multi-hypothesis approach. Since there are three types of forgeries in the test set, the average error rate is calculated as

$$AER(\gamma) = (FNR(\gamma) + FPR(\gamma)_{rand} + FPR(\gamma)_{simp} + FPR(\gamma)_{skil})/4 \tag{2.6}$$

Which is equivalent to consider equal *a priori* probabilities, that is, $P(genuine) = P(random) = P(simple) = P(skilled) = 0.25$, since the test set of each writer is composed of 10 samples per category of signature.

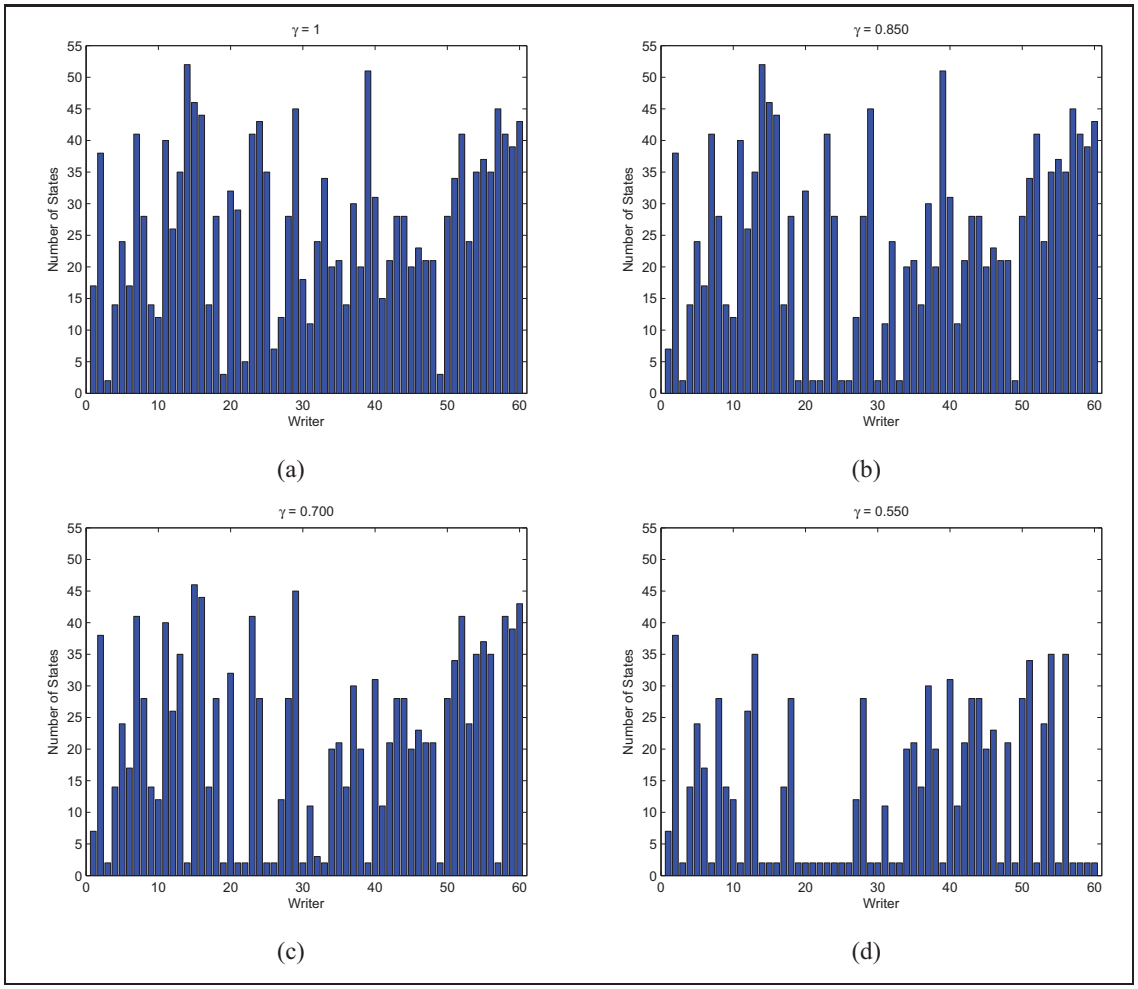

Figure 2.14 Number of HMM states used by different operating points in the averaged ROC space. The complexity of the HMMs increases with the value of γ, indicating that the operating points in the upper-left part of the ROC space are harder achieved. In other words, the best operating points are achieved with more number of states.

In general, the multi-hypothesis system provided smaller error rates. Moreover, the $FPR(\gamma)_{rand}$ are closer to the expected error rates given by 1-γ (recalling that γ can be viewed as the TNR, and that $FPR = 1 - TNR$). Additional results obtained with the multi-hypothesis system are presented in Table 2.2.

In order to analyze the impact of repairing individual ROC curves, the proposed approach was applied only to the 20 writers having ROC curves with concavities. On average, 75.91% of the

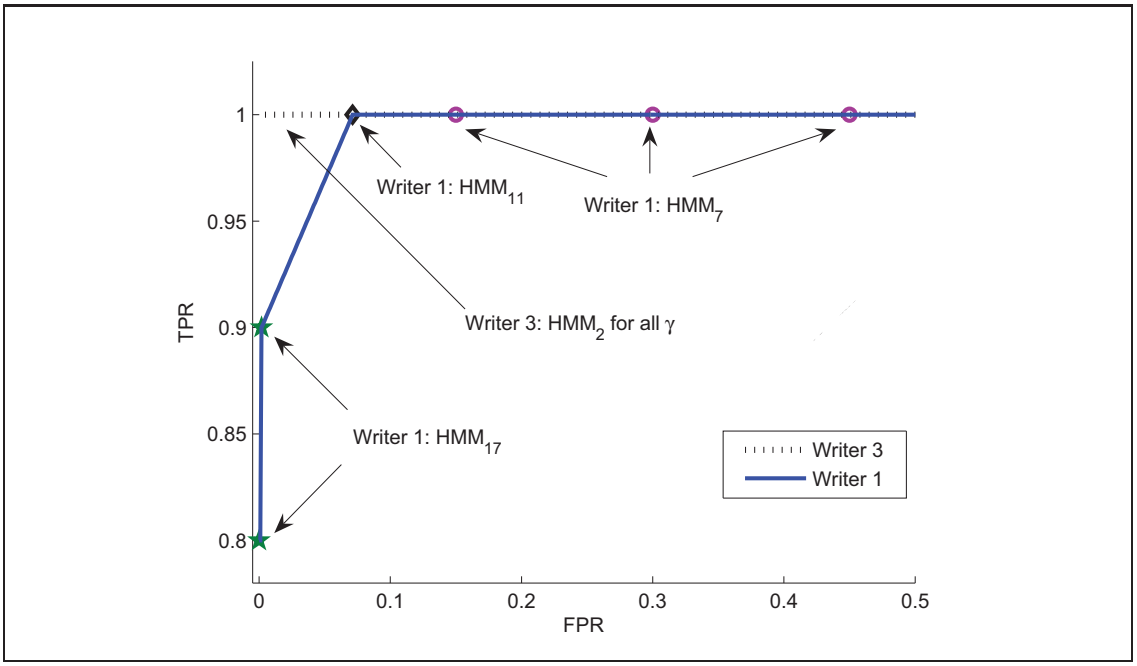

Figure 2.15 User-specific MRROC curves of two writers in DB_{exp}. While writer 1 can use HMMs with 7, 11, or 17 states depending on the operating point, writer 3 employs the same HMM all the time. Note that writer 3 obtained a curve with AUC = 1, which indicates a perfect separation between genuine signatures and random forgeries in the validation set.

problematic writers had their $AERs$ on test enhanced with the multi-hypothesis system in the region between $\gamma = 0.9$ and $\gamma = 1$; while 18.64% performed better with the single-hypothesis system. For the remaining 5.45%, both systems performed equally. Figure 2.16 presents the results for some γ values, where the improvements obtained with the multi-hypothesis system are located in the positive side, that is, below the dotted line. For instance, with the single-hypothesis system, the writer indicated by the arrow in (a) had an AER of 22.5%. When using the multi-hypothesis system, the respectiveAER was reduced to 4.9%, that is, 17.6% lower.

Finally, the multi-hypothesis system required fewer HMM states than the single-hypothesis system. Figure 2.17 shows the number of HMM states used by each writer in the single-hypothesis system. Note that these models, applied to all operating points, are more complex than those ones previously shown in Figure 2.14. Regarding the entire ROC space, the pro-

Table 2.1 Error rates (%) on test

Single-hypothesis system

γ	FNR	FPR_{random}	FPR_{simple}	$FPR_{skilled}$	AER
0.96	0.50	6.00	10.83	64.83	20.54
0.97	0.83	5.67	9.00	60.17	18.92
0.98	1.17	4.00	5.67	52.50	15.83
0.99	2.33	2.67	4.00	42.67	12.92
1	12.67	0.33	1.17	19.83	8.50

Multi-hypothesis system without combination

γ	FNR	FPR_{random}	FPR_{simple}	$FPR_{skilled}$	AER
0.96	3.17	5.17	11.00	62.33	20.42
0.97	3.33	4.17	9.33	58.50	18.83
0.98	3.83	1.83	6.67	51.17	15.88
0.99	5.00	1.17	4.17	41.17	12.88
1	12.83	0.33	1.17	20.50	8.71

Multi-hypothesis system

γ	FNR	FPR_{random}	FPR_{simple}	$FPR_{skilled}$	AER
0.96	4.13	4.67	8.70	54.81	18.07
0.97	4.15	3.17	7.35	52.23	16.72
0.98	4.48	2.50	5.51	47.05	14.88
0.99	5.55	1.17	4.00	39.63	12.58
1	12.83	0	1.17	20.50	8.62

Table 2.2 Additional error rates (%) on test obtained with the multi-hypothesis system

γ	FNR	FPR_{random}	FPR_{simple}	$FPR_{skilled}$	AER
0.991	5.71	1.00	3.83	38.01	12.13
0.992	5.81	0.67	3.83	37.38	11.92
0.993	6.00	0.67	3.50	36.15	11.58
0.994	6.17	0.67	3.50	35.90	11.56
0.995	6.30	0.67	3.17	34.80	11.23
0.996	7.10	0.67	2.67	33.73	11.04
0.997	7.63	0.67	2.67	32.48	10.86
0.998	8.21	0.67	2.67	30.60	10.54
0.999	9.37	0.17	1.91	26.83	9.57
1	12.83	0	1.17	20.50	8.62

posed approach reduced by 48.09% the number of states employed by the HMMs. This occurs because during the model selection step (see Algorithm 2.2), when two or more HMMs achieve the same TPR, the model with fewer states is chosen.

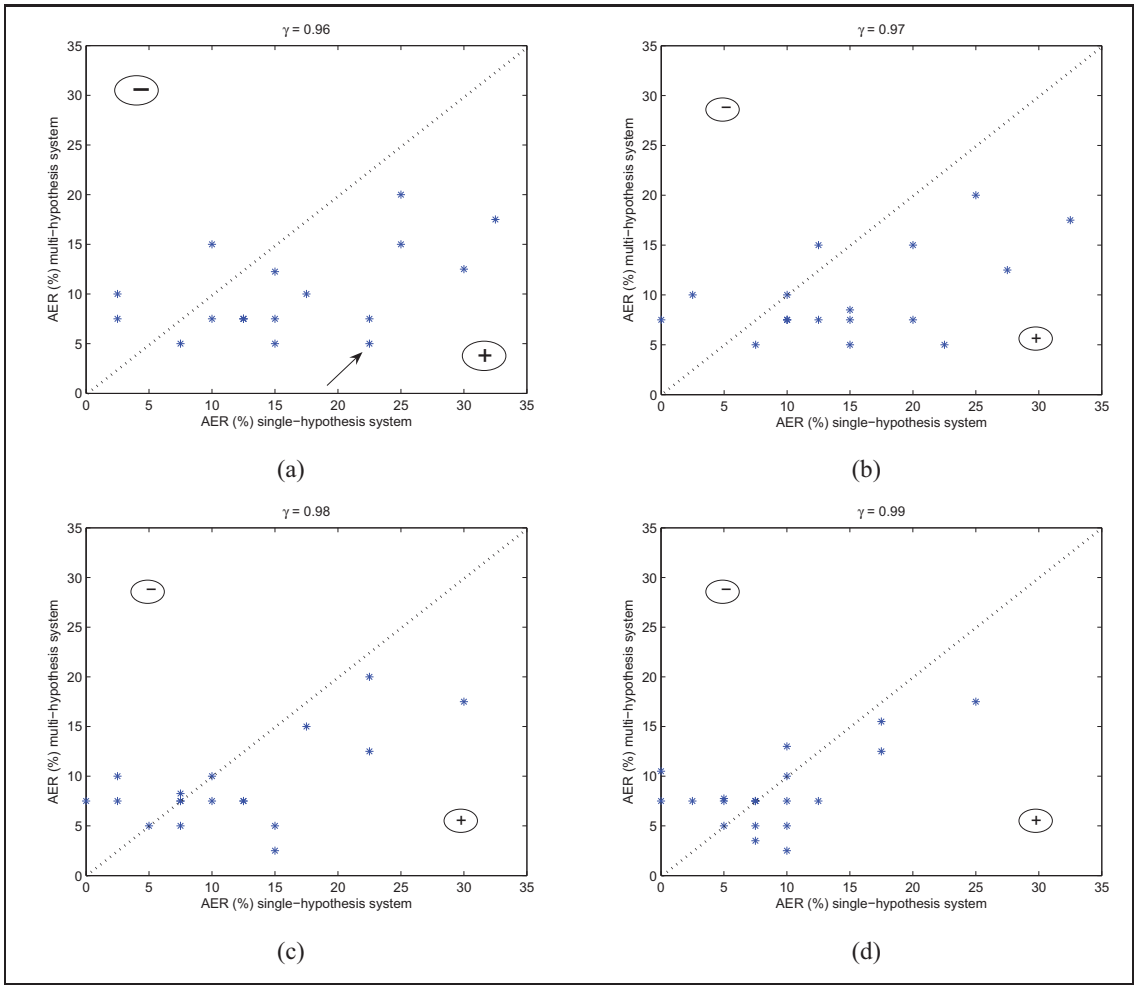

Figure 2.16 User-specific $AERs$ obtained on test with the single- and multi-hypothesis systems. The stars falling below the dotted lines represent the writers who improved their performances with multi-hypothesis system.

2.5.2 Off-line SV based on user-specific codebooks

This experiment explored the idea of using user-specific codebooks in order to reduce individual error rates. Since each writer must be evaluated separately, the selection of the best user-specific codebook was performed after the combination step, by choosing that one providing the MRROC curve with greatest AUC in the region of interest (i.e., between $FPR = 0$ and $FPR = 0.1$). Figure 2.18 (a) presents the codebook selected for each writer. For some

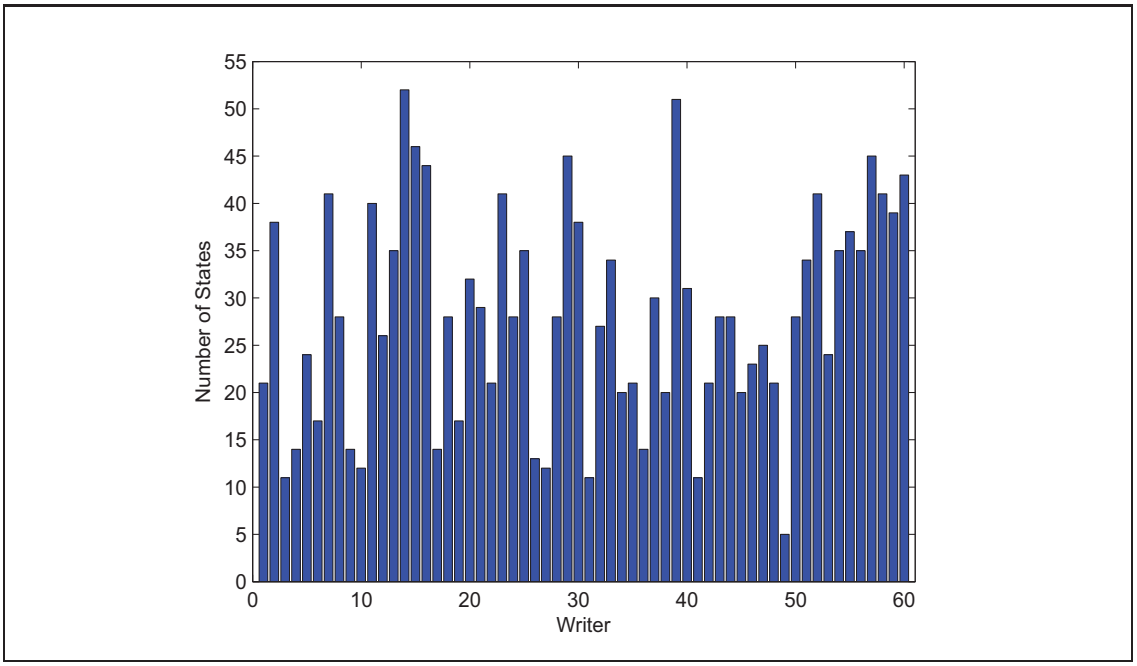

Figure 2.17 Number of HMM states selected by the cross-validation process in the single-hypothesis system. These models are used in all operating points of the ROC space.

writers, due to the high variability inter-class on validation (i.e., genuine signatures *versus* random forgeries), all codebooks provided AUC = 1. In these cases, the universal codebook CB_{35}, found in the previous experiment, was used. Figure 2.18 (b) indicates that only 13 codebooks (out of 29) were selected by this experiment; where 58% of the writers used the universal codebook CB_{35}, and 15% used a codebook with 150 clusters.

After selecting the best codebook per user, the user-specific MRROC curves were averaged by using Algorithm 2.4. The dash-dot line in Figure 2.19 shows the resulting averaged ROC curve (AUC = 0.9989), which is better than the curve obtained with the previous version of multi-hypothesis system (i.e., with CB_{35}) in the region between $\gamma = 0.995$ and $\gamma = 1$. This improvement was also observed on test, as shows Table 2.3; specially for $\gamma = 1$. The results for $\gamma = 0.96$ to 0.99 are not shown in Table 2.3 since both systems performed similarly for $\gamma < 0.995$. Figure 2.20 presents the $AERs$ of the 20 problematic writers obtained with the two multi-hypothesis systems. On average, 36.25% of these writers had their $AERs$ enhanced

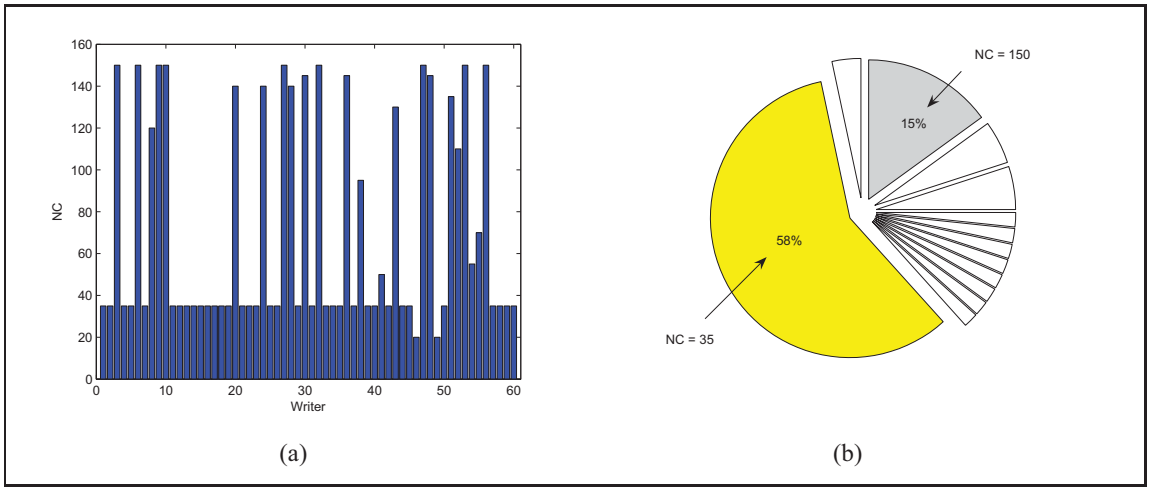

Figure 2.18 (a) Distribution of codebooks per writer. In the cases where all codebooks provided AUC = 1, the universal codebook CB_{35} was used. (b) Among the 13 codebooks selected by this experiment, CB_{35} was employed by 58% of the population, while 15% of the writers used a codebook with 150 clusters.

with the use of user-specific codebooks. This represents 12.08% of the whole population, which may indicate a considerable amount of users in a real world application. Only 16.25% performed better with CB_{35}; and for the remaining 47.50%, both systems performed equally.

Table 2.3 Error rates (%) on test

Results obtained with the multi-hypothesis system when using user-specific codebooks

γ	FNR	FPR_{random}	FPR_{simple}	$FPR_{skilled}$	AER
0.995	5.93	1.00	3.22	35.10	11.31
0.996	6.60	0.83	2.85	33.15	10.86
0.997	6.87	0.67	2.83	31.82	10.55
0.998	7.73	0.67	2.60	29.22	10.05
0.999	8.63	0.17	1.60	26.00	9.10
1	9.83	0	1.00	20.33	7.79

Results obtained with the multi-hypothesis system when using CB_{35}

γ	FNR	FPR_{random}	FPR_{simple}	$FPR_{skilled}$	AER
0.995	6.30	0.67	3.17	34.80	11.23
0.996	7.10	0.67	2.67	33.73	11.04
0.997	7.63	0.67	2.67	32.48	10.86
0.998	8.21	0.67	2.67	30.60	10.54
0.999	9.37	0.17	1.91	26.83	9.57
1	12.83	0	1.17	20.50	8.62

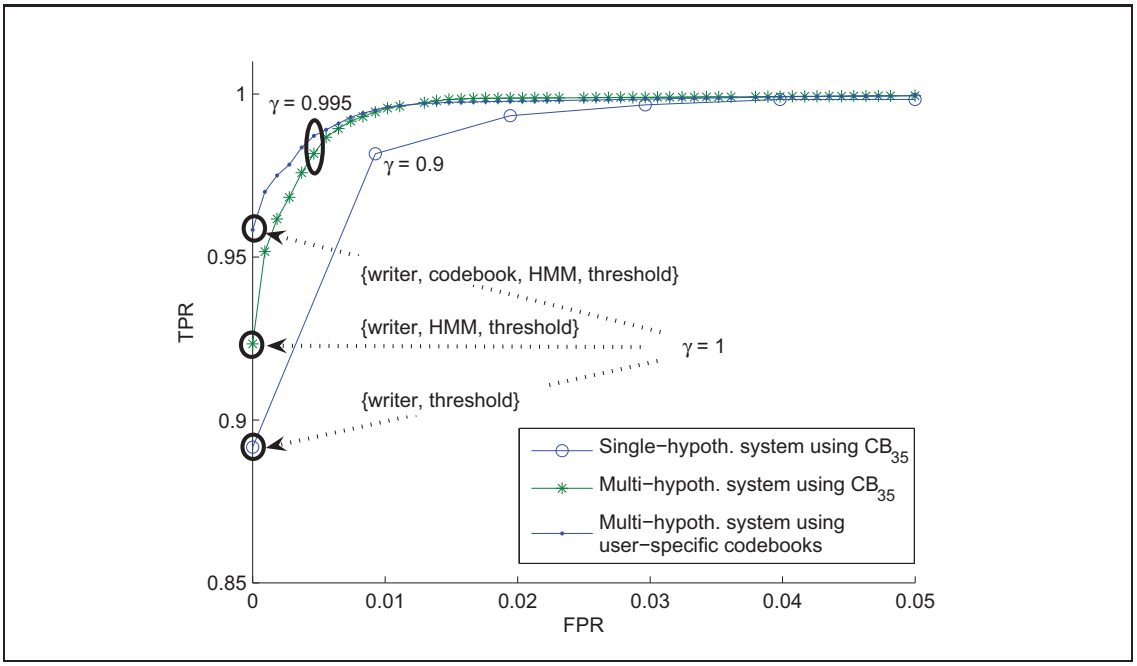

Figure 2.19 Averaged ROC curves obtained for three different systems, where the multi-hypothesis system with user-specific codebooks provided the greatest AUC. While the single-hypothesis system stores only the user-specific thresholds in the operating points, the multi-hypothesis systems can store information about user-specific thresholds, classifiers and codebooks in each operating point of the composite ROC curve.

Besides being used to retrieve the set of user-specific classifiers and thresholds, the operating points of the last multi-hypothesis system also stores information about what codebook to use; taking into account that a same codebook may be shared by different writers. In the single-hypothesis system, on the other hand, only the user-specific thresholds are stored, since each writer employs his/her single classifier in all operating points. It is worth noting that another variation of the proposed system could be developed by finding the best codebook at each operating point. However, since the 13 codebooks selected by this experiment already provided composite ROC curves with AUC equal or very close to 1, this approach was not investigated.

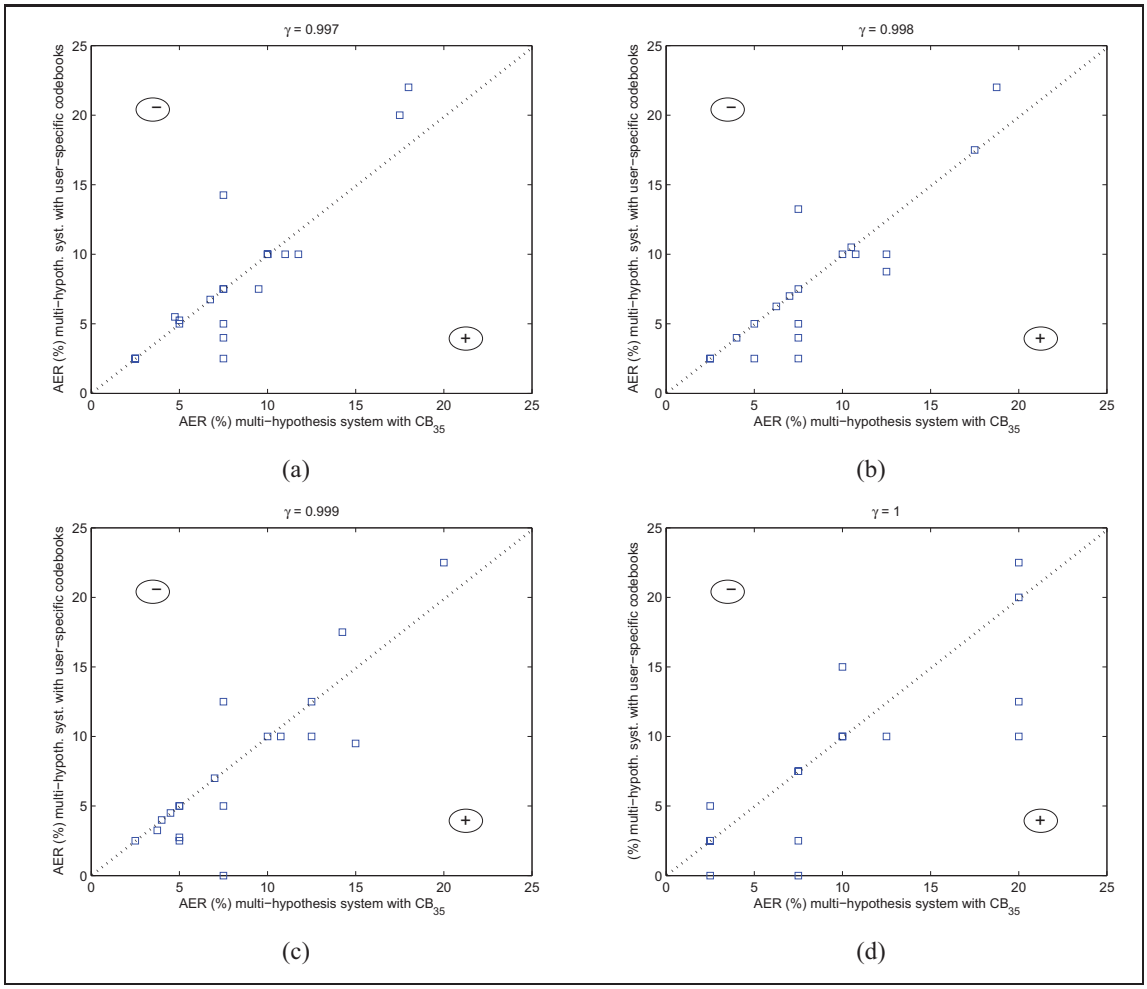

Figure 2.20 User-specific $AERs$ obtained on test with two versions of the multi-hypothesis system. The squares falling below the dotted lines represent the writers who improved their performances with multi-hypothesis system based on user-specific codebooks.

2.6 Discussion

In this chapter, an approach based on the combination of classifiers in the ROC space was proposed in order to improve performance of off-line SV systems designed from limited and unbalanced data. By training an ensemble of HMMs with different number of states and different codebooks, and then selecting the best model(s) for each operating point, it is possible

to construct a composite ROC curve that provides a more accurate estimation of system performance during training and significantly reduces the error rates during operations.

Experiments carried out on the Brazilian SV database, with random, simple and skilled forgeries, show that the multi-hypothesis approach leads to a significant improvement in overall performance, besides reducing the number of HMM states by up to 48%. The results also show that the use of user-specific codebooks can improve class separability.

Moreover, the multi-hypothesis system using an universal codebook obtained a considerable reduction in the number of codebook clusters and in the error rates[3] when comparing with another off-line SV system developed with the same SV database (Justino et al., 2001). Therefore, since ROC concavities are observed, the proposed approach is suitable to improve system performance. It can be easily adapted to any neural or statistical classifier designed to solve similar two-class problems. Of course, given a set of features able to provide adequate class separation, the multi-hypothesis approach would give no advantage.

The multi-hypothesis approach can be used for dynamic selection of the best classification model – that is, the best codebook, HMM and threshold – according to the risk linked to an input sample. In banking applications, for example, the decision to use a specific operating point may be associated with the amount of the check. In the simplest case, for a user that rarely signs high value checks, big amounts would require operating points related to low $FPRs$, such as would be provided by a γ close to 1; while lower amounts would require operating points related to low $FNRs$, since the user would not feel comfortable with frequent rejections. Note that, in the cases where a validation set is not available, the ROC curves may be generated by using the training set.

The proposed approach may require greater computational complexity (training time and memory consumption) than a single-hypothesis approach due to the generation of a set of candidate codebooks and HMMs. However, once the multi-hypothesis ROC space is obtained, all sub-

[3]Error rates reported in (Justino et al., 2001) with pixel density features: FNR = 2.17%, FPR_{random} = 1.23%, FPR_{simple} = 3.17%, $FPR_{skilled}$ = 36.57%, AER = 10.78%.

optimal solutions can be discarded, and only the HMMs associated with useful operating points should be stored. During the test phase, no additional time is required, since the process consists in the use of one HMM at a time.

Since HMMs are generative classifiers, they need more training data than discriminative classifiers to achieve a high level of performance. Indeed, while a generative classifier learns the full joint distribution of a class, i.e., a model of the joint probability $P(X|Y)$, of the inputs X and the label Y, a discriminative classifier models the decision boundary between class distributions by learning the posterior probability $P(Y|X)$ directly, or by learning a direct map from inputs X to the class labels (Drummond, 2006; Ng and Jordan, 2001). In this work, each HMM was built using 30 genuine signatures samples (i.e., 20 samples for training and 10 samples for validation), which is considered a limited set for a generative classifier. Other pattern recognition problems, such as handwritten character recognition, employ thousands of samples to train a HMM (Cavalin et al., 2009; Ko et al., 2009a,b). On the other hand, acquiring 30 signature samples per writer for designing a real-world SV system may be a costly and time consuming process. In the next chapter, a hybrid generative-discriminative SV system is proposed in order to take advantage of both classification paradigms. As both genuine and impostor classes are modeled, fewer training samples are needed to obtain satisfactory results.

CHAPTER 3

DYNAMIC SELECTION OF GENERATIVE-DISCRIMINATIVE ENSEMBLES

Since HMMs are generative classifiers, they need more training data than discriminative classifiers to achieve a high level of performance during operations. In this chapter, the problem of having a limited amount of genuine signature samples for training is addressed by designing a hybrid multi-classifier off-line SV system based on the dynamic selection of generative-discriminative ensembles. By taking advantage of both generative and discriminative classification paradigms, the objective is to achieve a more robust learning than a pure generative approach when a limited amount of training data is available.

To design the generative stage, multiple discrete *left-to-right* HMMs are trained using a different number of states and codebook sizes, allowing the system to learn signatures at different levels of perception. The codebooks are generated using signature samples of an independent database (also called development database), supplied by writers not enrolled to the SV system. This *prior* knowledge ensures that the SV system can be design even with a single user. To design the discriminative stage, HMM likelihoods are measured for each training signature, and assembled into feature vectors that are used to train a diversified pool of 2-Class Classifiers (2-CCs) through a specialized Random Subspace Method (RSM).

Given an input signature during operations, the most accurate subset of 2-CCs is selected to form an EoC using a Dynamic Selection (DS) strategy based on K-Nearest Oracles (KNORA) (Ko et al., 2008) and on Output Profile (OP) (Cavalin et al., 2010). As opposed to Static Selection (SS), where a single Ensemble of Classifiers (EoC) is selected before operations, and applied to all input samples, DS allows for a different selection of EoCs according to each input sample. Moreover, when new reference samples become available, they can be incorporated to the system, incrementally, to improve the selection of the most adequate EoC.

To validate the proposed SV system, proof-of-concept experiments are carried out on real-world signature data from two datasets, namely, the Brazilian SV database (Batista et al.,

2010a) (comprised of genuine samples and random, simple and skilled forgeries) and the GPDS database (Vargas et al., 2007) (comprised of genuine samples and random and skilled forgeries). The performance of the generative-discriminative ensembles formed with the proposed DS strategy is compared to that of other well-know DS and SS strategies, with a traditional system based on HMMs, and with other relevant SV systems found in the literature. Moreover, the adaptive properties of the proposed SV system for incremental learning of new signature samples are investigated.

The rest of this chapter is organized as follows. The next section briefly presents the state-of-the-art on hybrid generative-discriminative classifiers and on Ensemble of Classifiers. Section 3.2 presents the hybrid generative-discriminative off-line SV system, as well as the proposal of a new DS strategy. Section 3.3 describes the experimental methodology, including datasets, training protocol and measures used to evaluate system performance. The experiments are presented and discussed in Section 3.4. Finally, Section 3.5 concludes the chapter with a general discussion. The contents of this chapter have been publishedas conference articles in (Batista et al., 2010b) and (Batista et al., 2010c), accepted for publication in (Batista et al., 2011), and submitted to Pattern Recognition (december, 2010).

3.1 Hybrid Generative-Discriminative Ensembles

Generative classifers differ from discriminative ones in that they can reproduce an input pattern in addition to recognizing it. A generative classifier learns the full joint distribution of a class, i.e., a model of the joint probability $P(X|Y)$, of the inputs X and the label Y, and may generate labeled instances according to this distribution. Prediction is performed via the Bayes rule to compute $P(Y = y_j|X = x_i)$, and then by assigning x_i to the most likely y_j. In contrast, a discriminative classifier models the decision boundary between class distributions by learning the posterior probability $P(Y|X)$ directly, or by learning a direct map from inputs X to the class labels (Drummond, 2006; Ng and Jordan, 2001).

Despite the success of HMMs in SV, several important systems have been developed with discriminative classifiers (Batista et al., 2007; Impedovo and Pirlo, 2008). In fact, both generative and discriminative paradigms hold advantages and drawbacks. In classification problems, literature states that learning the full distribution $P(X|Y)$ is unnecessary. According to Vapnik (Vapnik, 1999), "one should solve the classification problem directly and never solve a more general problem as an intermediate step such as modeling $P(X|Y)$". Indeed, discriminative classifiers have been favored over generative ones in many pattern recognition problems due to their low asymptotic error (Abou-Moustafa et al., 2004), although comparisons between both paradigms have shown that a discriminative classifier does not necessarily yield better performance (Ng and Jordan, 2001; Rubinstein and Hastie, 1997). Moreover, generative classifiers may handle missing data (Raina et al., 2004), novelty detection, and supervised, unsupervised and incremental training more easily, since class densities are considered separately one from another (Rubinstein and Hastie, 1997). It is therefore easy to add and remove classes as the operational environment unfolds.

Some hybrid approaches found in literature appear promising to exploit both generative and discriminative paradigms. In the hybrid handwritten 10-digit recognition system proposed by Abou-Moustafa et al. (2004), a set of 20 discrete HMMs (two per class) is used to map the variable-lenght input patterns into single fixed-size likelihood vectors. In the classification stage, these vectors are presented to 10 SVMs (one per class) that provide the final decision through the one-against-all strategy. With a similar hybrid architecture, Bicego et al. (2004) proposed a system for 2D-shape/face recognition where each sample of a class is modeled by a continuous HMM. This type of architecture can be viewed as a dissimilarity representation (DR) approach, in which input patterns are described by their distance with respect to a predetermined set of prototypes (Pekalska and Duin, 2000, 2005). Therefore, while the HMMs model a set of prototypes, the likelihoods provide similarity measures that define a new input feature space. This new space of similarities can, in principle, be used to train any discriminative classifier. The fact that two patterns x_1 and x_2 present similar degrees of similarity with respect to several HMMs enforces the hypothesis that x_1 and x_2 belong to the same class

(Bicego et al., 2004). In a pure generative approach, an input pattern x_1 would be assigned to the most similar class model, neglecting all the information provided by a DR space (i.e., the distances with respect to the other classes).

The hybrid system achitectures presented in (Abou-Moustafa et al., 2004; Bicego et al., 2004) are particularly relevant for SV since they allow to model not only the genuine class, but also the impostor class. Traditional SV approches based on HMMs generally use only genuine signatures to train the system. Then, a decision threshold is defined by using a validation set composed of genuine and random forgery samples (in practice, only random forgeries are available during the design of a SV system).

Multi-Classifier Systems (MCS) have been used to reduce error rates of many challenging pattern recognition problems, including SV (Bajaj and Chaudhury, 1997; Bertolini et al., 2010; Blatzakis and Papamarkos, 2001; Huang and Yan, 2002; Sabourin and Genest, 1995; Sansone and Vento, 2000). The motivation of using MCS stems from the fact that different classifiers usually make different errors on different samples. Indeed, it has been shown that, when the response of a set of $\mathcal{C}$ classifiers is averaged, the variance contribution in the bias-variance decomposition decreases by $1/\mathcal{C}$, resulting in a smaller expected classification error (Tax, 2001; Tumer and Ghosh, 1996).

Bagging (Breiman, 1996), boosting (Freund, 1990) and random subspaces (Ho, 1998) are well-known methods for creating diverse classifiers. While bagging and boosting use different samples subsets to train different classifiers, the random subspace method (RSM) use different subspaces of the original input feature space. The RSM is, therefore, well-suited for generating a pool of classifiers in applications that must deal with a limited number of training samples. While many classification methods suffer from the curse of dimensionality, large amounts of features can be exploited by the RSM to improve the system performance (Ho, 1998).

Given a pool of classifiers, an important issue is the selection of a diversified subset of classifiers to form an EoC, such that the recognition rates are maximized during operations (Ko et al., 2008). This task may be performed either statically or dynamically. Given a set of reference

samples (generally not used to train the classifiers), a static selection (SS) approach selects the EoC that provides the best classification rates on that set. Then, this EoC is used during operations to classify any input sample. Dynamic selection (DS) also needs a reference set to select the best EoC; however, this task is performed on-line, by taking into account the specific characteristics of the sample to be classified. The KNORA strategy (Ko et al., 2008), for instance, finds for each input sample its K-nearest neighbors in the reference set, and then selects the classifiers that have correctly classified those neighbors. Finally, the selected classifiers are combined in order to classify the input sample.

In a biometric system that starts with a limited number of reference samples, it is difficult to define *a priori* a single best EoC for the application. Ideally, the EoC should be continuously adapted whenever new reference samples become available. With DS, this new data can be incorporated to the reference set (after being classified by the pool of classifiers) without any additional step.

3.2 A System for Dynamic Selection of Generative-Discriminative Ensembles

In this section, a hybrid generative-discriminative multi-classifier system is proposed for off-line SV. It consists of two stages – a generative stage that provides feature vectors for input patterns using a bank of HMMs; and a discriminative stage that classifies these feature vectors using an ensemble of two-class classifiers (2-CCs).

3.2.1 System Overview

Let $\mathcal{T}^i = I^i_{trn(l)}$, $1 \leq l \leq N$, be the training set used to design a SV system for writer i. $\mathcal{T}^i$ contains genuine signature samples supplied by writer i, as well as random forgery samples supplied by other writers not enrolled to the system (these random forgeries are part of a development database, and represent a *prior* knowledge of the problem). For each signature $I^i_{trn(l)}$, in the training set $\mathcal{T}^i$, a set of features is generated such as depicted in Figure 3.1. First, $I^i_{trn(l)}$ is described by means of pixel densities, which are extracted through a grid composed

of rectangular cells. Each column of cells j is converted into a feature vector $\mathbf{F}_j^i$, where each vector element is a value between 0 and 1 corresponding to the number of black pixels in a cell divided by the total number of pixels of this cell. The signature $I_{trn(l)}^i$ is therefore represented by a set of feature vectors $\boldsymbol{\mathcal{F}}_{\boldsymbol{trn(l)}}^{\boldsymbol{i}} = \left\{\mathbf{F}_{\boldsymbol{j}}^{\boldsymbol{i}}\right\}$, $1 \leq j \leq col$, where col is the number of columns in the grid.

Then, $\boldsymbol{\mathcal{F}}_{\boldsymbol{trn(l)}}^{\boldsymbol{i}}$ is quantized into a sequence of discrete observations $\mathbf{O}_{\boldsymbol{q}}^{\boldsymbol{i}} = \left\{o_j^i\right\}$, $1 \leq j \leq col$, where each observation o_j^i is a symbol provided by the codebook q (which is generated using the *K-means* algorithm (Makhoul et al., 1985)). As $\mathcal{Q}$ different codebooks are employed, a set of observation sequences $\boldsymbol{O}_{\boldsymbol{trn(l)}}^{\boldsymbol{i}} = \{\mathbf{O}_q^i\}$, $1 \leq q \leq \mathcal{Q}$, is obtained for a same training signature $I_{trn(l)}^i$. The set of observation sequences, $\boldsymbol{O}_{\boldsymbol{trn(l)}}^{\boldsymbol{i}}$, is then sent as input to the bank of *left-to-right* HMMs $\boldsymbol{\mathcal{M}}^{\boldsymbol{i}} = \{\lambda_b^i\}$, $1 \leq b \leq B$, from which a new feature vector $\mathbf{D}\left(\boldsymbol{O}_{\boldsymbol{trn(l)}}^{\boldsymbol{i}}, \boldsymbol{\mathcal{M}}^{\boldsymbol{i}}\right)$ is extracted. Each vector element in $\mathbf{D}\left(\boldsymbol{O}_{\boldsymbol{trn(l)}}^{\boldsymbol{i}}, \boldsymbol{\mathcal{M}}^{\boldsymbol{i}}\right)$ is a likelihood P_b computed between an observation sequence $\mathbf{O}_q^i$ and a HMM λ_b^i, where λ_b^i can be either from the genuine class (i.e., trained with genuine samples from writer i), or from the impostor class (i.e., trained with random forgery samples). It is worth noting that the same sequences $\boldsymbol{O}_{\boldsymbol{trn(l)}}^{\boldsymbol{i}}$, $1 \leq l \leq N$, used to obtain the HMM likelihood vectors, $\mathbf{D}\left(\boldsymbol{O}_{\boldsymbol{trn(l)}}^{\boldsymbol{i}}, \boldsymbol{\mathcal{M}}^{\boldsymbol{i}}\right)$, $1 \leq l \leq N$, are also used to train the HMMs in $\boldsymbol{\mathcal{M}}^{\boldsymbol{i}}$.

Since long HMM likelihood vectors are produced during the feature generation phase, a specialized random subspace method (RSM) is used to select the input space in which multiple discriminative 2-CCs are trained. For each random subspace r, $1 \leq r \leq \mathcal{R}$, a smaller subset of likelihoods is randomly selected, with replacement, from $\mathbf{D}\left(\boldsymbol{O}_{\boldsymbol{trn(l)}}^{\boldsymbol{i}}, \boldsymbol{\mathcal{M}}^{\boldsymbol{i}}\right)$, $1 \leq l \leq N$, and used to train a different 2-CC. As depicted in Figure 3.2, $\mathcal{R}$ random subspaces result in $\mathcal{R}$ different 2-CCs.

During operations (see Figure 3.3), a given input signature I_{tst}^i follows the same steps of feature extraction, vector quantization and likelihood extraction as performed with a training signature, resulting in the HMM likelihood vector $\mathbf{D}\left(\boldsymbol{O}_{\boldsymbol{tst}}^{\boldsymbol{i}}, \boldsymbol{\mathcal{M}}^{\boldsymbol{i}}\right)$. Then, based on signature samples previously classified – stored on the dynamic selection (DS) database –, the most accurate

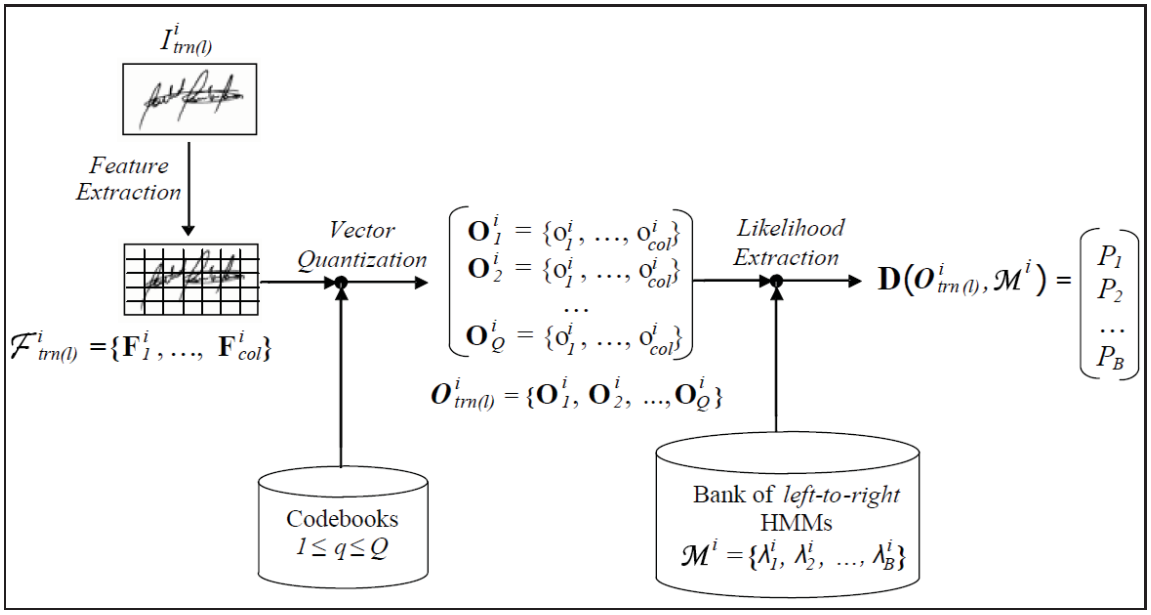

Figure 3.1 Design of the generative stage for a specific writer i.

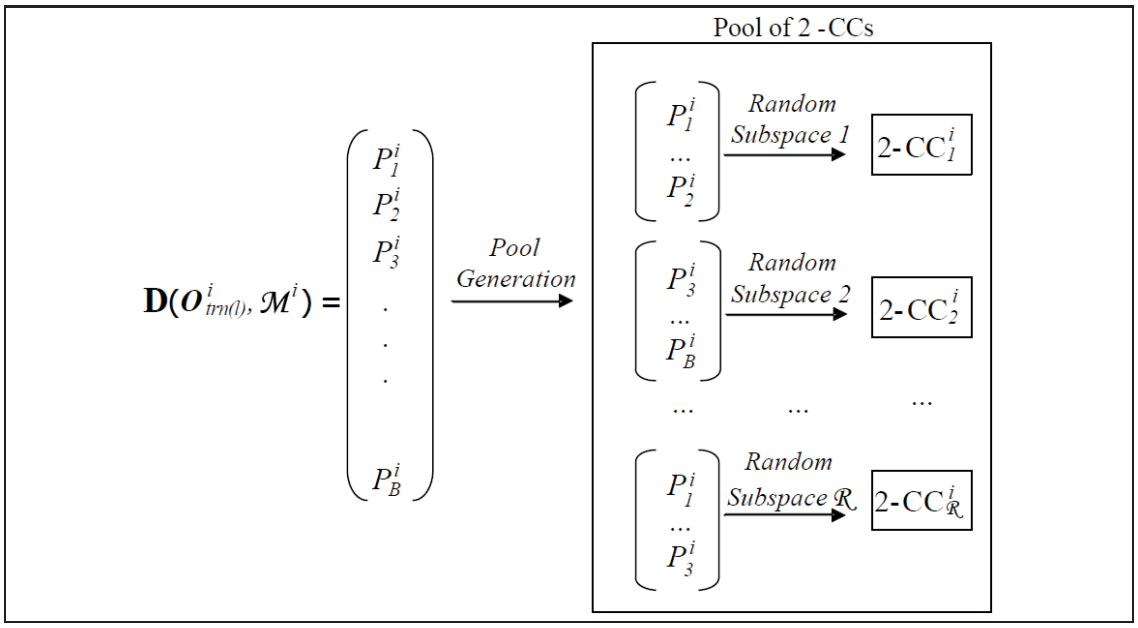

Figure 3.2 Design of the discriminative stage for a specific writer i.

ensemble of 2-CCs is dynamically selected and used to classify $\mathbf{D}\left(\boldsymbol{O}_{\boldsymbol{tst}}^{\boldsymbol{i}}, \boldsymbol{\mathcal{M}}^{\boldsymbol{i}}\right)$. Such as the training set, the DS database contains genuine signature samples supplied by writer i, as well as random forgery samples taken from the developement database. Section 3.3 explains the partitioning of each dataset used in this work.

The dynamic selection strategy proposed in this work is based on the K-nearest-oracles (KNORA) (briefly described in Section 3.1), which has been successfully applied to handwritten-numeral recognition (Ko et al., 2008). The main drawback of KNORA is that a robust set of features must be defined in order to compute similarity between the input sample and the samples in the DS database. As an alternative, the strategy proposed in this work inputs vector $\mathbf{D}\left(\boldsymbol{O}_{\boldsymbol{tst}}^{\boldsymbol{i}}, \boldsymbol{\mathcal{M}}^{\boldsymbol{i}}\right)$ to all 2-CCs in the pool, and the resulting output labels are used to find the K-nearest neighbors in the DS database. Then, the 2-CCs that have correctly classified those neighbors are selected to classify $\mathbf{D}\left(\boldsymbol{O}_{\boldsymbol{tst}}^{\boldsymbol{i}}, \boldsymbol{\mathcal{M}}^{\boldsymbol{i}}\right)$.

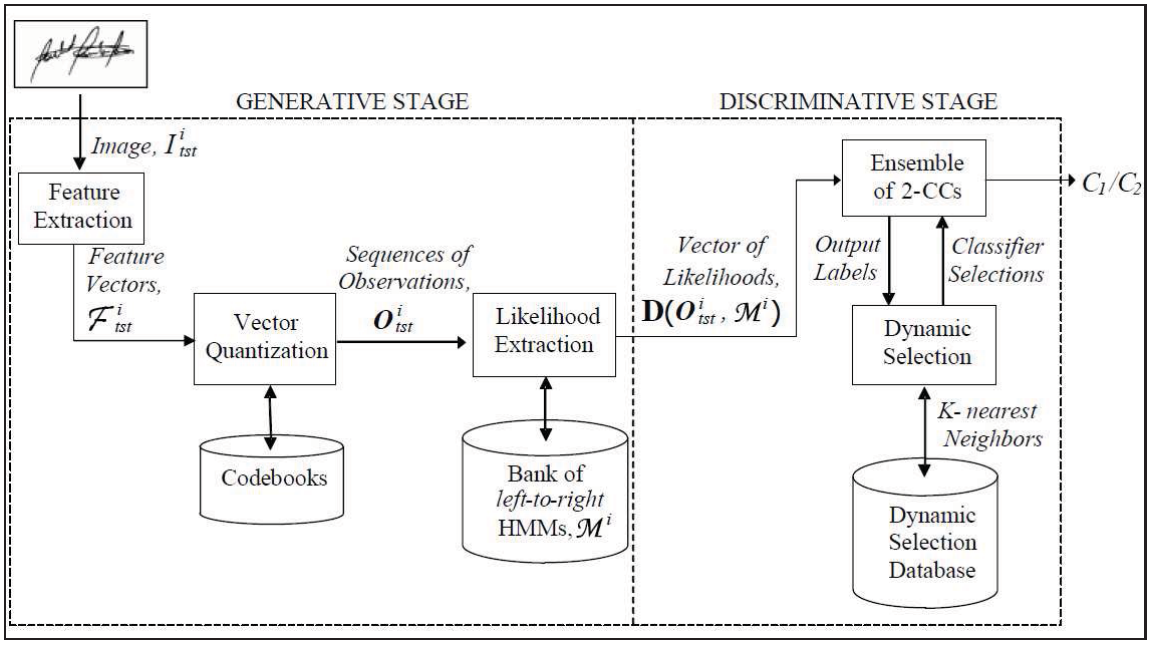

Figure 3.3 Entire hybrid generative-discriminative system employed during operations (for a specific writer i).

The rest of this section presents additional details on the bank of HMMs, the specialized algorithms to generate random subspaces and to perform dynamic selection of classifiers, and a complexity analysis of different components of the system.

3.2.2 Bank of HMMs

Let $\boldsymbol{\mathcal{M}^i} = \{\boldsymbol{w_1} \cup \boldsymbol{w_2}\}$ be the bank of *left-to-right* HMMs, where $\boldsymbol{w_1} = \{\lambda_1^{(C_1)}, \lambda_2^{(C_1)}, ..., \lambda_R^{(C_1)}\}$ is the set of R HMMs of the genuine class C_1, and $\boldsymbol{w_2} = \{\lambda_1^{(C_2)}, \lambda_2^{(C_2)}, ..., \lambda_S^{(C_2)}\}$ is the set of S HMMs of the impostor's class C_2. Each HMM in $\boldsymbol{w_1}$ is trained on genuine signature sequences of a specific writer i by using a different number of states. In a similar manner, the HMMs in $\boldsymbol{w_2}$ are trained on random forgery sequences, that is, genuine signature sequences from writers not enrolled to the system. Besides the different number of states, different codebooks are used, allowing the system to learn a signature at different levels of perception. Section 3.3.3 presents the training strategy adopted for the HMMs.

Once the bank $\mathcal{M}^i$ is obtained, it is used to extract likelihood vectors (see Figure 3.4). Given the set of observation sequences $\boldsymbol{O^i_{trn(l)}} = \{\mathbf{O}_1^i, \mathbf{O}_2^i, ..., \mathbf{O}_Q^i\}$ extracted from a training signature $I^i_{trn(l)}$, the vector $\mathbf{D}\left(\boldsymbol{O^i_{trn(l)}}, \boldsymbol{\mathcal{M}^i}\right)$ is obtained by computing the likelihoods of $\boldsymbol{O^i_{trn(l)}}$ for each HMM in $\boldsymbol{\mathcal{M}^i}$, that is,

$$\mathbf{D}\left(\boldsymbol{O^i_{trn(l)}}, \boldsymbol{\mathcal{M}^i}\right) = \begin{bmatrix} P(\mathbf{O}_q^i/\lambda_1^{(C_1)}) \\ P(\mathbf{O}_q^i/\lambda_2^{(C_1)}) \\ ... \\ P(\mathbf{O}_q^i/\lambda_S^{(C_2)}) \end{bmatrix} \tag{3.1}$$

If, for instance, $\lambda_1^{(C_1)}$ and $\lambda_S^{(C_2)}$ were trained with observation sequences extracted from the codebook $q = 10$, a compatible sequence from $\boldsymbol{O^i_{trn(l)}}$, that is, $\mathbf{O}^i_{q=10}$, must be sent to both. Finally, the vector $\mathbf{D}\left(\boldsymbol{O^i_{trn(l)}}, \boldsymbol{\mathcal{M}^i}\right)$ is labeled according to the class of $\boldsymbol{O^i_{trn(l)}}$. Observe that, if $\boldsymbol{O^i_{trn(l)}}$ belongs to class C_1, $\mathbf{D}\left(\boldsymbol{O^i_{trn(l)}}, \boldsymbol{\mathcal{M}^i}\right)$ should contain higher values in the first R positions and lower values in the remaining S positions, allowing a two-class classifier to discriminate between classes C_1 and C_2.

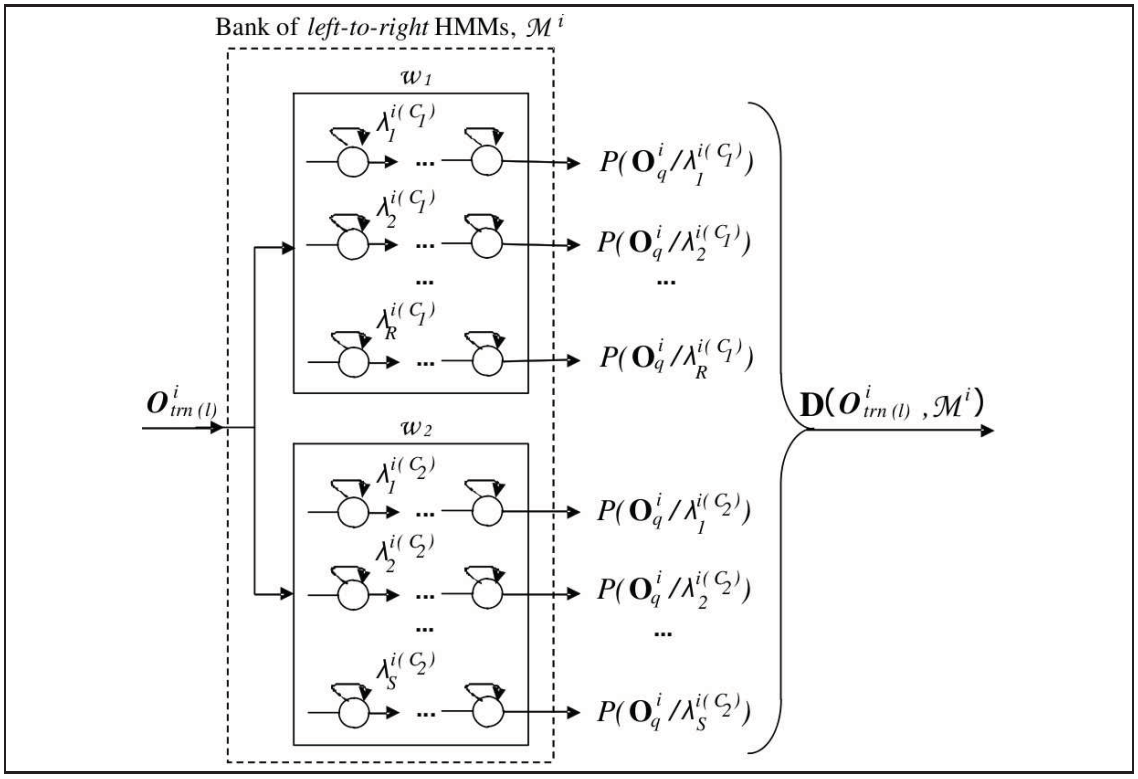

Figure 3.4 Bank of *left-to-right* HMMs used to extract a vector of likelihoods.

This procedure is performed on all $\boldsymbol{O}^{\boldsymbol{i}}_{\boldsymbol{trn}(\boldsymbol{l})}$, $1 \leq l \leq N$, and the resulting likelihood vectors $\mathbf{D}\left(\boldsymbol{O}^{\boldsymbol{i}}_{\boldsymbol{trn}(\boldsymbol{l})}, \boldsymbol{\mathcal{M}}^{\boldsymbol{i}}\right)$, $1 \leq l \leq N$, are used to train a pool of 2-CCs in the discriminative stage.

3.2.3 A Random Subspace Method for Two-Class Classifiers

Let $\boldsymbol{O}^{\boldsymbol{i}}_{\boldsymbol{trn}(\boldsymbol{l})}$, $1 \leq l \leq N$, be the sequences of observations extracted from the training signatures of writer i and $\mathbf{D}\left(\boldsymbol{O}^{\boldsymbol{i}}_{\boldsymbol{trn}(\boldsymbol{l})}, \boldsymbol{\mathcal{M}}^{\boldsymbol{i}}\right)$, $1 \leq l \leq N$, be their corresponding likelihood vectors – refered in this section as training vectors. From the first training vector, that is, $\mathbf{D}\left(\boldsymbol{O}^{\boldsymbol{i}}_{\boldsymbol{trn}(1)}, \boldsymbol{\mathcal{M}}^{\boldsymbol{i}}\right)$, Algorithm 3.1 randomly selects, with replacement, R' likelihoods from its R first positions (corresponding to $\boldsymbol{w_1}$), and S' likelihoods from its S last positions (corresponding to $\boldsymbol{w_2}$). Then, for each training vector $\mathbf{D}\left(\boldsymbol{O}^{\boldsymbol{i}}_{\boldsymbol{trn}(\boldsymbol{l})}, \boldsymbol{\mathcal{M}}^{\boldsymbol{i}}\right)$, $1 \leq l \leq N$, the selected positions, R' and S', are used to form a new vector $\mathbf{D'}\left(\boldsymbol{O}^{\boldsymbol{i}}_{\boldsymbol{trn}(\boldsymbol{l})}, \boldsymbol{\mathcal{M}}^{\boldsymbol{i}}\right)$, which is stored in the training set $\mathcal{T}'$.

Finally, the vectors $\mathbf{D'}\left(\boldsymbol{O}^{\boldsymbol{i}}_{\boldsymbol{trn(l)}}, \boldsymbol{\mathcal{M}^i}\right), 1 \leq l \leq N$, in $\mathcal{T}'$, are used to train a two-class classifier c_r, where r, $1 \leq r \leq \mathcal{R}$, is the actual random subspace. This procedure is repeated for $\mathcal{R}$ random subspaces, resulting in a pool $\mathcal{C}$ of $\mathcal{R}$ different two-class classifiers (2-CCs).

Inputs:
– the number of random subspaces, $\mathcal{R}$
– the training likelihood vectors, $\mathbf{D}\left(\boldsymbol{O}^{\boldsymbol{i}}_{\boldsymbol{trn(l)}}, \boldsymbol{\mathcal{M}^i}\right), 1 \leq l \leq N$
– the number of likelihoods associated to $\boldsymbol{w_1}$, R
– the number of likelihoods associated to $\boldsymbol{w_2}$, S
– the size of the subspace associated to $\boldsymbol{w_1}$, R'
– the size of the subspace associated to $\boldsymbol{w_2}$, S'
Outputs:
– the pool of trained 2-CCs, $\mathcal{C}$

for each subspace $r = 1, 2, ..., \mathcal{R}$ **do**
  STEP 1:
  from the first training vector $\mathbf{D}\left(\boldsymbol{O}^{\boldsymbol{i}}_{\boldsymbol{trn(1)}}, \boldsymbol{\mathcal{M}^i}\right)$, select at random and with replacement R' likelihoods from its R first positions and S' likelihoods from its S last positions
  let $\mathbf{D'}\left(\boldsymbol{O}^{\boldsymbol{i}}_{\boldsymbol{trn(1)}}, \boldsymbol{\mathcal{M}^i}\right)$ be the a new vector containing only R' and S'
  store $\mathbf{D'}\left(\boldsymbol{O}^{\boldsymbol{i}}_{\boldsymbol{trn(1)}}, \boldsymbol{\mathcal{M}^i}\right)$ in the training set $\mathcal{T}'$
  STEP 2:
  for each training vector $\mathbf{D}\left(\boldsymbol{O}^{\boldsymbol{i}}_{\boldsymbol{trn(l)}}, \boldsymbol{\mathcal{M}^i}\right), l = 2, 3, ..., N$ **do**
    let $\mathbf{D'}\left(\boldsymbol{O}^{\boldsymbol{i}}_{\boldsymbol{trn(l)}}, \boldsymbol{\mathcal{M}^i}\right)$ be the a new vector containing only the R' and S' positions selected in STEP 2
    store $\mathbf{D'}\left(\boldsymbol{O}^{\boldsymbol{i}}_{\boldsymbol{trn(l)}}, \boldsymbol{\mathcal{M}^i}\right)$ in the training set $\mathcal{T}'$
  end for
  STEP 3:
  use the vectors in $\mathcal{T}'$ to train a 2-CC c_r
  store c_r in the pool $\mathcal{C}$
end for

Algorithm 3.1 Random Subspace Method for 2-CCs.

3.2.4 A New Strategy for Dynamic Ensemble Selection

Let $\boldsymbol{O}^{\boldsymbol{i}}_{\boldsymbol{ds(j)}}$, $1 \leq j \leq M$, be the sequences of observations extracted from the DS database of writer i, and $\mathbf{D}\left(\boldsymbol{O}^{\boldsymbol{i}}_{\boldsymbol{ds(j)}}, \boldsymbol{\mathcal{M}^i}\right)$, $1 \leq j \leq M$, be their corresponding likelihood vectors – refered in this section as DS vectors. For each DS vector $\mathbf{D}\left(\boldsymbol{O}^{\boldsymbol{i}}_{\boldsymbol{ds(j)}}, \boldsymbol{\mathcal{M}^i}\right)$, an output profile (OP) is calculated by using Algorithm 3.2. First, $\mathbf{D}\left(\boldsymbol{O}^{\boldsymbol{i}}_{\boldsymbol{ds(j)}}, \boldsymbol{\mathcal{M}^i}\right)$ is sent to all two-class classifiers c_r, $r = 1, 2, ..., \mathcal{R}$, in the pool $\mathcal{C}$, where each c_r receives as input only the vector positions related to its respective subspace. Then, the resulting output labels are stored in a vector to form a DS output profile, $\mathbf{OP}\left(\mathbf{D}\left(\boldsymbol{O}^{\boldsymbol{i}}_{\boldsymbol{ds(j)}}, \boldsymbol{\mathcal{M}^i}\right)\right)$. This procedure is repeated for all DS vectors, resulting in a set of DS-OPs. For simplicity, we consider that the DS-OPs are also stored in the DS database.

Inputs:
– the input vector, $\mathbf{D}\left(\boldsymbol{O}^{\boldsymbol{i}}_{\boldsymbol{ds(j)}}, \boldsymbol{\mathcal{M}^i}\right)$
– the number of random subspaces, $\mathcal{R}$
– the pool of 2-CCs, $\mathcal{C}$
Outputs:
– the output profile, $\mathbf{OP}\left(\mathbf{D}\left(\boldsymbol{O}^{\boldsymbol{i}}_{\boldsymbol{ds(j)}}, \boldsymbol{\mathcal{M}^i}\right)\right)$
1: **for** each 2-CC c_r, $r = 1, 2, ..., \mathcal{R}$, in $\mathcal{C}$ **do**
2: classify $\mathbf{D}\left(\boldsymbol{O}^{\boldsymbol{i}}_{\boldsymbol{ds(j)}}, \boldsymbol{\mathcal{M}^i}\right)$ using c_r
3: store the classification label $y_r(\ \mathbf{D}\left(\boldsymbol{O}^{\boldsymbol{i}}_{\boldsymbol{ds(j)}}, \boldsymbol{\mathcal{M}^i}\right)\ )$ in the output profile vector:
$\mathbf{OP}(\mathbf{D}\left(\boldsymbol{O}^{\boldsymbol{i}}_{\boldsymbol{ds(j)}}, \boldsymbol{\mathcal{M}^i}\right))\ [r] = y_r(\ \mathbf{D}\left(\boldsymbol{O}^{\boldsymbol{i}}_{\boldsymbol{ds(j)}}, \boldsymbol{\mathcal{M}^i}\right)\ )$
4: **end for**
5: return $\mathbf{OP}\left(\mathbf{D}\left(\boldsymbol{O}^{\boldsymbol{i}}_{\boldsymbol{ds(j)}}, \boldsymbol{\mathcal{M}^i}\right)\right)$

Algorithm 3.2 Output Profile Algorithm.

When a test vector $\mathbf{D}\left(\boldsymbol{O}^{\boldsymbol{i}}_{\boldsymbol{tst}}, \boldsymbol{\mathcal{M}^i}\right)$ is presented, four main steps are performed (see Figure 3.5). First, the output profile $\mathbf{OP}\left(\mathbf{D}\left(\boldsymbol{O}^{\boldsymbol{i}}_{\boldsymbol{tst}}, \boldsymbol{\mathcal{M}^i}\right)\right)$ is calculated, such as performed for the DS vectors. Second, $\mathbf{OP}\left(\mathbf{D}\left(\boldsymbol{O}^{\boldsymbol{i}}_{\boldsymbol{tst}}, \boldsymbol{\mathcal{M}^i}\right)\right)$ is compared to each DS-OP, through the Euclidean distance, in order to find its K-nearest neighbors. Third, the 2-CCs that correctly classify the K

corresponding DS vectors are selected and used to classify $\mathbf{D}\left(\boldsymbol{O}_{\boldsymbol{tst}}^{\boldsymbol{i}}, \boldsymbol{\mathcal{M}}^{\boldsymbol{i}}\right)$. Fourth, the 2-CCs decisions are fused by majority vote.

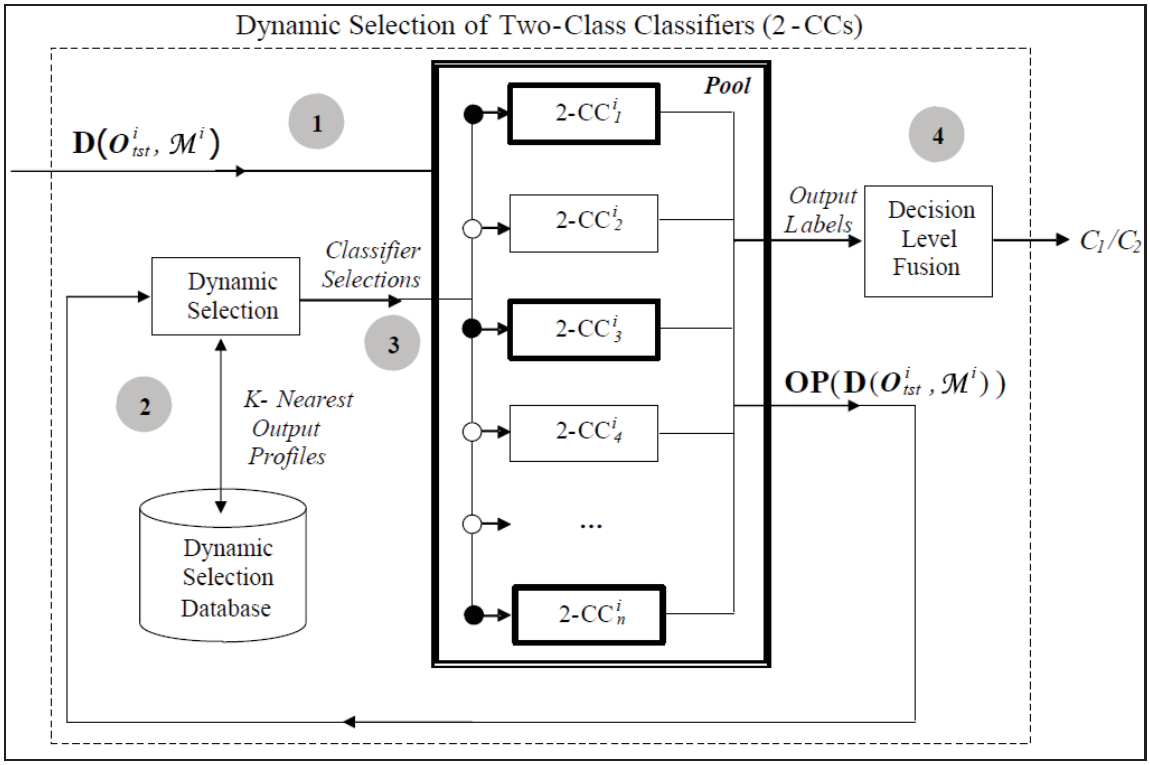

Figure 3.5 Illustration of the dynamic selection process for two-class classifiers based on output profiles. In this example, 2-CC_1^i, 2-CC_3^i and 2-CC_n^i are selected.

In this work, the two following variants of KNORA are proposed to deal with output profiles.

OP-UNION (see Algorithm 3.3). Given the test vector $\mathbf{D}\left(\boldsymbol{O}_{\boldsymbol{tst}}^{\boldsymbol{i}}, \boldsymbol{\mathcal{M}}^{\boldsymbol{i}}\right)$ and its K-nearest neighbors in the DS database, the objective of this second variant is to find for each neighbor k, $1 \leq k \leq K$, an ensemble of up to K 2-CCs that correctly classify it. First, the test output profile, $\mathbf{OP}\left(\mathbf{D}\left(\boldsymbol{O}_{\boldsymbol{tst}}^{\boldsymbol{i}}, \boldsymbol{\mathcal{M}}^{\boldsymbol{i}}\right)\right)$, and its K-nearest DS-OPs, $\mathbf{OP}\left(\mathbf{D}\left(\boldsymbol{O}_{\boldsymbol{ds(k)}}^{\boldsymbol{i}}, \boldsymbol{\mathcal{M}}^{\boldsymbol{i}}\right)\right)$, $1 \leq k \leq K$, are obtained, such as performed for OP-ELIMINATE. For each neighbor k, and for each two-class classifier c_r, $r = 1, 2, ..., \mathcal{R}$, in the pool $\mathcal{C}$, the OP-UNION algorithm then verifies if c_r has previously classified the DS vector $\mathbf{D}\left(\boldsymbol{O}_{\boldsymbol{ds(k)}}^{\boldsymbol{i}}, \boldsymbol{\mathcal{M}}^{\boldsymbol{i}}\right)$ correctly. If yes, c_r is added to the

ensemble E_k; otherwise, the next 2-CC in the pool is verified. After applying this procedure to all K-nearest neighbors, the 2-CCs in each ensemble E_k are combined in order to classify the test vector $\mathbf{D}\left(\boldsymbol{O}_{\boldsymbol{tst}}^{\boldsymbol{i}}, \boldsymbol{\mathcal{M}}^{\boldsymbol{i}}\right)$. Finally, the final classification label $\mathcal{L}$ is obtained by using the majority vote rule. Note that a same 2-CC can give more than one vote if it correctly classifies more than one DS vectors.

Inputs:
– the number of nearest neighbors, K
– the input vector, $\mathbf{D}\left(\boldsymbol{O}_{\boldsymbol{tst}}^{\boldsymbol{i}}, \boldsymbol{\mathcal{M}}^{\boldsymbol{i}}\right)$
– the number of random subspaces, $\mathcal{R}$
– the pool of 2-CCs, $\mathcal{C}$
– the DS output profiles, $\mathbf{OP}\left(\mathbf{D}\left(\boldsymbol{O}_{\boldsymbol{ds(j)}}^{\boldsymbol{i}}, \boldsymbol{\mathcal{M}}^{\boldsymbol{i}}\right)\right)$, $1 \leq j \leq M$, previously calculated with Algorithm 3.2
Outputs:
– the final classification label, $\mathcal{L}$
STEP 1:
use Algorithm 3.2 to obtain $\mathbf{OP}\left(\mathbf{D}\left(\boldsymbol{O}_{\boldsymbol{tst}}^{\boldsymbol{i}}, \boldsymbol{\mathcal{M}}^{\boldsymbol{i}}\right)\right)$, where the input vector is $\mathbf{D}\left(\boldsymbol{O}_{\boldsymbol{tst}}^{\boldsymbol{i}}, \boldsymbol{\mathcal{M}}^{\boldsymbol{i}}\right)$
STEP 2:
find its K nearest output profiles by calculating the Euclidean distance between $\mathbf{OP}\left(\mathbf{D}\left(\boldsymbol{O}_{\boldsymbol{tst}}^{\boldsymbol{i}}, \boldsymbol{\mathcal{M}}^{\boldsymbol{i}}\right)\right)$ and each $\mathbf{OP}\left(\mathbf{D}\left(\boldsymbol{O}_{\boldsymbol{ds(j)}}^{\boldsymbol{i}}, \boldsymbol{\mathcal{M}}^{\boldsymbol{i}}\right)\right)$, where $1 \leq j \leq M$
STEP 3:
for each neighbor k, $1 \leq k \leq K$, **do**
    set $count = 1$; // number of 2-CCs added to the ensemble
    for each 2-CC c_r, $r = 1, 2, ..., \mathcal{R}$, in $\mathcal{C}$ **do**
        if 2-CC c_r has previously classified $\mathbf{D}\left(\boldsymbol{O}_{\boldsymbol{ds(k)}}^{\boldsymbol{i}}, \boldsymbol{\mathcal{M}}^{\boldsymbol{i}}\right)$ correctly **and** $count \leq K$ **then**
            store c_r in the ensemble E_k, that is, $E_k(count) = c_r$
            increment the variable $count$;
        end if
    end for
end for
STEP 4:
use all E_k, $1 \leq k \leq K$, to classify $\mathbf{D}\left(\boldsymbol{O}_{\boldsymbol{tst}}^{\boldsymbol{i}}, \boldsymbol{\mathcal{M}}^{\boldsymbol{i}}\right)$
return the final classification label $\mathcal{L}$ by majority voting

Algorithm 3.3 OP-UNION Algorithm.

OP-ELIMINATE (see Algorithm 3.4). Given the test vector $\mathbf{D}\left(\boldsymbol{O}_{\boldsymbol{tst}}^{\boldsymbol{i}}, \boldsymbol{\mathcal{M}}^{\boldsymbol{i}}\right)$, the objective this first variant is to find an ensemble of up to K 2-CCs that simultaneously classify its K-nearest neighbors in the DS database correctly. First, the test output profile, $\mathbf{OP}\left(\mathbf{D}\left(\boldsymbol{O}_{\boldsymbol{tst}}^{\boldsymbol{i}}, \boldsymbol{\mathcal{M}}^{\boldsymbol{i}}\right)\right)$, is calculated. Its K-nearest DS-OPs, $\mathbf{OP}\left(\mathbf{D}\left(\boldsymbol{O}_{\boldsymbol{ds(k)}}^{\boldsymbol{i}}, \boldsymbol{\mathcal{M}}^{\boldsymbol{i}}\right)\right)$, $1 \leq k \leq K$, are then obtained by using the Euclidean distance. For each two-class classifier c_r, $r = 1, 2, ..., \mathcal{R}$, in the pool $\mathcal{C}$, the OP-ELIMINATE algorithm verifies if c_r has previously classified all corresponding DS vectors

$\mathbf{D}\left(\boldsymbol{O}^{\boldsymbol{i}}_{\boldsymbol{ds(k)}}, \boldsymbol{\mathcal{M}^i}\right)$, $1 \leq k \leq K$, correctly. If yes, c_r is added to the ensemble E; otherwise, the next 2-CC in the pool is verified. In the case where no classifier ensemble can correctly classify all K DS vectors, the value of K is decreased until at least one 2-CC can correctly classify one DS vector. Finally, each 2-CC in the ensemble E submites a vote on the test vector $\mathbf{D}\left(\boldsymbol{O}^{\boldsymbol{i}}_{\boldsymbol{tst}}, \boldsymbol{\mathcal{M}^i}\right)$, where final classification label $\mathcal{L}$ is obtained by using the majority vote rule.

Inputs:
– the number of nearest neighbors, K
– the input vector, $\mathbf{D}\left(\boldsymbol{O}^{\boldsymbol{i}}_{\boldsymbol{tst}}, \boldsymbol{\mathcal{M}^i}\right)$
– the number of random subspaces, $\mathcal{R}$
– the pool of 2-CCs, $\mathcal{C}$
– the DS output profiles, $\mathbf{OP}\left(\mathbf{D}\left(\boldsymbol{O}^{\boldsymbol{i}}_{\boldsymbol{ds(j)}}, \boldsymbol{\mathcal{M}^i}\right)\right)$, $1 \leq j \leq M$, previously calculated with Algorithm 3.2
Outputs:
– the final classification label, $\mathcal{L}$

STEP 1:
use Algorithm 3.2 to obtain $\mathbf{OP}\left(\mathbf{D}\left(\boldsymbol{O}^{\boldsymbol{i}}_{\boldsymbol{tst}}, \boldsymbol{\mathcal{M}^i}\right)\right)$, where the input vector is $\mathbf{D}\left(\boldsymbol{O}^{\boldsymbol{i}}_{\boldsymbol{tst}}, \boldsymbol{\mathcal{M}^i}\right)$
STEP 2:
find its K nearest output profiles by calculating the Euclidean distance between $\mathbf{OP}\left(\mathbf{D}\left(\boldsymbol{O}^{\boldsymbol{i}}_{\boldsymbol{tst}}, \boldsymbol{\mathcal{M}^i}\right)\right)$ and each $\mathbf{OP}\left(\mathbf{D}\left(\boldsymbol{O}^{\boldsymbol{i}}_{\boldsymbol{ds(j)}}, \boldsymbol{\mathcal{M}^i}\right)\right)$, where $1 \leq j \leq M$
STEP 3:
set $count = 1$; // number of 2-CCs added to the ensemble
for each 2-CC c_r, $r = 1, 2, ..., \mathcal{R}$, in $\mathcal{C}$ **do**
    if 2-CC c_r has previously classified all $\mathbf{D}\left(\boldsymbol{O}^{\boldsymbol{i}}_{\boldsymbol{ds(k)}}, \boldsymbol{\mathcal{M}^i}\right)$, $1 \leq k \leq K$, correctly **and** $count \leq K$ **then**
        store c_r in the ensemble E, that is, $E(count) = c_r$;
        increment the variable $count$;
    end if
end for
STEP 4:
if size$(E) == 0$ **then**
    decrement K
    repeat the process from STEP 3
end if
STEP 5:
use the 2-CCs in E to classify $\mathbf{D}\left(\boldsymbol{O}^{\boldsymbol{i}}_{\boldsymbol{tst}}, \boldsymbol{\mathcal{M}^i}\right)$
by majority voting, return the final classification label $\mathcal{L}$

Algorithm 3.4 OP-ELIMINATE Algorithm.

3.2.5 Complexity Analysis

The following complexity analysis considers the use of the Forward-Backward algorithm (Rabiner, 1989) for HMMs employed in the generative stage, and Support Vector Machines (SVM) with Radial Basis Function (RBF) kernel (Burges, 1998) in the discriminative stage. Assume a *left-to-right* HMM with $\mathcal{S}$ states, in which only transitions between two consecutive states are allowed, and a sequence of lenght L. The Forward-Backward algorithm has a complexity of $\mathcal{O}(L\mathcal{S})$ per iteration, in terms of both time and memory (Alpaydin, 2004; Khreich et al., 2010). For the SVM-RBF, the time and memory complexity during training is $\mathcal{O}(\mathcal{D}N^2)$, where N is the size of the training set and $\mathcal{D}$ is the number of input dimensions. During operations, the evaluation of each input sample has a time and memory complexity of $\mathcal{O}(\mathcal{D}V)$, where V is the number of support vectors (Burges, 1998; Cao et al., 2008).

Table 3.1 presents the overall time complexities associated with the generative and discriminative stages, where the proposed SV system is composed of a bank of B HMMs and a pool of $\mathcal{R}$ SVMs, respectively. In the discriminative stage, α genuine samples *vs.* β forgery samples are used to train the SVMs (i.e., $N = \alpha + \beta$), while only α genuine samples are used to train each HMM in the generative stage. The DS strategies proposed in this paper are applied only during operations, where K is the number of nearest output profiles. Note that the output profiles are obtained from the pool of SVMs, whose complexity is shown in the second column.

Table 3.1 Time complexities of the generative and discriminative stages

Phase	Bank of HMMs	Pool of SVMs	OP-ELIM./UNION
Training	$\mathcal{O}(\alpha BL\mathcal{S})$	$\mathcal{O}(\mathcal{R}\mathcal{D}N^2)$	-
Test	$\mathcal{O}(BL\mathcal{S})$	$\mathcal{O}(\mathcal{R}\mathcal{D}V)$	$\mathcal{O}(K\mathcal{R})$

3.3 Experimental Methodology

Given the generative-discriminative system proposed in Section 3.2, two scenarios are investigated:

1) **Scenario 1 – abundant data.** A considerable number of genuine signatures per writer (i.e., 30) is assumed to be available to design an off-line SV system. The objective of this scenario is to analyse the impact of using the proposed DS strategies over other relevant ensemble selection strategies found in the literature.

2) **Scenario 2 – sparse data** A limited number of genuine signatures per writer is assumed to be available to design an off-line SV system. The objective of this scenario is to apply the proposed system to two realistic cases of SV. In the first case, three different systems are designed, each one with 4, 8 and 12 genuine signatures per writer. In the second case, a system is initially designed with 4 genuine signatures per writer, and new genuine samples available overtime are incrementaly added to system, without retraining the actual classifiers.

The rest of this section describes the signature databases, the grid segmentation scheme, the classifier training specifications and the performance evaluation method used in the experiments.

3.3.1 Off-line SV Databases

Two different off-line signature databases are used for proof-of-concept computer simulations: the Brazilian SV database from PUCPR, used by our research group (Batista et al., 2010a; Justino et al., 2000; Bertolini et al., 2010; Batista et al., 2010b), and the GPDS database (Vargas et al., 2007), used by other researchers (Ferrer et al., 2005; Martinez et al., 2004; Pirlo et al., 2009; Vargas et al., 2011). While the Brazilian SV database is composed of random, simple and skilled forgeries, the GPDS database is composed of random and skilled forgeries.

3.3.1.1 Brazilian SV database

As presented in Chapter 2, the Brazilian SV database contains 7920 samples of signatures that were digitized as 8-bit greyscale images over 400X1000 pixels, at resolution of 300 dpi. The signatures were provided by 168 writers and are organized in two sets: the development database (DB_{dev}) and the exploitation database (DB_{exp}).

DB_{dev} contains signature samples from writers not enrolled to the system, and is used as *prior* knowledge to design the codebooks and the impostor class. It is composed of 4320 genuine samples supplied by 108 writers. Each writer j has 40 genuine samples, where 20 are available for training ($\mathcal{T}^{j}_{dev(20)}$) and 10 for validation ($\mathcal{V}^{j}_{dev(10)}$). The remaining 10 samples, available for test, are not employed in this work.

DB_{exp} contains signature samples from writers enrolled to the system, and is used to model the genuine class. It is composed of 3600 signatures supplied by 60 writers. Each writer has 40 genuine samples, 10 simple forgeries and 10 skilled forgeries. In the first scenario, 20 genuine samples are available for training ($\mathcal{T}^{i}_{exp(20)}$) and 10 for validation ($\mathcal{V}^{i}_{exp(10)}$). In the second scenario, 4, 8 and 12 genuine samples are available for training, taken from $\mathcal{T}^{i}_{exp(20)}$. The test set is the same for Scenarios 1 and 2, that is, each writer in DB_{exp} has 10 genuine samples ($TST^{i}_{true(10)}$), 10 random ($TST^{i}_{rand(10)}$) forgeries, 10 simple ($TST^{i}_{simp(10)}$) forgeries and 10 skilled forgeries ($TST^{i}_{skil(10)}$); where the random forgeries are genuine samples randomly selected from other writers in DB_{exp}.

Given a writer i enrolled to the system, DB_{dev} and DB_{exp} are used to compose different datasets employed in different phases of the system design (see Table 3.2).

3.3.1.2 GPDS database

The GPDS database is composed of 16200 signature images digitized as 8-bit greyscale at resolution of 300 dpi. It contains 300 writers, where the first 160 are set as DB_{exp} and the remaining 140, as DB_{dev}. For each writer in both DB_{exp} and DB_{dev}, there are 24 genuine

Table 3.2 Datasets for a specific writer i, using the Brazilian SV database

(a) Scenario 1 – design

Dataset Name	Task	Genuine Samples	Random Forgery Samples
DB^i_{hmm}	HMM Training	$\mathcal{T}^i_{exp(20)} + \mathcal{V}^i_{exp(10)}$	$\mathcal{T}^{j=1:108}_{dev(20)} + \mathcal{V}^{j=1:108}_{dev(10)}$
DB^i_{svm}	SVM Training	$\mathcal{T}^i_{exp(20)}$	20 from $\mathcal{T}^{j=1:108}_{dev(20)}$
DB^i_{grid}	SVM Grid Search	$\mathcal{V}^i_{exp(10)}$	10 from $\mathcal{V}^{j=1:108}_{dev(10)}$
DB^i_{roc}	ROC Curve		$\mathcal{V}^{j=1:108}_{dev(10)}$
DB^i_{ds}	Dynamic Selection		

(b) Scenario 2 – design

Dataset Name	Task	Genuine Samples	Random Forgery Samples
DB^i_{hmm}	HMM Training	4, 8, 12 from $\mathcal{T}^i_{exp(20)}$	4x108, 8x108, 12x108 from $\mathcal{T}^{j=1:108}_{dev(20)}$
DB^i_{svm}	SVM Training		4, 8, 12 from $\mathcal{T}^{j=1:108}_{dev(20)}$
DB^i_{grid}	SVM Grid Search		4, 8, 12 from $\mathcal{V}^{j=1:108}_{dev(10)}$
DB^i_{roc}	ROC Curve		$\mathcal{V}^{j=1:108}_{dev(10)}$
DB^i_{ds}	Dynamic Selection		

(c) Scenarios 1 and 2 – operations

Dataset Name	Genuine Samples	Forgery Samples
DB^i_{tst}	$TST^i_{true(10)}$	$TST^i_{rand(10)} + TST^i_{simp(10)} + TST^i_{skil(10)}$

signatures and 30 skilled forgeries. In the literature, only 80 to 160 writers (out of 300) are used to develop the SV systems, which allow us to work with two datasets.

As this database has a limited number of genuine signatures per writer, it is employed only in Scenario 2 (see Table 3.3). For each writer j in DB_{dev}, 14 genuine signatures are available for training ($\mathcal{T}^j_{dev(14)}$) and 10 for validation ($\mathcal{V}^j_{dev(10)}$); while in DB_{exp}, each writer i has 14 genuine signatures available for training ($\mathcal{T}^i_{dev(14)}$) and 10 for test ($TST^i_{true(10)}$). Moreover, 10 random forgeries ($TST^i_{rand(10)}$) and 10 skilled forgeries ($TST^i_{skil(10)}$) are used for test, where the random forgeries are genuine samples randomly selected from other writers in DB_{exp}.

During the comparative analysis performed with systems in the literature (presented in Section 3.4.4), 30 skilled forgeries ($TST^i_{skil(30)}$) are used for test, instead of 10.

In the following sections, the GPDS database is refered as GPDS-160, since a set of 160 writers (that is, DB_{exp}) is actually modeled by the proposed system.

Table 3.3 Datasets for a specific writer i, using the GPDS database

(a) Scenario 2 – design

Dataset Name	Task	Genuine Samples	Random Forgery Samples
DB^i_{hmm}	HMM Training	4, 8, 12 from $\mathcal{T}^i_{exp(14)}$	4x140, 8x140, 12x140 from $\mathcal{T}^{j=1:140}_{dev(14)}$
DB^i_{svm}	SVM Training		4, 8, 12 from $\mathcal{T}^{j=1:140}_{dev(14)}$
DB^i_{grid}	SVM Grid Search		4, 8, 12 from $\mathcal{V}^{j=1:140}_{dev(10)}$
DB^i_{roc}	ROC Curve		$\mathcal{V}^{j=1:140}_{dev(10)}$
DB^i_{ds}	Dynamic Selection		

(b) Scenario 2 – operations

Dataset Name	Genuine Samples	Forgery Samples
DB^i_{tst}	$TST^i_{true(10)}$	$TST^i_{rand(10)}$+$TST^i_{skil(10)}$
		$TST^i_{rand(10)} + TST^i_{skil(30)}$

3.3.2 Grid Segmentation

For the Brazilian SV database, the signature images (composed of 400x1000 pixels) are divided in 62 horizontal cells, where each cell is a rectangle composed of 40x16 pixels. This grid size along with density of pixels have been successfully applied to this database in (Justino et al., 2000).

A similar grid segmentation scheme is applied to the GPDS-300 database, even if no previous work have been done in order to find the best cell size. Although this database contains images

of different sizes (that vary from 51x82 pixels to 402x649 pixels), they are represented in a grid of 400x650 pixels, and segmented in 65 horizontal cells of 40x10 pixels.

To absorb the horizontal variability of the signatures, the images are aligned to the left and the blank cells in the end of the images are discarded. Therefore, the images may have a variable number of horizontal cells, while the number of vertical cells is always 10, as shows the example of Figure 3.6.

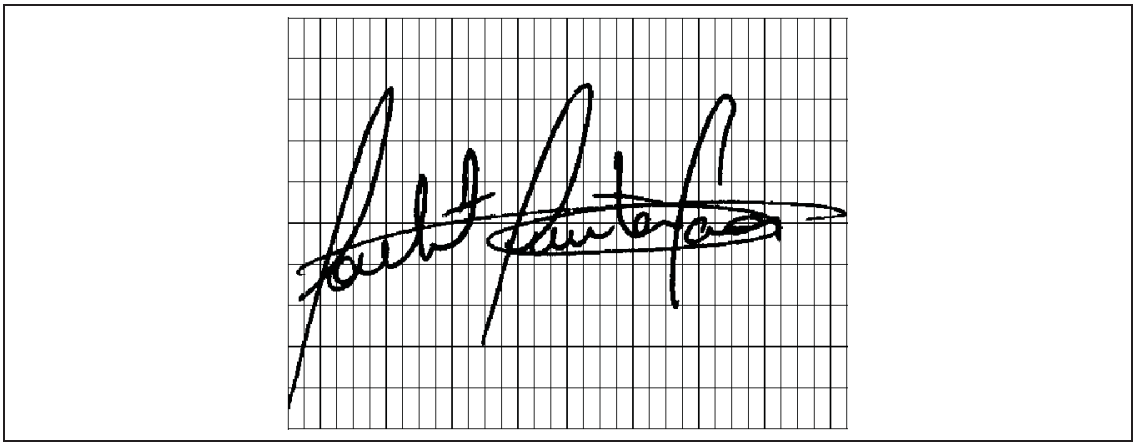

Figure 3.6 Example of grid segmentation scheme.

3.3.3 Training of the Generative Stage

29 different codebooks q $(1 \leq q \leq 29)$ are generated by varying the number of clusters from 10 to 150, in steps of 5; using all training and validation signatures of DB_{dev}. In Scenario 1, given a writer i and a codebook q, 20 genuine samples are taken from DB^i_{hmm} (i.e., $\mathcal{T}^i_{exp(20)}$) and used to train a set of discrete *left-to-right* HMMs with different number of states. As the number of states varies from 2 to the lenght of the smallest sequence used for training (L_{min}), the genuine space, $\boldsymbol{w_1}$, is composed of a variable number HMMs (i.e., 29x(L_{min}-1)) that depends on the writer's signature size. On the other hand, to compose the impostor space, $\boldsymbol{w_2}$, there

are thousands of HMMs taken from the writers in DB_{dev} (each writer j in DB_{dev} has a set of HMMs trained with his/her genuine samples).

As performed in Chapter 2, each HMM is trained by using the Baum-Welch Forward-Backward algoritm (Rabiner, 1989), and at each iteration t, the error $\mathcal{E}_t$ is calculated (see Equation 2.5). The goal is to reach an error of 10^{-5} or smaller (Justino, 2001). Besides this stop criteria, a validation set (i.e., $\mathcal{V}^i_{exp(10)}$, available only for Scenario 1) is used in order to select the optimal training point before overfitting.

In Scenario 2, the number of training sequences is dramatically reduced to 4, 8 and 12. For a given training sequence $\mathbf{O}^i_q$, a set of HMMs is trained by varying the number of states from 2 to $\frac{1}{3}$ of the sequence's size. The use of a single training sequence per HMM was previoulsy investigated in (Bicego et al., 2004). The main advantage of this strategy is that it allows to obtain a higher number of HMMs, adding more diversity to the next system stage.

3.3.4 Training of the Discriminative Stage

Although any discriminative two-class classifier can be used in the second stage, the SVM classifier with RBF kernel (Chang and Lin, 2001) was chosen because of its successful use in different pattern recognition problems.

By employing the LIBSVM toolbox (Chang and Lin, 2001), the parameters C and γ are found through a gridsearch technique. For each different pair {C, γ}, 10 different SVMs are trained using a variant of the cross-validation method, where the genuine samples performs the usual rotation, and the random forgery samples are changed each time. Since the number of genuine samples in DB^i_{grid} can be smaller than the number of SVMs to be trained (i.e., in Scenario 2), the same genuine samples are used to train more than one SVM. On the other hand, new random forgery samples are selected, randomly and with remplacement, each time that a new SVM training is performed. Finally, the error rates provided by the 10 SVMs are averaged, and the pair {C, γ} providing the smallest error rates are used to train the final SVMs.

By using the specialized RSM (see Algorithm 3.1) with $R' = S' = 15$, 100 SVMs are trained per writer. Note that, for a same writer i, the training set, DB^i_{svm}, remains the same for all 100 SVMs.

3.3.5 Classifier Ensemble Selection

In this work, the simulation results obtained with OP-UNION and OP-ELIMINATE are compared with KNORA-UNION/ELIMINATE (Ko et al., 2008), the standard combination of all classifiers, and Decision Templates (DT) (Kuncheva et al., 2001).

With OP-UNION and OP-ELIMINATE, the search for the K-nearest neighbors is done by using the output labels provided by all 100 SVMs; while with KNORA-UNION and KNORA-ELIMINATE, only the SVM input subspace providing the lowest error rates on DB^i_{ds} is used during the search. The value of K is defined as being half of the number of genuine samples in DB^i_{ds}. If the value of K is even, $K+1$ classifiers are used in order to avoid votes that result in a tie. In Scenario 1, K is set as 5; while in Scenario 2, K is set as 3, 5 and 7.

The standard combination of classifiers consists of sending the test vector $\mathbf{D}\left(\boldsymbol{O^i_{tst}}, \boldsymbol{\mathcal{M}^i}\right)$ to all 100 SVMs and then fusing their corresponding output labels by majory vote. If a tie vote is obtained, the final output label is randomly chosen.

The decision templates (DTs) is a well-known DS method in the multi-classifier system (MCS) community (Kuncheva et al., 2001). First, each DS vector $\mathbf{D}\left(\boldsymbol{O^i_{ds(j)}}, \boldsymbol{\mathcal{M}^i}\right)$, $1 \leq j \leq M$, is sent to all SVMs, and its corresponding output labels are organized in a decision profile (DP) matrix, where each line corresponds to a different SVM and each column corresponds to a different class. Since we work with 100 two-class SVMs, each $\mathbf{DP}\left(\mathbf{D}\left(\boldsymbol{O^i_{ds(j)}}, \boldsymbol{\mathcal{M}^i}\right)\right)$ is composed of 2 columns and 100 lines, where each cell contains the value 1 or 0. For instance, if the 100th SVM classifies $\mathbf{D}\left(\boldsymbol{O^i_{ds(j)}}, \boldsymbol{\mathcal{M}^i}\right)$ as belonging to the genuine class C_1, the cell located in line 100 and column 1 will contain the value 1, while the cell located in line 100 and column 2 (which corresponds to the class C_2) will contain the value 0. Then, a decision

template (DT) is calculated for each class C_j ($j = 1, 2$) by averaging the DPs of the DS vectors belonging to this class. When a test vector $\mathbf{D}\left(\boldsymbol{O}^{\boldsymbol{i}}_{\boldsymbol{tst}}, \boldsymbol{\mathcal{M}^i}\right)$ is presented, its decision profile matrix $\mathbf{DP}\left(\mathbf{D}\left(\boldsymbol{O}^{\boldsymbol{i}}_{\boldsymbol{tst}}, \boldsymbol{\mathcal{M}^i}\right)\right)$ is calculated and compared to the decision templates $\mathbf{DT}(C_j)$. The comparison is done by using the Euclidean distance, and the higher the similarity between $\mathbf{DP}\left(\mathbf{D}\left(\boldsymbol{O}^{\boldsymbol{i}}_{\boldsymbol{ds(j)}}, \boldsymbol{\mathcal{M}^i}\right)\right)$ and $\mathbf{DT}(C_j)$, the higher the support for class C_j. Finally, the most likely $\mathbf{DT}(C_j)$ is selected and the output label the most represented in this template is assigned to $\mathbf{D}\left(\boldsymbol{O}^{\boldsymbol{i}}_{\boldsymbol{ds(j)}}, \boldsymbol{\mathcal{M}^i}\right)$.

The DS strategies proposed in this paper are compared as well with two reference systems proposed in our previous work, that is, (i) a traditional generative system based on HMMs (Batista et al., 2010a) (refered in this paper as baseline system), and (ii) a hybrid system based on the static selection of generative-discriminative ensembles (Batista et al., 2010b). Both systems are briefly described in Section 3.4.1.

3.3.6 Performance Evaluation

The system performance is measured by an averaged ROC curve generated using DB^i_{roc}, according to the method of Jain and Ross (2002). As explained in Chapter 2, the operating points associated with a same γ value (and related to different users) are averaged. Recall that γ corresponds to the true negative rate (TNR) and that it may be associated with different thresholds. Since different 2-CCs are trained through the Random Subspace Method, each 2-CC results in a different averaged ROC curve.

During operations, FNR and FPR are calculated regarding different γ values of the averaged ROC curves. The average error rate (AER), also computed for different γ values, indicates the total error of the system, where FNR and FPR are averaged taking into account the *a priori* probabilities. When the Brazilian SV database is used, the FPR is calculated with respect to three forgery types: random, simple and skilled (see DB^i_{tst} of Table 3.2); while for GPDS database, FPR is calculated with respect to random and skilled forgeries (see DB^i_{tst} of Table

3.3).

3.4 Simulation Results and Discussions

3.4.1 Reference Systems

In Chapter 2, a baseline off-line SV system was designed under a traditional HMM-based approach, which consists of training a single HMM per writer (see also ref. Batista et al. (2010a)). By using DB^i_{hmm} (see Table 3.2 (a)) and a single codebook, multiple HMMs were trained with a different number of states in order to isolate an HMM order that provides the smallest error $\mathcal{E}_t$ (see Equation 2.5). This resulted in an AER ($\gamma = 1.0$) of 8.50% on test data. To reduce error rates and exploit the sub-optimal HMMs discarded by this baseline system, a multi-hypothesis system was also designed. By training a set of HMMs with a different number of states, and then selecting the most accurate HMM for each operating point of the ROC space, an AER ($\gamma = 1.0$) of 7.79% was obtained on test data.

In another work, a hybrid system based on the static selection of generative-discriminative ensembles was proposed (see also ref. Batista et al. (2010b) and Appendix I). Given the same HMMs generated through the multi-hypothesis approach, only the most representative HMMs were selected to compose the generative stage, by using a greedy search algorithm. The representative HMMs were then employed as a feature extractors for the discriminative stage. To generate a pool of SVMs, a different SVM was trained using DB^i_{svm} (see Table 3.2 (a)), each time that the greedy algorithm added a new representative HMM to the system. Then, the ICON algorithm (Ulas et al., 2009) was applied in order to incrementally construct the ensemble. Like the model selection algorithm, ICON consists in a greedy process that, during each iteration, chooses the SVM that most improves system performance on validation data when added to the ensemble. A margin-based measure called CI (from Chebishev's inequality) (Breiman, 2001; Kapp et al., 2007) was employed to assess the performance of each ensemble. This resulted in an AER ($\gamma = 1.0$) of 5.50% on test data – which represents an improvement of 2.50% with

respect to the baseline system of Chapter 2. Figure 3.8 shows the corresponding $AERs$ curves.

3.4.2 Scenario 1 – abundant data

In this experiment, each DB^i_{ds} is composed of 10 genuine samples supplied by writer i (in DB_{exp}) *versus* 1080 random forgery samples taken from writers not enrolled to the system (see Table 3.2 (a)). Note that the random forgery samples are the same for all writers in DB_{exp}. Figure 3.7 shows the averaged ROC curves obtained with scores produced from 100 different SVMs using DB^i_{roc} , while Figure 3.8 presents the $AERs$ curves on test data (DB^i_{tst}), as function of operating points (γ).

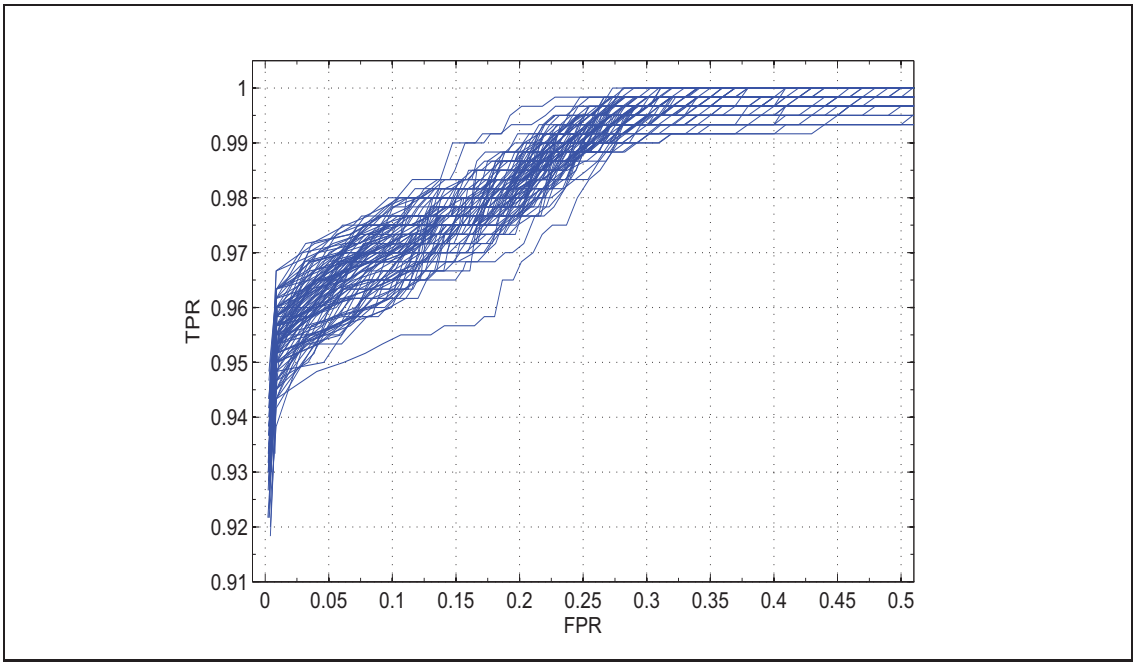

Figure 3.7 Averaged ROC curves obtained with scores produced from 100 different SVMs using DB^i_{roc} (from Brazilian data), under Scenario 1.

Results indicate that OP-ELIMINATE and OP-UNION strategies provided the lowest $AERs$, demonstrating the advantage of using a DS approach based on output profiles – as opposed to

KNORA, where the input feature space is used to find the K-nearest DS samples. It is also beneficial to employ EoCs composed of a small set of base classifiers – in contrast to Decision Templates and to the standard combination of classifiers, where all base classifiers in the pool are part of the ensemble.

OP-ELIMINATE and OP-UNION also achieved $AERs$ that are lower than those obtained with SS, showing that the proposed DS strategies are more suitable for SV, where a significant level of uncertainty resides due to the availability of partial knowledge during system design. Generaly, only genuine and random forgery samples are available to design a SV system. This system, in turn, must detect other forgery types during operations. Finally, the fewer performance of the baseline system is obtained because a pure generative approach was adopted for system design, where only the genuine class is modeled. Tables 3.4 and 3.5 present the overall results for $\gamma = 0.90$ and $\gamma = 1.0$, respectively.

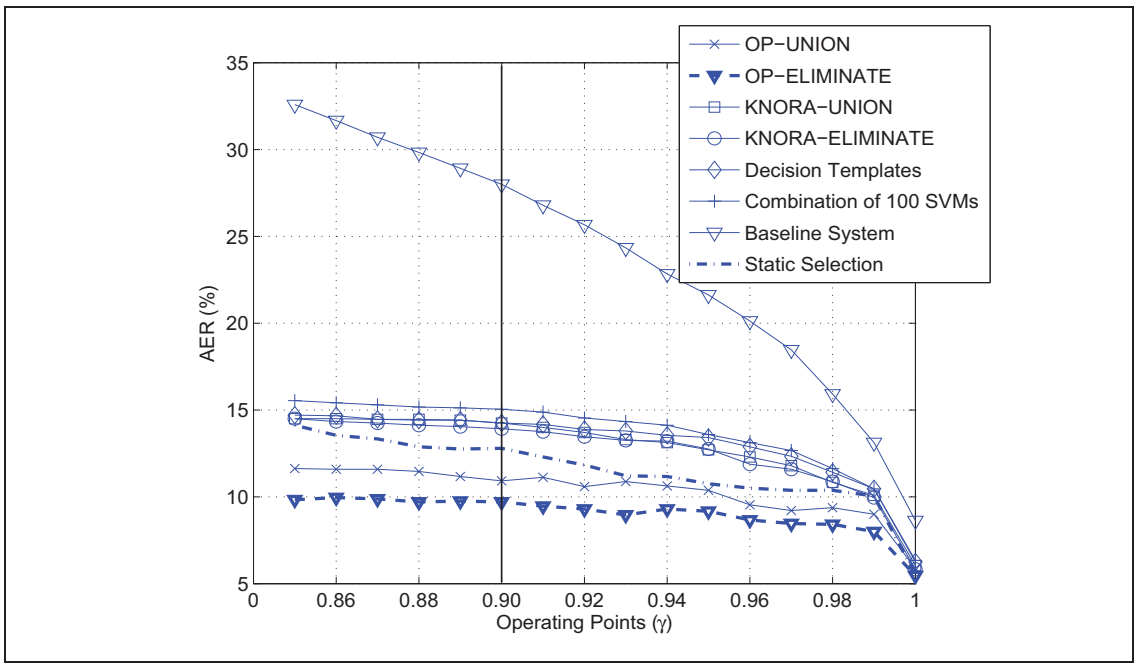

Figure 3.8 $AERs$ *versus* operating points (γ) obtained on Brazilian test data with different SV systems, under Scenario 1.

Table 3.4 Overall error rates (%) obtained on Brazilian test data for $\gamma = 0.90$, under Scenario 1

Method	FNR	FPR_{random}	FPR_{simple}	$FPR_{skilled}$	AER
OP-UNION	3.33	1.67	3.83	34.83	10.92
OP-ELIMINATE	**4.67**	**1.33**	**2.83**	**30.00**	**9.71**
KNORA-UNION	2.17	2.50	7.00	45.33	14.25
KNORA-ELIMINATE	2.33	2.67	6.33	44.33	13.92
Decision Templates	2.17	2.17	7.17	45.50	14.25
Combination of 100 SVMs	2.00	2.67	8.17	47.33	15.04
Static Selection (Batista et al., 2010b)	2.17	8.00	5.83	35.17	12.79
Baseline (Batista et al., 2010a)	0.33	12.17	20.67	78.83	28.00

Table 3.5 Overall error rates (%) obtained on Brazilian test data for $\gamma = 1.0$, under Scenario 1

Method	FNR	FPR_{random}	FPR_{simple}	$FPR_{skilled}$	AER
OP-UNION	8.17	0.67	0.67	14.00	5.88
OP-ELIMINATE	**7.50**	**0.33**	**0.50**	**13.50**	**5.46**
KNORA-UNION	8.17	0.67	0.67	14.67	6.04
KNORA-ELIMINATE	7.83	0.67	0.67	14.17	5.83
Decision Templates	8.67	0.50	0.67	15.17	6.25
Combination of 100 SVMs	8.83	0.50	0.67	15.33	6.33
Static Selection (Batista et al., 2010b)	13.50	0.00	0.17	8.33	5.50
Baseline (Batista et al., 2010a)	12.67	0.33	1.17	19.83	8.50

3.4.3 Scenario 2 – sparse data

In this experiment, each DB^i_{ds} is composed of 4, 8 and 12 genuine samples supplied by writer i (in DB_{exp}) *versus* several random forgery samples taken from writers not enrolled to the system (see Tables 3.2 (b) and 3.3 (a)), where the random forgery samples are the same for all writers in DB_{exp}. Figure 3.9 presents a comparison between the baseline system (Batista et al., 2010b) and OP-ELIMINATE, when trained with 4, 8 and 12 genuine samples from the Brazilian SV database. The results obtained by these systems when trained with 20 genuine samples, previously presented in Scenario 1, are also shown in this graph. As expected, system performance improves as more genuine samples are used for training. Such an improvement

is less pronounced with the baseline system. As with Scenario 1, the proposed system reached the smallest $AERs$.

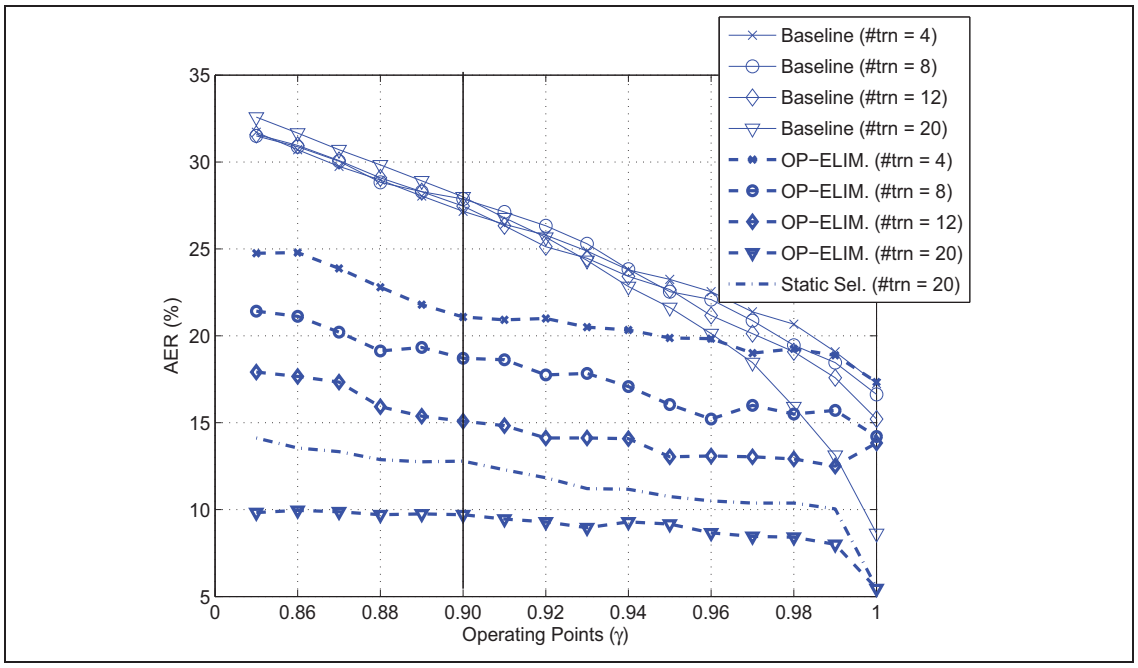

Figure 3.9 $AERs$ *versus* operating points (γ) obtained on Brazilian test data with the baseline system and OP-ELIMINATE, under Scenario 2.

Figures 3.10 and 3.11 show the $AERs$ obtained with the proposed systems for both Brazilian and GPDS-160 databases, and Table 3.6 presents the overall error rates obtained for $\gamma = 0.9$; where $\#trn$ indicates the number of genuine signatures in the training set (i.e., DB^i_{hmm} and DB^i_{svm}), and $\#ds$ indicates the number of genuine signatures in DB^i_{ds}. Note that Table 3.6 (d) is related to the Scenario 1, where the training and DS sets differ. See Appendix II for error rates related to other operating points (γ).

The proposed system achieved higher error rates with the GPDS-160 database because it contains different image sizes, which vary (vertically and horizontally) even for a same writer. In this work, no normalization technique was employed. As explained in Section 3.3.2, a fixed-sized grid – suitable for the Brazilian SV database – was applied to the GPDS-160 database.

With the Brazilian SV database, the region used for signing does not vary, since it simulates the case where the signature samples come from a same type of document, i.e., checks from a specific bank.

OP-UNION seems to be more suitable than OP-ELIMINATE when the base classifiers are trained with a very small number of signatures (for instance, 4 genuine signatures *vs.* 4 random forgeries). In fact, since classifiers trained with few signature samples are not very accurate, it is desirable to select a higher number of classifiers to form an EoC.

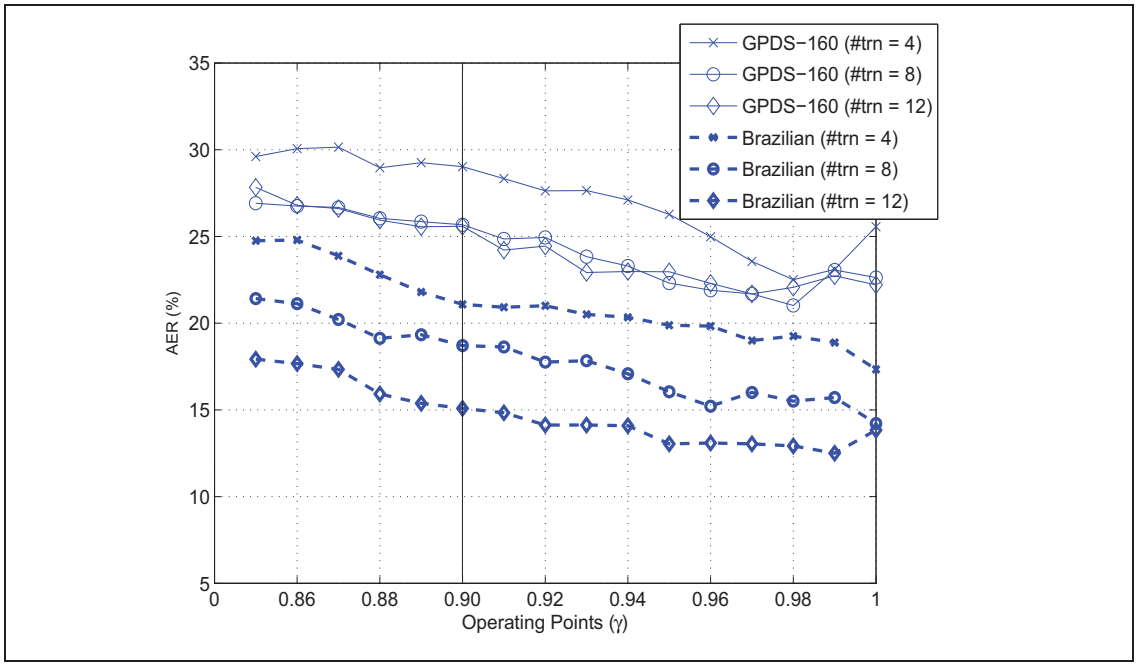

Figure 3.10 $AERs$ *versus* operating points (γ) obtained on Brazilian and GPDS-160 test data with OP-ELIMINATE strategy, under Scenario 2.

The final experiment investigates the adaptive capabilities of the proposed system when new genuine signatures are integrated incrementally. A limited number of genuine signatures are used to design both generative and discriminative stages. Then, the goal is to gradually improve system performance by adding new genuine signatures to DB^i_{ds}.

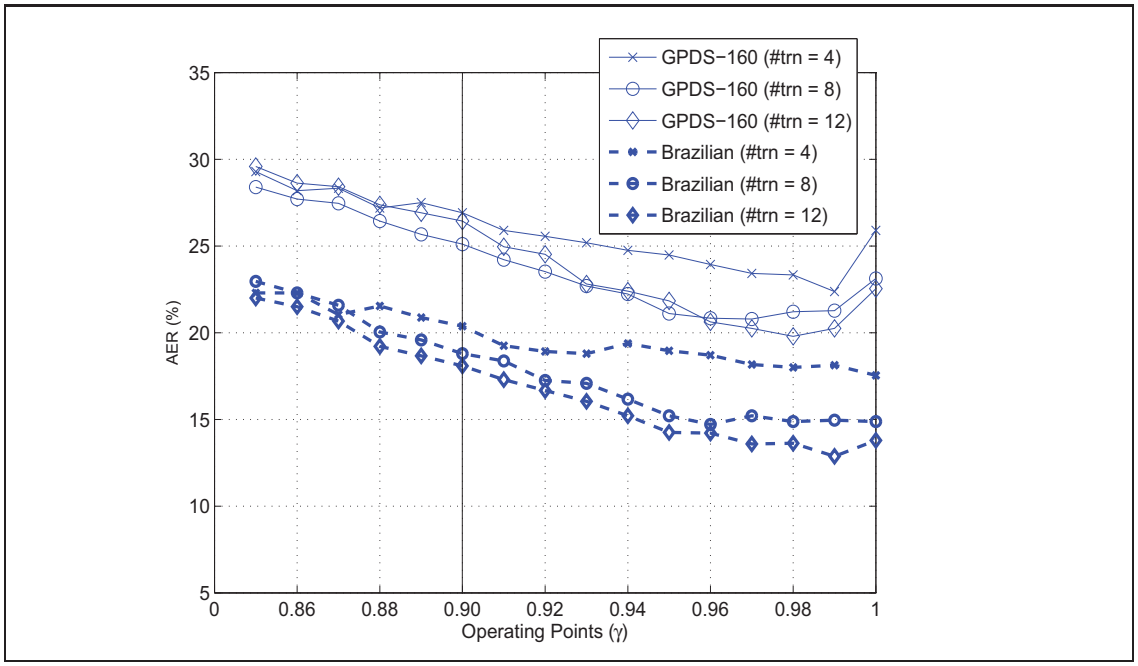

Figure 3.11 $AERs$ *versus* operating points (γ) obtained on Brazilian and GPDS-160 test data with OP-UNION strategy, under Scenario 2.

First, DB^i_{ds} is composed of 4 genuine signatures *versus* 1080 random forgeries from DB_{dev}, as performed in the previous experiment. Then, DB^i_{ds} is updated twice, by adding 4 new genuine signatures each time. Figures 3.12 and 3.13 show the AER curves (in bold) obtained with OP-ELIMINATE using the Brazilian and GPDS-160 databases, respectively. The AER curves related to the systems trained with 8 genuine samples and 12 genuine samples, from the previous experiment, are also presented in these figures.

The addition of newly-obtained genuine samples in DB^i_{ds} improved system performance in almost all operating points. With the Brazilian SV database (see Figure 3.12), the performance of the system using 4 genuine samples for training and 8 for DS is comparable to that of using 8 genuine samples for both training and DS in some operating points, such as $\gamma = 0.91$ and $\gamma = 0.87$. With the GPDS-160 database (see Figure 3.13), the performance of the system using 4 signatures for training and 12 for DS is comparable to or better than that of using 12 genuine samples for both training and DS, when $\gamma \leq 0.92$.

Table 3.6 Overall error rates (%) obtained on Brazilian and GPDS-160 test data for $\gamma = 0.90$, under Scenario 2.

(a) $\#trn = 4, \#ds = 4, K = 3$

Database	Method	FNR	FPR_{random}	FPR_{simple}	$FPR_{skilled}$	AER
Brazilian	Baseline	16.17	9.67	15.00	67.83	27.17
	OP-UNION	**26.17**	**10.83**	**9.33**	**35.17**	**20.38**
	OP-ELIMINATE	27.33	11.67	10.50	34.83	21.08
GPDS-160	**OP-UNION**	**19.44**	**12.62**	N/A	**48.69**	**26.92**
	OP-ELIMINATE	20.69	16.56	N/A	50.50	29.25

(b) $\#trn = 8, \#ds = 8, K = 5$

Database	Method	FNR	FPR_{random}	FPR_{simple}	$FPR_{skilled}$	AER
Brazilian	Baseline	8.00	11.00	19.17	73.33	27.87
	OP-UNION	11.33	11.83	9.67	42.33	18.79
	OP-ELIMINATE	**16.00**	**11.33**	**8.67**	**38.83**	**18.71**
GPDS-160	**OP-UNION**	**14.88**	**11.44**	N/A	**49.00**	**25.10**
	OP-ELIMINATE	16.62	11.62	N/A	48.75	25.67

(c) $\#trn = 12, \#ds = 12, K = 7$

Database	Method	FNR	FPR_{random}	FPR_{simple}	$FPR_{skilled}$	AER
Brazilian	Baseline	5.17	11.50	19.33	73.83	27.46
	OP-UNION	7.83	10.67	10.50	43.33	18.08
	OP-ELIMINATE	**13.50**	**5.67**	**6.83**	**34.33**	**15.08**
GPDS-160	OP-UNION	13.75	11.62	N/A	53.94	26.44
	OP-ELIMINATE	**19.19**	**9.81**	N/A	**47.25**	**25.42**

(d) $\#trn = 20, \#ds = 10, K = 5$ (from Scenario 1)

Database	Method	FNR	FPR_{random}	FPR_{simple}	$FPR_{skilled}$	AER
Brazilian	Baseline	0.33	12.17	20.67	78.83	28.00
	Static Selection	2.17	8.00	5.83	35.17	12.79
	OP-UNION	3.33	1.67	3.83	34.83	10.92
	OP-ELIMINATE	**4.67**	**1.33**	**2.83**	**30.00**	**9.71**

The main advantage of adapting DB^i_{ds} incrementally is that the actual classifiers need not be retrained. Moreover, more genuine signatures may be exploited by OP-UNION and OP-ELIMINATE during the dynamic selection of classifiers. Although more complexes, the systems trained with 8 and 12 genuine samples provide, in general, lower error rates compared to the system trained with 4 genuine samples and using 8 and 12 samples for DS, respectively. Therefore, incremental updating of DB^i_{ds} represents a viable measure to improve system performance, and may be used in conjuction with incremental learning (IL) of classifiers.

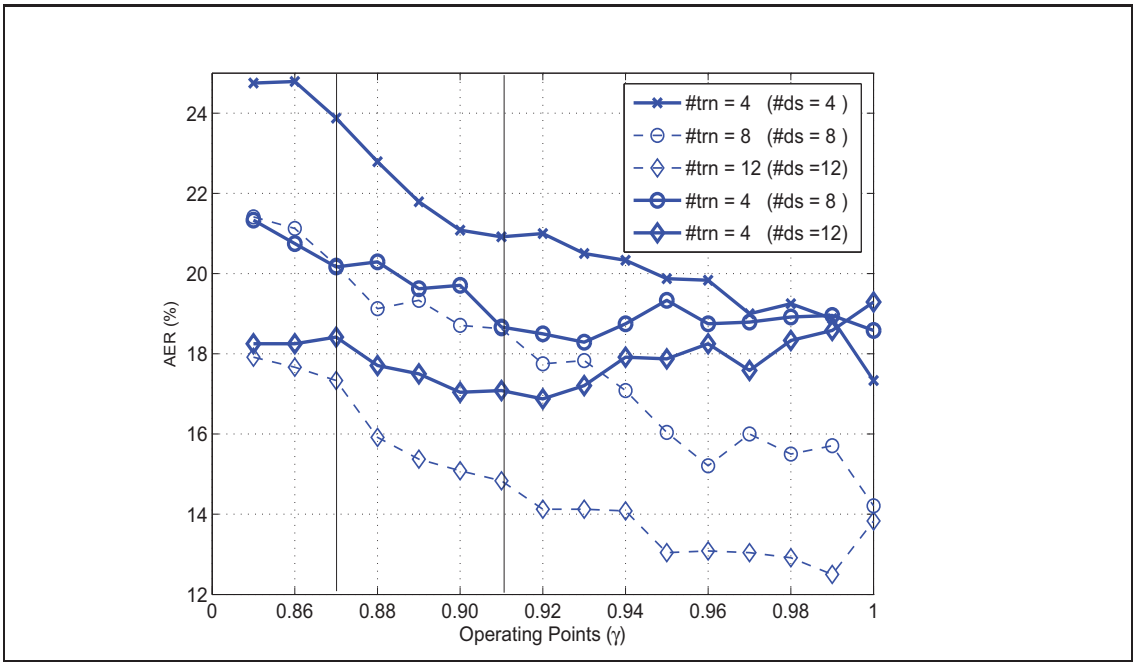

Figure 3.12 $AERs$ *versus* operating points (γ) obtained on Brazilian test data with incremental updating and OP-ELIMINATE strategy, under Scenario 2.

3.4.4 Comparisons with systems in the literature

Table 3.7 presents the error rates provided by systems designed with the Brazilian SV database. While Bertolini et al. (2010) and Santos et al. (2004) proposed discriminative systems based on dissimilarity representation, Justino et al. (2001) proposed a traditional generative system based on HMMs. Finally, Batista et al. (2010a) proposed a multi-hypothesis system based on HMMs (note that it represents the same system of Chapter 2). Since these systems required a considerable number of signatures for training, they are compared with the best system obtained in Scenario 1.

Comparisons with other systems is difficult because of the use of different features, databases and experimentation protocols. In our research, only genuine signatures and random forgeries are considered during training, validation and thresholding, since other forgery types are not available during the design of a real-world SV system. However, some authors have used

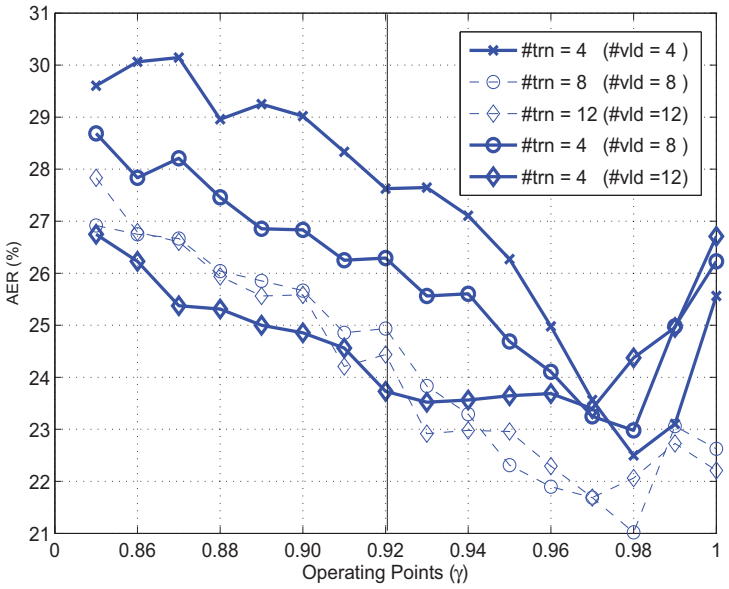

Figure 3.13 $AERs$ *versus* operating points (γ) obtained on GPDS test data with incremental updating of DB^i_{ds} and OP-ELIMINATE strategy, under Scenario 2.

Table 3.7 Overall error rates (%) provided by systems designed with the Brazilian SV database

Reference	FNR	FPR_{random}	FPR_{simple}	$FPR_{skilled}$	AER
Batista et al. (2010a)	9.83	0.00	1.00	20.33	7.79
Bertolini et al. (2010)	11.32	4.32	3.00	6.48	6.28
Justino et al. (2001)	2.17	1.23	3.17	36.57	7.87
Santos et al. (2004)	10.33	4.41	1.67	15.67	8.02
OP-ELIMINATE ($\gamma = 1.0$)	**7.50**	**0.33**	**0.50**	**13.50**	**5.46**

skilled forgeries to select optimal decision thresholds. In order to compare with systems that use the GPDS database, the equal error rate (EER) – obtained when the threshold is set to have the FNR approximately equal to the FPR – is employed. Two operating points are chosen from the test scores: one regarding genuine signatures *vs.* random forgeries, and a second regarding genuine signatures *vs.* skilled forgeries (where 30 skilled forgeries are employed, instead of 10). Table 3.8 presents the $EERs$ provided by the proposed system and other

systems designed with different subsets of the GPDS database. Following the same evaluation critera, the results obtained with the Brazilian SV database are also shown in Table 3.8.

Table 3.8 $EERs$ (%) provided by the proposed system and by other systems in the literature

(a) genuine signatures *vs.* random forgeries

Reference	Database	$\#trn$	FNR (%)	FPR (%)
Ferrer et al. (2005)	GPDS-160	4	4.30	3.80
		8	2.50	2.40
		12	2.20	3.30
Vargas et al. (2011)	GPDS-100	5	3.75	3.75
		10	1.76	1.76
OP-UNION	GPDS-160	4	7.75	6.56
		8	5.38	5.44
		12	4.50	5.19
OP-UNION	Brazilian	4	7.67	8.33
		8	4.17	4.67
		12	2.83	3.67

(b) genuine signatures *vs.* skilled forgeries

Reference	Database	$\#trn$	FNR (%)	FPR (%)
Ferrer et al. (2005)	GPDS-160	4	17.30	14.90
		8	13.40	14.90
		12	14.10	12.60
Martinez et al. (2004)	GPDS-160	-	9.56	9.56
Pirlo et al. (2009)	GPDS-40	-	19.00	21.00
Vargas et al. (2011)	PDS-100	5	12.06	12.06
		10	9.02	9.02
OP-UNION	GPDS-160	4	20.75	20.31
		8	16.69	17.38
		12	16.81	16.88
OP-UNION	Brazilian	4	19.00	20.17
		8	14.33	14.67
		12	12.17	12.67

3.4.5 System Complexity

In Scenario 1, $Q(L_{min}-1)$ HMMs are trained per writer, where Q is the number of codebooks (i.e., 29) and L_{min} is the size of the smallest training sequence. On the other hand, $\alpha Q(\frac{1}{3}L-1)$ HMMs are trained per writer in Scenario 2, where α is the number of genuine signatures used for training and L is the size of the training sequence being modeled. This indicates that this scenario produces about $\alpha/3$ times more HMMs than the previous one. Nevertheless, the time

complexity to train an individual HMM is lower in Scenario 2, since HMMs are trained with a single observation sequence, and with a smaller number of states. Recall that the number of HMM states varies from 2 to L_{min} in Scenario 1 and from 2 to $\frac{1}{3}L$ in Scenario 2. Regarding the discriminative stage, each SVM has a fixed input feature dimension of 15+15 (i.e., $R' + S'$).

During the experiments, the number of HMM states varied from 2 to 33 in Scenario 1 and from 2 to 12 in Scenario 2, on average. By considering only the genuine space, $\boldsymbol{w_1}$, 29x(33-1) HMMs were trained per writer in Scenario 1, and 4x29x(12-1) HMMs were trained per writer in Scenario 2, when $\alpha = 4$. Table 3.9 presents the average number of HMMs, states, SVM inputs and support vectors employed in each scenario. Despite the overproduction of base classifiers in both generative and discriminative stages, each individual base classifier holds a very low complexity.

Table 3.9 Average number of HMMs, states, SVM inputs, and support vectors (SVs) in each scenario

Scenario	α	HMMs per writer ($\boldsymbol{w_1}$)	HMM states	SVM inputs ($R' + S'$)	SVs per SVM
1	20	928	2 to 33	15+15	25
2	4	1276	2 to 12		7
	8	2552			11
	12	3828			16

3.5 Discussion

In this chapter, the challenge of designing off-line SV systems from a limited amount of genuine signature samples was addressed through the dynamic selection of hybrid generative-discriminative ensembles. In the generative stage, multiple discrete *left-to-right* HMMs are trained using a different number of states and codebook sizes, and employed as feature extractors for the discriminative stage. In the discriminative stage, HMM likelihoods are measured for each training signature, and assembled into feature vectors that are used to train a diversified pool of 2-CCs through a specialized RSM. During operations, a DS strategy selects the most accurate ensemble of 2-CCs to classify a given input signature. Experiments performed

with two real-world signature databases (comprised of genuine samples and random, simple and skilled forgeries) indicate that the proposed DS strategy can significantly reduce the overall error rates, with respect to other EoCs formed using well-known dynamic and static selection strategies. Moreover, the performance of the hybrid generative-discriminative system is greater than or comparable to that of relevant systems found in the literature.

The use of different codebooks and HMM states allows the system to learn each signature at different levels of perception. The codebooks – as well as the impostor class – are obtained from signatures of an independent database (i.e., DB_{dev}), ensuring that the SV system can be designed with a single user (Appendix III investigates the use of DB_{exp} for both designing codebooks and the SV system, such as performed by most SV systems based on discrete HMMs). Another important contribution is the proposal of two new DS strategies (OP-ELIMINATE and OP-UNION), based on KNORA (Ko et al., 2008) and on output profiles (OP) (Cavalin et al., 2010), which were shown to be more suitable for off-line SV than other well-known dynamic and static selection strategies.

A challenging issue in biometrics is to take into account the aging of reference data in long-lived systems (Pato and Millett, 2010). In this respect, the proposed generative-discriminative SV system can be adapted such that newly-obtained genuine samples are used to incrementally improve its performance overtime, without the need of retraining the actual classifiers.

CONCLUSION

This Thesis focused on the challenge of designing accurate and adaptive off-line SV systems, based on *left-to-right* HMMs, with a limited and unbalanced amount of data. Instead of trying to increase the number of training samples or to select the most discriminative features, the off-line SV approaches proposed in this Thesis take advantage of the potential availability of a large number of extracted features to overcome the problem of having a limited amount of training data. In other words, signatures are represented at different levels of perception and used to produce multiple classifiers that collaborate together in order to reduce error rates. Besides, an independent signature database, supplied by writers not enrolled to the SV system, is employed as *prior* knowledge of the problem to design the codebooks and the impostor class.

Based on the multi-hypotheses principle, a new approach for combining classifiers in the ROC space is proposed. By training a set of HMMs with different number of states and codebooks and then selecting the most accurate HMM(s) for each operating point of the ROC space, we propose a solution to repair concavities of individual ROC curves, while generating a high quality composite ROC curve. Besides providing a more accurate estimation of system performance during training, the operating points of the composite ROC curve significantly reduces the error rates during operations. Therefore, since ROC concavities are observed, this approach is suitable to improve system performance. Another advantage of the multi-hypothesis approach is that it can be used for dynamic selection of the best classification model – that is, the best codebook, HMM and threshold – according to the risk linked to an input sample. In banking applications, for instance, the decision to use a specific operating point may be associated with the amount of the check. As an example, if a user rarely signs high value checks, signing for large amounts would require operating points related to low $FPRs$, as would be provided by a γ value close to 1. Lower amounts would translate to operating points related to low $FNRs$, since the bank and user would not feel comfortable with frequent false rejections.

Still taking advantage of multiple *left-to-right* HMMs trained with different states and codebooks, a hybrid generative-discriminative classification architecture is proposed. The use of

HMMs as feature extractors in the generative stage followed by SVMs as classifiers in the discriminative stage allows for a better design not only of the genuine class, but also of the impostor class. Moreover, this approach provides a more robust learning than a traditional HMM-based approach when a limited amount of training data is available. Despite the over-production of base classifiers in both generative and discriminative stages, each individual base classifier holds a very low complexity.

The last contribution of this Thesis is the proposal of two new strategies for the dynamic selection (DS) of ensemble of classifiers, namely OP-UNION and OP-ELIMINATE. Experiments performed with the PUCPR and GPDS signature databases indicate that the proposed DS strategies achieve a higher level of performance in off-line SV than other reference DS and static selection (SS) strategies from literature. This represents a situation where DS is superior to SS, i.e., in a problem where a significant level of uncertainty resides due to the availability of partial knowledge during system design. Finally, OP-UNION and OP-ELIMINATE allow for the SV system to be adapted such that new genuine signature samples may be integrated incrementally. As new genuine signature samples become available, the system performance may be improved overtime, without the need of retraining the actual classifiers.

Although the proposed approaches were validated for the specific problem of off-line SV, they can be easly adapted to any similar two-class problem, e.g., other applications in biometrics. Regardless the biometric trait, applications in biometrics generally suffer from the problem of having a limited number of genuine samples to train a classifier. With respect to the choice of classifiers, the multi-hypothesis approach can be employed with any generative or discriminative classifier, with the condition that it is possible to generate ROC curves from its outputs. Similarly, other generative and discriminative classifiers can be investigated in the hybrid generative-discriminative architecture, such as, Gaussian Mixture Models (GMMs) followed by Multi-Layer Perceptrons (MLPs).

Future work

Due to time constraints, some interesting issues were not investigated in this Thesis. Therefore, proposals for future work consist of:

1) *Generation of a composite ROC curve for the hybrid generative-discriminative system.* As an alternative to the classifier selection/combination strategies proposed for the hybrid generative-discriminative system of Chapter 3, the multiple SVMs generated through the random subspace method could be used to obtain a composite ROC curve (such as proposed in Chapter 2), so that the best SVM(s) would be associated to each operating point of the curve.

2) *Learning of new features incrementally*. In Chapter 3, we have shown that each HMM in the generative stage may be trained by using a single signature sample. In this respect, new HMMs – and, consequently, new likelihoods – may be added to the system whenever a new training sample is available. The discriminative stage, however, should be composed of classifiers able to deal with the addition of new dimensions to the input feature vectors, such as the K-NN classifier.

3) *Investigation of other grid resolutions and features.* Although the grid resolution and the features employed in this Thesis were previously validated by Justino (2001) with the Brazilian SV database, different grid resolutions/features could be analysed taking into account other SV databases.

LIST OF PUBLICATIONS

Journal Articles

- Batista, L., E. Granger, and R. Sabourin. Dynamic Selection of Generative-Discriminative Ensembles for Off-Line Signature Verification. Submitted to *Pattern Recognition*.

- Batista, L., E. Granger, and R. Sabourin. Improving Performance of HMM-based Off-line Signature Verification Systems through a Multi-Hypothesis Approach. *International Journal on Document Analysis and Recognition (IJDAR)*, 13:33–47, March 2010.

Conference Articles

- Batista, L., E. Granger, and R. Sabourin. Dynamic Ensemble Selection for Off-Line Signature Verification. To appear in the *Tenth International Workshop on Multiple Classifier System (MCS'11)*, Jun 2011.

- Batista, L., E. Granger, and R. Sabourin. Applying Dissimilarity Representation to Off-Line Signature Verification. In *Twentieth International Conference Pattern Recognition (ICPR'10)*, pages 1293–1297, August 2010.

- Batista, L., E. Granger, and R. Sabourin. A Multi-Classifier System for Off-line Signature Verification based on Dissimilarity Representation. In *Ninth International Workshop on Multiple Classifier System (MCS'10)*, pages 264–273, April 2010.

- Batista, L., E. Granger, and R. Sabourin. A Multi-Hypothesis Approach for Off-line Signature Verification with HMMs. In *International Conference on Document Analysis and Recognition (ICDAR'09)*, pages 1315–1319, July 2009.

Book Chapter

- Batista, L., D. Rivard, R. Sabourin, E. Granger, and P. Maupin. State of the Art in Off-line Signature Verification. In B. Verma and M. Blumenstein, editors, *Pattern Recognition Technologies and Applications: Recent Advances*. IGI Global, 1st edition, pages 39-62, 2007.

APPENDIX I

STATIC SELECTION OF GENERATIVE-DISCRIMINATIVE ENSEMBLES

The contents of this appendix have been published as a conferece article in (Batista et al., 2010b). In that work, a hybrid generative-discriminative off-line SV system was proposed, similar to that of Chapter 3, where the generative stage is composed of HMMs trained by using a single universal codebook (i.e., CB_{35}) and different number of states, and the discriminative stage is composed of one or more two-class classifiers, selected through a static strategy.

This system is depicted in Figure AI.1, where only the most representative HMMs, $\mathcal{H}^i$, are chosen to compose the genuine (w_1) and impostor (w_2) subspaces for a specific writer i.

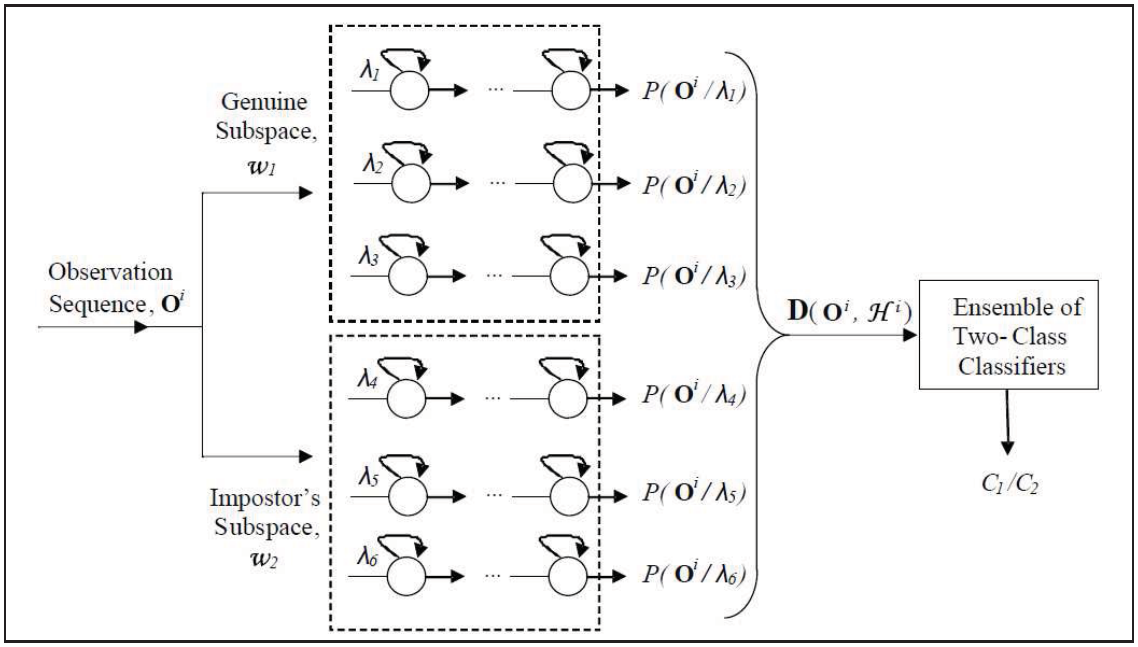

Figure AI.1 The hybrid generative-discriminative system, for a specific writer i, using three representative HMMs per subspace.

Let $\mathcal{M}^i = \{\Phi_1 \cup \Phi_2\}$be the bank of available HMMs for a specific writer i, where $\Phi_1$is the set of HMMs trained with genuine samples of writer i, and $\Phi_2$is the set of HMMs trained with

random forgery samples (i.e., genuine samples from writers not enrolled to the system). By starting with an empty subspace $\boldsymbol{w_n}$, $1 \leq n \leq 2$, a greedy algorithm incrementally adds a new HMM to $\boldsymbol{w_n}$, until a convergence criterion is reached (see Algorithm AI.1).

Basically, a HMM λ_b is chosen if its addition to the current subspace, $\boldsymbol{w_n}$, minimizes the AER provided by a 1-NN classifier (with Euclidean distance) on the validation set $\mathbf{O}^i_{vld(j)}$, $1 \leq j \leq M$. In other words, when a HMM λ_b is added to $\boldsymbol{w_n}$, a set of likelihood vectors $\mathbf{D}\left(\mathbf{O}^{\boldsymbol{i}}_{\boldsymbol{vld(j)}}, \boldsymbol{w_n}\right)$, $1 \leq j \leq M$, is obtained such as described in Chapter 3. Then, for each vector $\mathbf{D}\left(\mathbf{O}^{\boldsymbol{i}}_{\boldsymbol{vld(j)}}, \boldsymbol{w_n}\right)$, its nearest neighbor is found in the validation set (excluding itself), and its output label is calculated. After applying this procedure to all validation vectors, the AER is calculated. If the addition of λ_b to $\boldsymbol{w_n}$ minimizes the AER, it is permanently added to the bank of representative HMMs, $\boldsymbol{\mathcal{H}^i}$.

Inputs:
– the validation set of writer i, composed of genuine samples (class C_1) and random forgery samples (class C_2)
– the bank of available *left-to-right* HMMs $\boldsymbol{\mathcal{M}^i = \{\Phi_n\}}$, $1 \leq n \leq 2$, where Φ_n is the set of HMMs of class n
Outputs: the bank of representative HMMs $\boldsymbol{\mathcal{H}^i = \{w_n\}}$, $1 \leq n \leq 2$

```
for each class C_n, 1 ≤ n ≤ 2, do
    set w_n ← [ ];  //empty subspace
    set m ← 0;    //number of models stored in w_n
    repeat
        m ← m + 1;
        find the HMM λ_b in Φ_n that, when added to w_n(m), provides the smallest AER of a
        1-NN classifier using the validation set;
        remove λ_b from the set Φ_n;
    until AER reaches a minimum value
end for
store each subspace w_n in H^i, that is, H^i = {w_n}, 1 ≤ n ≤ 2;
return H^i;
```

Algorithm AI.1 Selection of representative HMMs for a specific writer i.

The rest of this appendix presents the experiments performed with the hybrid generative-discriminative system using the Brazilian SV database. Except for the fact that only one

codebook is used, the experimentation protocol is similar to that employed in Scenario 1 of Chapter 3.

Hybrid Generative-Discriminative System *vs.* Baseline System

Given the bank of available *left-to-right* HMMs, $\boldsymbol{\mathcal{M}^i = \{\Phi_1 \cup \Phi_2\}}$, and the validation set of writer i, Algorithm I.1 was applied to select the most representative HMMs, $\boldsymbol{\mathcal{H}^i = \{w_1 \cup w_2\}}$. This procedure was repeated for each writer in DB_{exp}, and, on average, 2 HMMs were selected to compose w_1, and 3 HMMs were selected to compose w_2. Then, by using $\boldsymbol{\mathcal{H}^i}$ and a set of training sequences $\mathbf{O}^i_{trn(l)}$, $1 \leq l \leq N$, likelihood vectors $\mathbf{D}\left(\mathbf{O}^{\boldsymbol{i}}_{\boldsymbol{trn(l)}}, \boldsymbol{\mathcal{H}^i}\right)$, $1 \leq l \leq N$ were obtained and used to train a single SVM per writer.

The averaged ROC curve representing the generative-discriminative system (obtained with validation scores) is indicated by the square-dashed line in Figure AI.2. The circle-dashed curve corresponds to the baseline system, designed under a traditional HMM-based SV approach (see Chapters 2 and 3). Table AI.1 (a) and (b) present the error rates on test for both systems regarding different operating points (γ). Note that the proposed system provided a reduction in the AER from 2.5%, for γ =1, up to 9.87%, for γ = 0.95.

Static Selection of SVMs Ensembles

The next experiment consisted of analyzing the impact of using an ensemble of SVMs per writer in the discriminative stage, where each SVM of the ensemble is selected through a static approach. In order to generate a pool, a different SVM is trained each time that a new HMM is selected by Algorithm I.1. For example, given that w_1 is represented by the HMMs $\{a, b, c\}$ and w_2, by $\{d, e\}$, six base SVMs can be produced by using $\{w_1 \cup w_2\}$, that is, $\{a, d\}$; $\{a, d, e\}$; $\{a, b, d\}$; $\{a, b, d, e\}$; $\{a, b, c, d\}$ and $\{a, b, c, d, e\}$.

Once the pool of SVMs is obtained, the algorithm ICON (Ulas et al., 2009) is applied in order to incrementally construct the ensemble. Such as Algorithm I.1, ICON consists in a greedy process, at each iteration, chooses the classifier that best improves the system performance (on validation data) when added to the current ensemble.

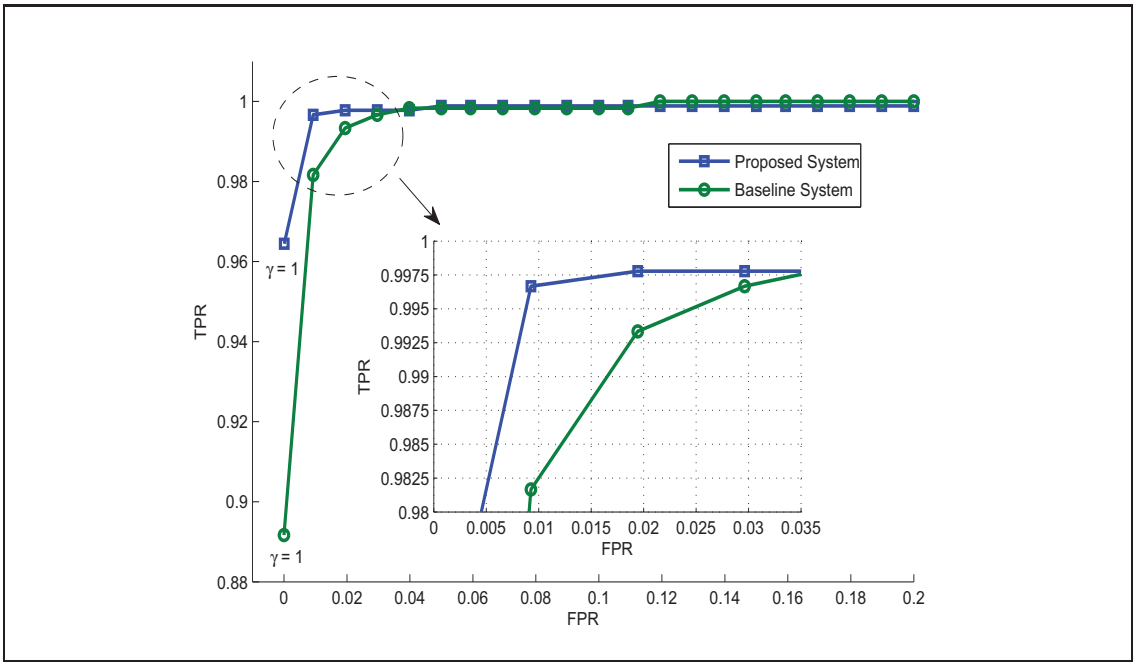

Figure AI.2 Averaged ROC curves of the baseline and proposed systems.

In this work, a measure called CI (from Chebishev's inequality) (Breiman, 2001; Kapp et al., 2007) was employed to evaluate the ensembles. It is computed as $CI = \sigma(\Omega)/\mu(\Omega)^2$, where σ and μ denote the variance and the average of the set of margins Ω provided by the samples in the validation set, respectively. Given a sample x_i from class C_1, its margin Ω_i is given by the difference between the number of votes assigned to the true class C_1, minus the number of votes assigned to class C_2. The ensemble providing the smallest CI value contains the strongest and less correlated classifiers (Kapp et al., 2007).

The overall error rates obtained on test data by using the majority vote are shown in Table AI.1 (c). Note that, except for γ = 1, the improvements were mostly related to the $FPRs$. Figure AI.3 presents the 60 individual $AERs$ for γ = 0.95. According to this graph, 48.33% of the writers had their $AERs$ on test reduced (in up to 10%) with the use of ensembles – which may indicate a considerable amount of users in a real world application –, while 15% performed better with single SVMs. For the remaining 36.67%, both versions of the system performed equally.

Table AI.1 Overall error rates (%) of baseline and proposed systems on the test data

(a) Baseline system (Batista et al., 2010a)

γ	FNR	FPR_{random}	FPR_{simple}	$FPR_{skilled}$	AER
0.95	0.50	6.83	12.83	68.00	22.04
0.96	0.50	6.00	10.83	64.83	20.54
0.97	0.83	5.67	9.00	60.17	18.92
0.98	1.17	4.00	5.67	52.50	15.83
0.99	2.33	2.67	4.00	42.67	12.92
1	12.67	0.33	1.17	19.83	8.50

(b) Generative-Discriminative system with single SVMs (Batista et al., 2010b)

γ	FNR	FPR_{random}	FPR_{simple}	$FPR_{skilled}$	AER
0.95	2.17	3.83	5.17	37.50	12.17
0.96	2.17	3.17	4.83	36.67	11.71
0.97	2.17	2.50	4.50	36.50	11.42
0.98	2.33	2.00	4.00	36.33	11.17
0.99	2.50	1.33	3.33	34.67	10.46
1	16.17	0.00	0.17	7.67	6.00

(c) Generative-Discriminative system with ensembles of SVMs (Batista et al., 2010b)

γ	FNR	FPR_{random}	FPR_{simple}	$FPR_{skilled}$	AER
0.95	2.83	2.33	4.50	33.33	10.75
0.96	3.00	1.67	3.67	33.67	10.50
0.97	2.83	1.33	3.67	33.67	10.37
0.98	2.83	1.00	3.50	34.17	10.37
0.99	3.00	1.00	3.50	32.67	10.04
1	13.50	0.00	0.17	8.33	5.50

(d) Generative-Discriminative system with AdaBoost (Batista et al., 2010c)

γ	FNR	FPR_{random}	FPR_{simple}	$FPR_{skilled}$	AER
0.95	3.33	6.00	11.50	67.67	22.12
0.96	3.33	4.83	10.83	64.33	20.83
0.97	3.50	4.00	7.67	58.83	18.50
0.98	3.67	3.17	5.17	52.33	16.08
0.99	4.50	1.67	3.50	41.83	12.87
1	13.67	0	0.50	12.00	6.54

Regarding γ = 1, only 34 writers (out of 60) were associated to ensembles by algorithm ICON. The remaining 26 writers kept using a single SVM with all HMMs selected by Algorithm 1. In Figure AI.4, observe that the AER was reduced in 7.5% for writers 4 and 10, in 10% for writer 9, and in 2.5% for writers 21, 26 and 38. Whereas for writer 20, the use of ensembles increased the AER in 2.5%.

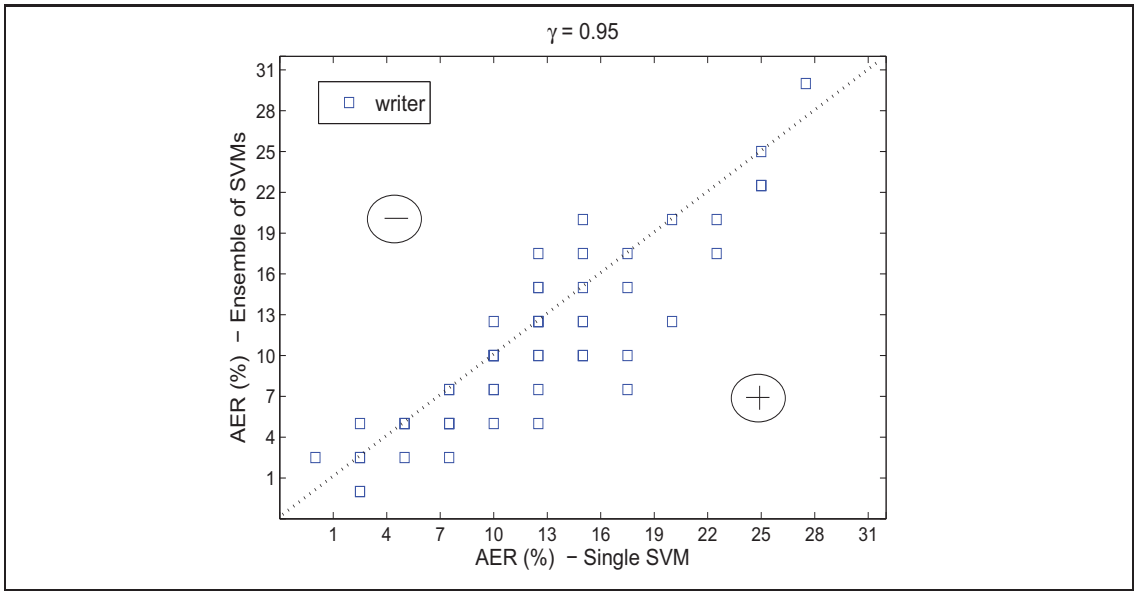

Figure AI.3 Individual $AERs$ obtained on test data for γ = 0.95, before and after using ensemble of SVMs. Note that the writers that had their $AERs$ reduced by using an ensemble of SVMs are located below the dotted line.

Comparison with Adaboost

Given its ability to perform feature selection while classifying, the Gentle Adaboost algorithm (Friedman et al., 2000) was investigated in the discriminative stage of the proposed system. Differently from the original AdaBoost algorithm, Gentle AdaBoost deals with overfitting by assigning less importance to outliers.

Although the maximum number of hypothesis was set as 1000 during the experiments, Adaboost reached training error equal to zero with a single hypothesis per writer – where a hypothesis corresponds to a decision stump, that is, a single-level decision tree constructed from the likelihoods of a single HMM. This occurred due to the fact that training set was easily separable, since it contains only genuine and random forgery samples. However, in the test phase, other forgery types were considered, and the problem became more difficult. Indeed, Adaboost did not reduce the error rates obtained by the generative-discriminative system based on SVMs, as shows Table AI.1 (d).

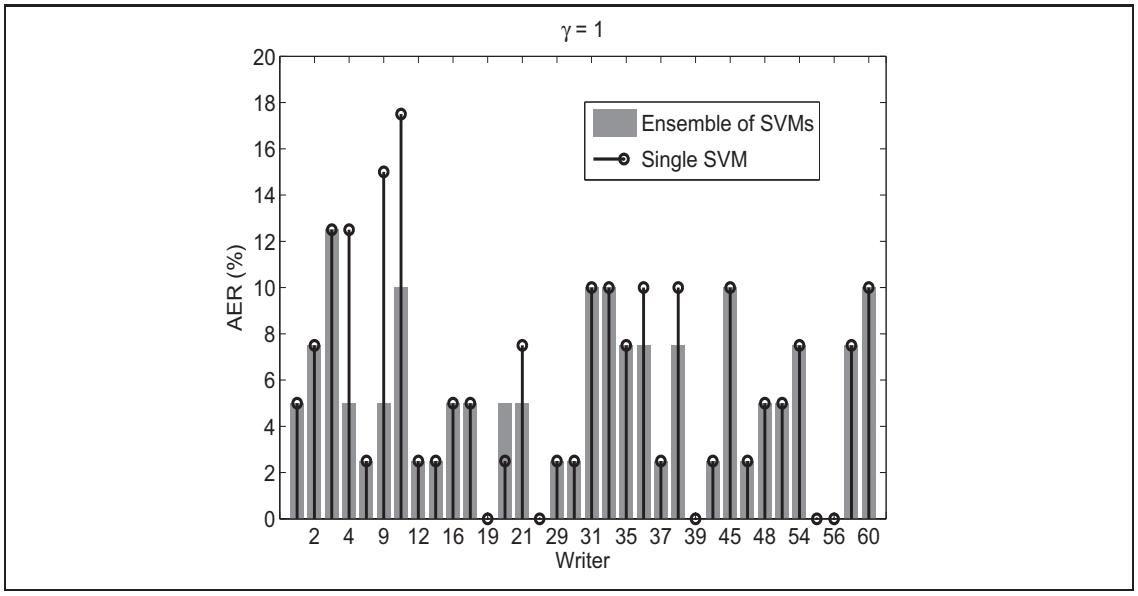

Figure AI.4 Individual $AERs$ obtained on test data for γ = 1, before and after using ensemble of SVMs.

The use of a validation set to select the most discriminative features (i.e., HMMs) and to select the best ensemble of SVMs provided a more robust solution and a higher level of performance on unknown data. Adaboost, on the other hand, performs feature selection based only on the training set.

APPENDIX II

ADDITIONAL RESULTS OBTAINED WITH THE HYBRID GENERATIVE-DISCRIMINATIVE SYSTEM

This appendix presents additional results obtained with the hybrid generative-discriminative system of Chapter 3, under Scenarios 1 and 2. Tables AII.1 to AII.6 present the overall error rates obtained on test data for different operating points (γ). Note that the error rates related to the Baseline System and Static Selection of Scenario 1 were previously presented by Tables AI.1 (a) and (c), respectively, in Appendix I.

Table AII.1 Overall error rates (%) obtained on Brazilian and GPDS-160 test data for $\gamma = 0.95$

(a) $\#trn = 4, \#ds = 4, K = 3$ (from Scenario 2)

Database	**Method**	FNR	FPR_{random}	FPR_{simple}	$FPR_{skilled}$	AER
Brazilian	Baseline	18.33	6.67	8.83	59.17	23.25
	OP-UNION	37.33	7.33	5.67	25.50	18.96
	OP-ELIMINATE	37.67	7.67	7.17	27.00	19.88
GPDS-160	OP-UNION	28.69	6.94	N/A	37.81	24.48
	OP-ELIMINATE	27.69	9.50	N/A	40.31	25.83

(b) $\#trn = 8, \#ds = 8, K = 5$ (from Scenario 2)

Database	**Method**	FNR	FPR_{random}	FPR_{simple}	$FPR_{skilled}$	AER
Brazilian	Baseline	8.33	6.83	10.00	65.00	22.54
	OP-UNION	20.50	5.83	5.33	29.17	15.21
	OP-ELIMINATE	21.00	7.67	5.83	29.67	16.04
GPDS-160	OP-UNION	22.50	5.56	N/A	35.25	21.10
	OP-ELIMINATE	19.62	7.50	N/A	39.81	22.31

(c) $\#trn = 12, \#ds = 12, K = 7$ (from Scenario 2)

Database	**Method**	FNR	FPR_{random}	FPR_{simple}	$FPR_{skilled}$	AER
Brazilian	Baseline	5.67	7.17	11.50	66.33	22.67
	OP-UNION	18.00	6.33	4.33	28.33	14.25
	OP-ELIMINATE	20.50	4.00	3.50	24.17	13.04
GPDS-160	OP-UNION	20.19	6.25	N/A	39.06	21.83
	OP-ELIMINATE	18.12	7.06	N/A	41.81	22.33

(d) $\#trn = 20, \#ds = 10, K = 5$ (from Scenario 1)

Database	**Method**	FNR	FPR_{random}	FPR_{simple}	$FPR_{skilled}$	AER
Brazilian	Baseline	0.50	6.83	12.83	68.00	22.04
	Static Selection	2.83	2.33	4.50	33.33	10.75
	OP-UNION	4.50	1.50	3.50	32.00	10.38
	OP-ELIMINATE	5.33	1.17	2.33	27.83	9.17

Table AII.2 Overall error rates (%) obtained on Brazilian and GPDS-160 test data for $\gamma = 0.96$

(a) $\#trn = 4, \#ds = 4, K = 3$ (from Scenario 2)

Database	**Method**	FNR	FPR_{random}	FPR_{simple}	$FPR_{skilled}$	AER
Brazilian	Baseline	19.50	5.83	8.33	56.50	22.54
	OP-UNION	39.50	5.67	5.33	24.33	18.71
	OP-ELIMINATE	39.33	7.17	6.33	26.50	19.83
GPDS-160	OP-UNION	33.44	6.00	N/A	32.38	23.94
	OP-ELIMINATE	31.56	7.38	N/A	36.50	25.15

(b) $\#trn = 8, \#ds = 8, K = 5$ (from Scenario 2)

Database	**Method**	FNR	FPR_{random}	FPR_{simple}	$FPR_{skilled}$	AER
Brazilian	Baseline	9.33	6.50	9.17	63.33	22.08
	OP-UNION	23.50	5.17	4.00	26.17	14.71
	OP-ELIMINATE	24.00	6.33	4.50	26.00	15.21
GPDS-160	OP-UNION	26.56	4.12	N/A	31.81	20.83
	OP-ELIMINATE	22.19	6.19	N/A	37.31	21.90

(c) $\#trn = 12, \#ds = 12, K = 7$ (from Scenario 2)

Database	**Method**	FNR	FPR_{random}	FPR_{simple}	$FPR_{skilled}$	AER
Brazilian	5.83	5.83	10.17	62.83	21.17	
	OP-UNION	20.83	5.50	4.50	26.00	14.21
	OP-ELIMINATE	23.17	4.00	2.67	22.50	13.08
GPDS-160	OP-UNION	22.81	5.12	N/A	33.94	20.62
	OP-ELIMINATE	19.38	6.75	N/A	39.94	22.02

(d) $\#trn = 20, \#ds = 10, K = 5$ (from Scenario 1)

Database	**Method**	FNR	FPR_{random}	FPR_{simple}	$FPR_{skilled}$	AER
Brazilian	Baseline	0.50	6.00	10.83	64.83	20.54
	Static Selection	3.00	1.67	3.67	33.67	10.50
	OP-UNION	3.67	1.50	3.00	30.00	9.54
	OP-ELIMINATE	5.33	1.00	2.33	26.00	8.67

Table AII.3 Overall error rates (%) obtained on Brazilian and GPDS-160 test data for $\gamma = 0.97$

(a) $\#trn = 4, \#ds = 4, K = 3$ (from Scenario 2)

Database	**Method**	FNR	FPR_{random}	FPR_{simple}	$FPR_{skilled}$	AER
Brazilian	Baseline	20.50	4.83	6.83	53.33	21.38
	OP-UNION	43.33	4.67	3.50	21.17	18.17
	OP-ELIMINATE	42.33	5.17	5.83	22.67	19.00
GPDS-160	OP-UNION	37.19	4.38	N/A	28.69	23.42
	OP-ELIMINATE	35.19	5.19	N/A	31.62	24.00

(b) $\#trn = 8, \#ds = 8, K = 5$ (from Scenario 2)

Database	**Method**	FNR	FPR_{random}	FPR_{simple}	$FPR_{skilled}$	AER
Brazilian	Baseline	9.67	5.50	7.67	60.67	20.87
	OP-UNION	30.67	3.83	2.67	23.67	15.21
	OP-ELIMINATE	29.00	6.00	4.00	25.00	16.00
GPDS-160	OP-UNION	29.44	3.75	N/A	29.19	20.79
	OP-ELIMINATE	23.12	5.81	N/A	36.12	21.69

(c) $\#trn = 12, \#ds = 12, K = 7$ (from Scenario 2)

Database	**Method**	FNR	FPR_{random}	FPR_{simple}	$FPR_{skilled}$	AER
Brazilian	Baseline	6.17	5.00	9.17	60.17	20.13
	OP-UNION	24.17	4.00	3.00	23.17	13.58
	OP-ELIMINATE	27.00	3.33	2.17	19.67	13.04
GPDS-160	OP-UNION	25.69	4.37	N/A	30.69	20.25
	OP-ELIMINATE	19.56	6.94	N/A	38.44	21.65

(d) $\#trn = 20, \#ds = 10, K = 5$ (from Scenario 1)

Database	**Method**	FNR	FPR_{random}	FPR_{simple}	$FPR_{skilled}$	AER
Brazilian	Baseline	0.83	5.67	9.00	60.17	18.92
	Static Selection	2.83	1.33	3.67	33.67	10.37
	OP-UNION	3.33	1.50	3.33	28.67	9.21
	OP-ELIMINATE	4.83	1.00	2.67	25.33	8.46

Table AII.4 Overall error rates (%) obtained on Brazilian and GPDS-160 test data for $\gamma = 0.98$

(a) $\#trn = 4, \#ds = 4, K = 3$ (from Scenario 2)

Database	**Method**	FNR	FPR_{random}	FPR_{simple}	$FPR_{skilled}$	AER
Brazilian	Baseline	22.00	4.33	6.00	50.33	20.67
	OP-UNION	49.50	3.50	3.00	16.00	18.00
	OP-ELIMINATE	46.50	5.83	5.83	18.83	19.25
GPDS-160	OP-UNION	45.31	2.69	N/A	22.00	23.33
	OP-ELIMINATE	40.19	3.62	N/A	23.75	22.52

(b) $\#trn = 8, \#ds = 8, K = 5$ (from Scenario 2)

Database	**Method**	FNR	FPR_{random}	FPR_{simple}	$FPR_{skilled}$	AER
Brazilian	Baseline	10.50	4.67	6.67	56.00	19.46
	OP-UNION	36.00	2.50	1.83	19.17	14.88
	OP-ELIMINATE	33.33	5.00	3.17	20.50	15.50
GPDS-160	OP-UNION	36.06	2.94	N/A	24.62	21.21
	OP-ELIMINATE	27.62	4.31	N/A	31.12	21.02

(c) $\#trn = 12, \#ds = 12, K = 7$ (from Scenario 2)

Database	**Method**	FNR	FPR_{random}	FPR_{simple}	$FPR_{skilled}$	AER
Brazilian	Baseline	6.83	4.00	8.67	56.83	19.08
	OP-UNION	28.33	3.33	2.50	20.33	13.62
	OP-ELIMINATE	29.50	2.83	1.50	17.83	12.92
GPDS-160	OP-UNION	32.44	2.56	N/A	24.38	19.79
	OP-ELIMINATE	24.06	7.38	N/A	34.62	22.02

(d) $\#trn = 20, \#ds = 10, K = 5$ (from Scenario 1)

Database	**Method**	FNR	FPR_{random}	FPR_{simple}	$FPR_{skilled}$	AER
Brazilian	Baseline	1.17	4.00	5.67	52.50	15.83
	Static Selection	2.83	1.00	3.50	34.17	10.37
	OP-UNION	3.83	1.50	2.50	29.67	9.38
	OP-ELIMINATE	5.00	1.00	2.17	25.50	8.42

Table AII.5 Overall error rates (%) obtained on Brazilian and GPDS-160 test data for $\gamma = 0.99$

(a) $\#trn = 4, \#ds = 4, K = 3$ (from Scenario 2)

Database	**Method**	FNR	FPR_{random}	FPR_{simple}	$FPR_{skilled}$	AER
Brazilian	Baseline	22.83	3.50	5.00	45.00	19.08
	OP-UNION	54.83	2.17	2.83	12.67	18.12
	OP-ELIMINATE	52.33	3.33	4.00	15.83	18.88
GPDS-160	OP-UNION	45.06	2.50	N/A	19.56	22.37
	OP-ELIMINATE	46.94	2.37	N/A	20.12	23.15

(b) $\#trn = 8, \#ds = 8, K = 5$ (from Scenario 2)

Database	**Method**	FNR	FPR_{random}	FPR_{simple}	$FPR_{skilled}$	AER
Brazilian	Baseline	11.17	4.33	5.67	52.67	18.46
	OP-UNION	42.00	2.00	1.17	14.67	14.96
	OP-ELIMINATE	38.00	3.83	2.67	18.33	15.71
GPDS-160	OP-UNION	35.25	3.19	N/A	25.38	21.27
	OP-ELIMINATE	37.62	4.00	N/A	27.56	23.06

(c) $\#trn = 12, \#ds = 12, K = 7$ (from Scenario 2)

Database	**Method**	FNR	FPR_{random}	FPR_{simple}	$FPR_{skilled}$	AER
Brazilian	Baseline	7.33	3.17	6.33	53.50	17.58
	OP-UNION	32.17	1.83	1.83	15.67	12.88
	OP-ELIMINATE	33.67	1.67	0.50	14.17	12.50
GPDS-160	OP-UNION	38.38	1.94	N/A	20.44	20.25
	OP-ELIMINATE	31.06	5.62	N/A	31.44	22.71

(d) $\#trn = 20, \#ds = 10, K = 5$ (from Scenario 1)

Database	**Method**	FNR	FPR_{random}	FPR_{simple}	$FPR_{skilled}$	AER
Brazilian	Baseline	2.33	2.67	4.00	42.67	12.92
	Static Selection	3.00	1.00	3.50	32.67	10.04
	OP-UNION	4.67	1.17	2.17	28.00	9.00
	OP-ELIMINATE	5.83	0.83	1.83	23.50	8.00

Table AII.6 Overall error rates (%) obtained on Brazilian and GPDS-160 test data for $\gamma = 1.0$

(a) $\#trn = 4, \#ds = 4, K = 3$ (from Scenario 2)

Database	**Method**	FNR	FPR_{random}	FPR_{simple}	$FPR_{skilled}$	AER
Brazilian	Baseline	27.00	2.00	2.83	37.17	17.25
	OP-UNION	60.50	0.17	1.33	8.17	17.54
	OP-ELIMINATE	59.33	0.33	1.33	8.33	17.33
GPDS-160	OP-UNION	67.56	1.19	N/A	8.94	25.90
	OP-ELIMINATE	67.31	1.19	N/A	9.06	25.85

(b) $\#trn = 8, \#ds = 8, K = 5$ (from Scenario 2)

Database	**Method**	FNR	FPR_{random}	FPR_{simple}	$FPR_{skilled}$	AER
Brazilian	Baseline	13.00	2.50	4.33	46.67	16.62
	OP-UNION	50.17	1.00	0.50	7.83	14.88
	OP-ELIMINATE	47.33	1.00	0.50	8.00	14.21
GPDS-160	OP-UNION	56.69	0.69	N/A	12.00	23.12
	OP-ELIMINATE	54.88	0.69	N/A	12.31	22.63

(c) $\#trn = 12, \#ds = 12, K = 7$ (from Scenario 2)

Database	**Method**	FNR	FPR_{random}	FPR_{simple}	$FPR_{skilled}$	AER
Brazilian	Baseline	8.00	2.00	4.50	46.33	15.21
	OP-UNION	45.33	0.83	0.83	8.17	13.79
	OP-ELIMINATE	43.67	1.33	1.00	9.33	13.83
GPDS-160	OP-UNION	56.25	0.81	N/A	10.56	22.54
	OP-ELIMINATE	53.69	1.00	N/A	11.38	22.02

(d) $\#trn = 20, \#ds = 10, K = 5$ (from Scenario 1)

Database	**Method**	FNR	FPR_{random}	FPR_{simple}	$FPR_{skilled}$	AER
Brazilian	Baseline	12.67	0.33	1.17	19.83	8.50
	Static Selection	13.50	0.00	0.17	8.33	5.50
	OP-UNION	8.17	0.67	0.67	14.00	5.88
	OP-ELIMINATE	7.50	0.33	0.50	13.50	5.46

APPENDIX III

USING SYSTEM-ADAPTED CODEBOOKS

This appendix investigates the use a single database, i.e., DB_{exp}, for both designing codebooks and the SV system, such as performed by most SV systems based on discrete HMMs. A hybrid generative-discriminative off-line SV system, similar to that proposed in Chapter 3, is designed using the data indicated in Table AIII.1. Since the 29 codebooks are designed using the same data used for training and validation of the classifiers (i.e., $\mathcal{T}^{i=1:60}_{exp(20)} + \mathcal{V}^{i=1:60}_{exp(10)}$), they are refered as system-adapted codebooks.

Table AIII.1 Datasets for a specific writer i, using the Brazilian SV database

(a) Design

Dataset Name	Task	Genuine Samples	Random Forgery Samples
DB^i_{hmm}	HMM Training	$\mathcal{T}^i_{exp(20)} + \mathcal{V}^i_{exp(10)}$	$\mathcal{T}^{j=1:60}_{exp(20)} + \mathcal{V}^{j=1:60}_{exp(10)}, j \neq i$
DB^i_{svm}	SVM Training	$\mathcal{T}^i_{exp(20)}$	20 from $\mathcal{T}^{j=1:60}_{exp(20)}, j \neq i$
DB^i_{grid}	SVM Grid Search	$\mathcal{V}^i_{exp(10)}$	10 from $\mathcal{V}^{j=1:60}_{exp(10)}, j \neq i$
DB^i_{roc}	ROC Curve		$\mathcal{V}^{j=1:60}_{exp(10)}, j \neq i$
DB^i_{ds}	Dynamic Selection		

(b) Operations

Dataset Name	Genuine Samples	Forgery Samples
DB^i_{tst}	$TST^i_{true(10)}$	$TST^i_{rand(10)} + TST^i_{simp(10)} + TST^i_{skil(10)}$

The main goal of the experiments presented in this appendix is to perform a comparison with Scenario 1 of Chapter 3 (see Section 3.4.2), which employs universal codebooks designed using an independent database (i.e., DB_{dev}).

Figure AIII.1 shows the averaged ROC curves obtained with scores produced from 100 different SVMs using DB^i_{roc}, while Figure AIII.2 presents the $AERs$ curves on test data (DB^i_{tst}), as

function of operating points (γ). As occurred with in Chapter 3 (see Figure 3.8), OP-ELIMINATE and OP-UNION strategies provided the lowest $AERs$.

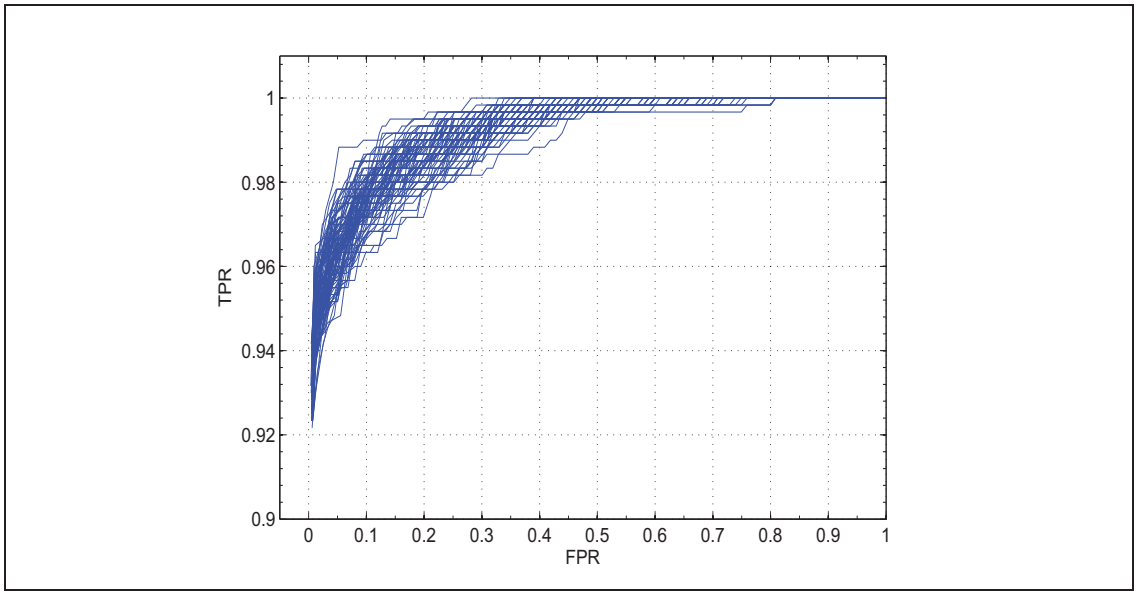

Figure AIII.1 Averaged ROC curves obtained with scores produced from 100 different SVMs, using DB^{i}_{roc} (from Brazilian data).

Tables AIII.2 and AIII.3 present the overall results for $\gamma = 0.90$ and $\gamma = 1.0$, respectively, where the different SV systems were designed with the data presented by Table AIII.1. Note that the error rates shown in Chapter 3 (see tables 3.4 and 3.5) are smaller, which proves that the universal codebooks generated using DB_{dev} are representative of the population in DB_{exp}.

The main advantage of using universal codebooks, over system-adapted codebooks, is that a SV system can be designed even for a single user, since the data used to generate the codebooks came from an independent database.

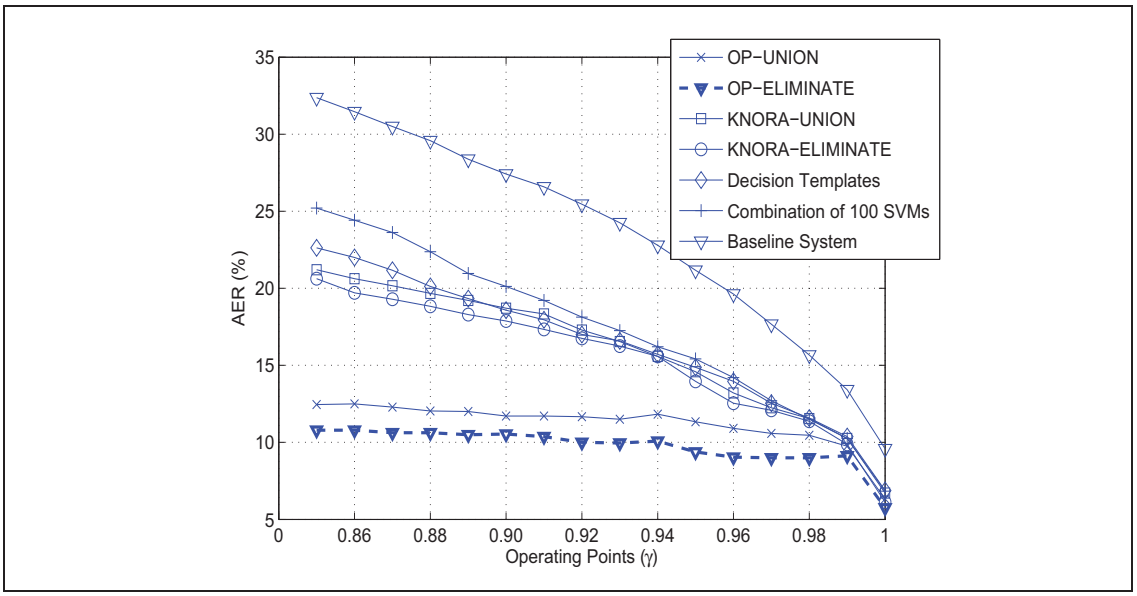

Figure AIII.2 *AERs versus* operating points (γ) obtained on Brazilian test data with different SV systems.

Table AIII.2 Overall error rates (%) obtained on Brazilian test data for $\gamma = 0.90$

Method	FNR	FPR_{random}	FPR_{simple}	$FPR_{skilled}$	AER
OP-UNION	3.50	1.33	5.00	37.00	11.71
OP-ELIMINATE	3.00	1.17	3.33	34.67	10.54
KNORA-UNION	2.17	13.83	9.33	49.50	18.71
KNORA-ELIMINATE	2.17	12.33	8.33	48.67	17.88
Decision Templates	1.00	14.83	8.83	49.67	18.58
Combination of 100 SVMs	1.00	17.50	10.33	51.67	20.12
Baseline	0.33	8.83	22.67	77.83	27.42

Table AIII.3 Overall error rates (%) obtained on Brazilian test data for $\gamma = 1.0$

Method	FNR	FPR_{random}	FPR_{simple}	$FPR_{skilled}$	AER
OP-UNION	8.00	0.17	0.50	16.67	6.33
OP-ELIMINATE	6.17	0.00	0.83	16.00	5.75
KNORA-UNION	8.33	0.33	0.83	17.33	6.71
KNORA-ELIMINATE	6.83	0.33	0.67	16.67	6.12
Decision Templates	8.33	0.50	0.83	17.83	6.88
Combination of 100 SVMs	9.00	0.50	0.67	17.17	6.83
Baseline	3.33	0.33	1.33	33.33	9.58

BIBLIOGRAPHY

Abou-Moustafa, K., M. Cheriet, and C. Suen, 2004. Classification of time-series data using a generative/discriminative hybrid. *Ninth International Workshop on Frontiers in Handwriting Recognition*, pages 51–56, Washington, DC, USA, 2004. IEEE Computer Society.

Al-Shoshan, A., 2006. Handwritten signature verification using image invariants and dynamic features. *2006 International Conference on Computer Graphics, Imaging and Visualisation*, pages 173–176.

Alpaydin, E., 2004. *Introduction to Machine Learning (Adaptive Computation and Machine Learning)*. The MIT Press.

Ammar, M., 1991. Progress in verification of skillfully simulated handwritten signatures. *International Journal of Pattern Recognition and Artificial Intelligence*, 5(1-2):337–351.

Ammar, M., Y. Yoshida, and T. Fukumura, 1985. Off-line verification of signature based on pressure features. *Tech. Group Meeting of Pattern Recognition Learn*, pages 134–144.

Ammar, M., Y. Yoshida, and T. Fukumura, 1988. Off-line pre-processing and verification of signatures. *International Journal of Pattern Recognition and Artificial Intelligence*, 2 (4):589–602.

Ando, S. and M. Nakajima, 2003. An active search method for local individual features in off-line signature verification. *Systems and Computers in Japan*, 34(12):64–76.

Armand, S., M. Blumenstein, and V. Muthukkumarasamy, 2006a. Off-line signature verification based on the modified direction feature. *18th International Conference on Pattern Recognition*, volume 4, pages 509–512.

Armand, S., M. Blumenstein, and V. Muthukkumarasamy, 2006b. Off-line signature verification using the enhanced modified direction feature and neural-based classification. *International Joint Conference on Neural Networks*, pages 684–691.

Bajaj, R. and S. Chaudhury, January 1997. Signature verification using multiple neural classifiers. *Pattern Recognition*, 30(1):1–7.

Bastos, L., F. Bortolozzi, R. Sabourin, and C. Kaestner, 1997. Mathematical modelation of handwritten signatures by conics. *Revista da Sociedade Paranaese de Matemática*, 18: 135–146.

Batista, L., D. Rivard, R. Sabourin, E. Granger, and P. Maupin, 2007. State of the art in off-line signature verification. Verma, B. and M. Blumenstein, editors, *Pattern Recognition Technologies and Applications: Recent Advances*, pages 39–62. IGI Global, 1st edition.

Batista, L., E. Granger, and R. Sabourin, July 2009. A multi-hypothesis approach for off-line signature verification with HMMs. *International Conference on Document Analysis and Recognition*, pages 1315–1319.

Batista, L., E. Granger, and R. Sabourin, March 2010a. Improving performance of HMM-based off-line signature verification systems through a multi-hypothesis approach. *International Journal on Document Analysis and Recognition*, 13:33–47. ISSN 1433-2833.

Batista, L., E. Granger, and R. Sabourin, April 2010b. A multi-classifier system for off-line signature verification based on dissimilarity representation. *Ninth International Workshop on Multiple Classifier Systems*, pages 264–273.

Batista, L., E. Granger, and R. Sabourin, August 2010c. Applying dissimilarity representation to off-line signature verification. *20th International Conference on Pattern Recognition*, pages 1293–1297.

Batista, L., E. Granger, and R. Sabourin, Jun 2011. Dynamic ensemble selection for off-line signature verification. *To appear in the Tenth International Workshop on Multiple Classifier Systems*.

Bertolini, D., L. Oliveira, E. Justino, and R. Sabourin, January 2010. Reducing forgeries in writer-independent off-line signature verification through ensemble of classifiers. *Pattern Recognition*, 43(1):387–396.

Bicego, M., V. Murino, and M. Figueiredo, 2004. Similarity-based clustering of sequences using hidden Markov models. *Pattern Recognition*, 37(12):2281–2291.

Blatzakis, H. and N. Papamarkos, 2001. A new signature verification technique based on a two-stage neural network classifier. *Engineering Applications of Artificial Intelligence*, 14:95–103.

Breiman, L., 1996. Bagging predictors. *Machine Learning*, 2:123–140.

Breiman, L., 2001. Random forests. *Machine Learning*, 45:5–32.

Britto, A., 2001. *A Two-Stage HMM-based Method for Recognizing Handwritten Numeral Strings*. PhD thesis, PUC-PR, Brasil.

Burges, C., 1998. A tutorial on support vector machines for pattern recognition. *Data mining and knowledge discovery*, 2(2):121–167.

Cao, H., T. Naito, and Y. Ninomiya, 2008. Approximate RBF kernel SVM and its applications in pedestrian classification. *1st International Workshop on Machine Learning for Vision-based Motion Analysis*.

Cardot, H., M. Revenu, B. Victorri, and M. Revillet, 1994. A static signature verification system based on a cooperating neural network architecture. *International Journal on Pattern Recognition and Artificial Intelligence*, 8(3):679–692.

Cavalin, P., R. Sabourin, C. Suen, and A. Britto, December 2009. Evaluation of incremental learning algorithms for HMM in the recognition of alphanumeric characters. *Pattern Recognition*, 42:3241–3253.

Cavalin, P., R. Sabourin, and C. Suen, 2010. Dynamic selection of ensembles of classifiers using contextual information. *Ninth International Workshop on Multiple Classifier Systems*, pages 145–154.

Cha, S., 2001. *Use of Distance Measures in Handwriting Analysis*. PhD thesis, State University of New York at Buffalo.

Chalechale, A., G. Naghdy, P. Premaratne, and A. Mertins, 2004. Document image analysis and verification using cursive signature. *IEEE International Conference on Multimedia and Expo*, volume 2, pages 887–890.

Chang, C. and C. Lin, 2001. LIBSVM: a library for support vector machines. *http://www.csie.ntu.edu.tw/˜cjlin/libsvm*.

Chen, S. and S. Srihari. Combining one- and two-dimensional signal recognition approaches to off-line signature verification. Taghva, K. and X. Lin, editors, *Document Recognition and Retrieval XIII*, volume 6067, pages 1–10. SPIE.

Chuang, P., 1977. Machine verification of handwritten signature image. *1977 International Conference on Crime Countermeasures–Science and Engineering*, pages 105–109.

Coetzer, H. and R. Sabourin, 2007. A human-centric off-line signature verification system. *International Conference on Document Analysis and Recognition*, pages 153–157.

Coetzer, J., 2005. *Off-line Signature verification*. PhD thesis, University of Stellenbosch.

Coetzer, J., B. Herbst, and J. du Preez, 2004. Offline signature verification using the discrete radon transform and a hidden Markov model. *Journal on Applied Signal Processing*, 2004(4):559–571.

Deng, P., H. Liao, C. Ho, and H. Tyan, December 1999. Wavelet-based off-line handwritten signature verification. *Computer Vision and Image Understanding*, 76(3):173–190.

Deng, P., L. Jaw, J. Wang, and C. Tung, 2003. Trace copy forgery detection for handwritten signature verification. *IEEE 37th Annual 2003 International Carnahan Conference on Security Technology*, pages 450–455.

Drouhard, J., R. Sabourin, and M. Godbout, March 1996. A neural network approach to off-line signature verification using directional PDF. *Pattern Recognition*, 29(3):415–424.

Drummond, C., 2006. Discriminative vs. generative classifiers for cost sensitive learning. *Canadian Conference on Artificial Intelligence. Lecture Notes in Artificial Intelligence*, pages 479–490.

El-Yacoubi, A., E. Justino, R. Sabourin, and F. Bortolozzi, 2000. Off-line signature verification using HMMs and cross-validation. *IEEE Workshop on Neural Networks for Signal Processing*, pages 859–868.

Fadhel, E. and P. Bhattacharyya, 1999. Application of a steerable wavelet transform using neural network for signature verification. *Pattern Analysis and Applications*, 2:184–195.

Fang, B. and Y. Tang, 2005. Improved class statistics estimation for sparse data problems in offline signature verification. *IEEE Transactions on Systems, Man and Cybernetics, Part C*, 35(3):276–286.

Fang, B., Y. Wang, C. Leung, and K. Tse, 2001. Off-line signature verification by the analysis of cursive strokes. *International Journal of Pattern Recognition and Artificial Intelligence*, 15(4):659–673.

Fang, B., C. Leung, Y. Tang, P. Kwok, K. Tse, and Y. Wong, 2002. Offline signature verification with generated training samples. *IEE Proceedings of Vision, Image and Signal Processing*, 149(2):85–90.

Fang, B., C. Leung, Y. Tang, K. Tse, P. Kwok, and Y. Wong, January 2003. Off-line signature verification by the tracking of feature and stroke positions. *Pattern Recognition*, 36(1): 91–101.

Fasquel, J. and M. Bruynooghe, March 2004. A hybrid opto-electronic method for fast off-line handwritten signature verification. *International Journal on Document Analysis and Recognition*, 7(1):56–68.

Fawcett, T., June 2006. An introduction to ROC analysis. *Pattern Recognition Letters*, 27(8): 861–874.

Ferrer, M., J. Alonso, and C. Travieso, 2005. Offline geometric parameters for automatic signature verification using fixed-point arithmetic. *IEEE Transactions on Pattern Analysis and Machine Intelligence*, 27(6):993–997.

Fierrez-Aguilar, J., N. Alonso-Hermira, G. Moreno-Marquez, and J. Ortega-Garcia, 2004. An off-line signature verification system based on fusion of local and global information. Maltoni, D. and A. K. Jain, editors, *Biometric Authentication, Lecture Notes In Computer Science*, pages 295–306. Springer-Verlag Berlin.

Flach, P. and S. Wu, 2003. Repairing concavities in ROC curves. *UK Workshop on Computational Intelligence*, pages 38–44.

Franke, K., Y. Zhang, and M. Koppen, 2002. Static signature verification employing a kosko-neuro-fuzzy approach. *International Conference on Fuzzy Systems*, volume 2275, pages 185–190. Springer Berlin / Heidelberg.

Freund, Y., 1990. Boosting a weak learning algorithm by majority. *third annual workshop on Computational learning theory*, pages 202–216, San Francisco, CA, USA, 1990. Morgan Kaufmann Publishers Inc.

Frias-Martinez, E., A. Sanchez, and J. Velez, September 2006. Support vector machines versus multi-layer perceptrons for efficient off-line signature recognition. *Engineering Applications of Artificial Intelligence*, 19(6):693–704.

Friedman, J., T. Hastie, and R. Tibshirani, 2000. Additive logistic regression: A statistical view of boosting. *The Annals of Statistics*, 38(2):337–374.

Fujisawa, H., 2007. *Robustness Design of Industrial Strength Recognition Systems*. Springer.

Gibbons, J., 1985. *Nonparametric Statistical Inference*. M. Dekker, 2nd edition.

Gonzalez, R. and R. Woods, editors, 2002. *Digital Image Processing*. Prentice Hall, 2nd edition.

Gotoh, Y., M. Hochberg, and H. Silverman, 1998. Efficient training algorithms for HMMs using incremental estimation. *IEEE Transactions on Speech and Audio Processing*, 6 (6):539–548.

Guo, J., D. Doermann, and A. Rosenfeld, 1997. Local correspondence for detecting random forgeries. *International Conference on Document Analysis and Recognition*, volume 1, pages 319–323.

Guo, J., D. Doermann, and A. Rosenfeld, 2000. Off-line skilled forgery detection using stroke and sub-stroke properties. *15th International Conference on Pattern Recognition*, volume 2, pages 355–358.

Hanmandlu, M., M. Yusof, and V. Madasu, March 2005. Off-line signature verification and forgery detection using fuzzy modeling. *Pattern Recognition*, 38(3):341–356.

Haykin, S., 1998. *Neural Networks: A Comprehensive Foundation*. Prentice Hall, 2 edition.

Ho, T., 1998. The random subspace method for constructing decision forests. *IEEE Transactions on Pattern Analysis and Machine Intelligence*, 20(8):832–844.

Huang, K. and H. Yan, January 1997. Off-line signature verification based on geometric feature extraction and neural network classification. *Pattern Recognition*, 30(1):9–17.

Huang, K. and H. Yan, 2002. Off-line signature verification using structural feature correspondence. *Pattern Recognition*, 35:2467–2477.

Huang, X., A. Acero, and H. Hon, editors, 2001. *Spoken Language Processing*. Prentice Hall.

Igarza, J., I. Hernaez, and I. Goirizelaia, 2005. Static signature recognition based on left-to-right hidden Markov models. *Journal of Electronic Imaging*, 14(4).

Impedovo, D. and G. Pirlo, 2008. Automatic signature verification: The state of the art. 38(5): 609–635.

Jain, A. and A. Ross, 2002. Learning user-specific parameters in a multibiometric system. *International Conference on Image Processing*, pages 57–60.

Jain, A., F. Griess, and S. Connell, 2002. On-line signature verification. *Pattern Recognition*, 35:2963–2972.

Justino, E., 2001. *O Grafismo e os Modelos Escondidos de Markov na Verificacao Automatica de Assinaturas*. PhD thesis, PUC-PR, Brasil.

Justino, E., A. El-Yacoubi, F. Bortolozzi, and R. Sabourin, 2000. An off-line signature verification system using HMM and graphometric features. *International Workshop on Document Analysis Systems*, pages 211–222.

Justino, E., F. Bortolozzi, and R. Sabourin, 2001. Off-line signature verification using HMM for random, simple and skilled forgeries. *International Conference on Document Analysis and Recognition*, pages 105–110.

Justino, E., F. Bortolozzi, and R. Sabourin, 2005. A comparison of SVM and HMM classifiers in the off-line signature verification. *Pattern Recognition Letters*, 26(9):1377–1385.

Kalera, M., S. Srihari, and A. Xu, 2004. Offline signature verification and identification using distance statistics. *International Journal of Pattern Recognition and Artificial Intelligence*, 18(7):1339–1360.

Kapp, M., R. Sabourin P., and Maupin, 2007. An empirical study on diversity measures and margin theory for ensembles of classifiers. *10th International Conference on Information Fusion*, pages 1–8.

Kholmatov, A., 2003. Biometric identity verification using on-line and off-line signature verification. Master's thesis, Sabanci University, Istanbul, Turkey.

Khreich, W., E. Granger, A. Miri, and R. Sabourin, 2010. On the memory complexity of the forward-backward algorithm. *Pattern Recognition Letters*, 31(2):91–99.

Ko, A., R. Sabourin, and A. Britto, 2008. From dynamic classifier selection to dynamic ensemble selection. *Pattern Recognition*, 41(5):1718–1731.

Ko, A., P. Cavalin, R. Sabourin, and A. Britto, December 2009a. Leave-one-out-training and leave-one-out-testing hidden Markov models for a handwritten numeral recognizer: The implications of a single classifier and multiple classifications. *IEEE Transactions on Pattern Analysis and Machine Intelligence*, 31:2168–2178.

Ko, A., R. Sabourin, and A. Britto, January 2009b. Ensemble of HMM classifiers based on the clustering validity index for a handwritten numeral recognizer. *Pattern Analysis and Applications*, 12:21–35.

Kuncheva, L., J. Bezdek, and R. Duin, 2001. Decision templates for multiple classifier fusion: an experimental comparison. *Pattern Recognition*, 34:299–314.

Kung, S., M. Mak, and S. Lin, 2004. *Biometric Authentication: A Machine Learning Approach*. Prentice Hall.

Lau, K., P. Yuen, and Y. Tang, 2005. Universal writing model for recovery of writing sequence of static handwriting images. *International Journal of Pattern Recognition and Artificial Intelligence*, 19(5):603–630.

Leclerc, F. and R. Plamondon, 1994. Automatic signature verification: the state of the art - 1989-1993. *International Journal of Pattern Recognition and Artificial Intelligence*, 8 (3):643–660.

Lee, L. and M. Lizarraga, 1996. An off-line method for human signature verification. *13th International Conference on Pattern Recognition*, volume 3, pages 195–198.

Lv, H., W. Wang, C. Wang, and Q. Zhuo, November 2005. Off-line chinese signature verification based on support vector machines. *Pattern Recognition Letters*, 26(15):2390–2399.

Madasu, V., April 2004. *Off-line signature verification and Bank Cheque processing*. PhD thesis, University of Queensland.

Madasu, V., M. Hanmandlu, and S. Madasu, 2003. Neuro-fuzzy approaches to signature verification. *2nd National Conference on Document Analysis and Recognition*.

Makhoul, J., S. Roucos, and H. Gish, 1985. Vector quantization in speech coding. *IEEE*, 73: 1551–1558.

Martinez, L., C. Travieso, J. Alonso, and M. Ferrer, 2004. Parameterization of a forgery handwritten signature verification system using svm. *38th Annual International Carnahan Conference on Security Technology*, pages 193–196.

Mighell, D., T. Wilkinson, and J. Goodman, 1989. *Advances in Neural Information Processing Systems I*. Morgan Kaufmann, San Mateo, CA.

Murshed, N., F. Bortolozzi, and R. Sabourin, 1995. Off-line signature verification using fuzzy artmap neural networks. *IEEE International Conference on Neural Networks*, pages 2179–2184.

Nagel, R. and A. Rosenfeld, 1977. Computer detection of freehand forgeries. *IEEE Transactions on Computers*, 26:895–905.

Nel, E., J. du Preez, and B. Herbst, 2005. Estimating the pen trajectories of static signatures using hidden Markov models. *IEEE Transactions on Pattern Analysis and Machine Intelligence*, 27(11):1733–1746.

Nemcek, W. and W. Lin, 1974. Experimental investigation of automatic signature verification. *IEEE Transactions on Pattern Analysis and Machine Intelligence*, 4:121–126.

Ng, A. and M. Jordan, 2001. On discriminative vs. generative classifiers: A comparison of logistic regression and naive Bayes. *Advances in Neural Information Processing Systems*, pages 841–848.

Oliveira, L., E. Justino, C. Freitas, and R. Sabourin, 2005. The graphology applied to signature verification. *12th Conference of the International Graphonomics Society*, pages 178–182.

Oliveira, L., E. Justino, and R. Sabourin, 2007. Off-line signature verification using writer-independent approach. *International Joint Conference on Neural Networks*, pages 2539–2544.

Oz, C., 2005. Signature recognition and verification with artificial neural network using moment invariant method. *Advances in Neural Networks.*, volume 3497 of *Lecture Notes in Computer Science*, pages 195–202. Springer Berlin / Heidelberg.

Ozgunduz, E., T. Senturk, and M. E. Karsligil, September 2005. Off-line signature verification and recognition by support vector machine. *13th European Signal Processing Conference*.

Pato, J. and L. Millett, 2010. *Biometric Recognition: Challenges and Opportunities*. National Academies Press.

Pekalska, E. and R. Duin, 2000. Classifiers for dissimilarity-based pattern recognition. *International Conference on Pattern Recognition*, volume 2, pages 12–16.

Pekalska, E. and R. Duin, 2005. *The Dissimilarity Representation for Pattern Recognition: Foundations And Applications (Machine Perception and Artificial Intelligence)*. World Scientific Publishing Co., Inc., River Edge, NJ, USA.

Perez-Hernandez, A., A. Sanchez, and J. F. Velez, 2004. Simplified stroke-based approach for off-line signature recognition. *2nd COST Workshop on Biometrics on the Internet: Fundamentals, Advances and Applications*, pages 89–94.

Pirlo, G., D. Impedovo, E. Stasolla, and C. Trullo, 2009. Learning local correspondences for static signature verification. *XIth International Conference of the Italian Association for Artificial Intelligence Reggio Emilia on Emergent Perspectives in Artificial Intelligence*, pages 385–394, Berlin, Heidelberg, 2009. Springer-Verlag.

Plamondon, R., 1994. *Progress in Automatic Signature Verification*. Word Scientific, Singapore.

Plamondon, R. and G. Lorette, 1989. Automatic signature verification and writer identification - the state of the art. *Pattern Recognition*, 22:107–131.

Qi, Y. and B. Hunt, 1994. Signature verification using global and grid features. *Pattern Recognition*, 27(12):1621–1629.

Quek, C. and R. Zhou, 2002. Antiforgery: A novel pseudo product based fuzzy neural network driven signature verification system. *Pattern Recognition Letters*, 23:1795–1816.

Rabiner, L., 1989. A tutorial on hidden Markov models and selected applications in speech recognition. *IEEE*, 77(2):257–286.

Raina, R., Yirong Shen, Andrew Y. Ng, and Andrew McCallum, 2004. Classification with hybrid generative/discriminative models. Thrun, S., Lawrence Saul, and Bernhard Schölkopf, editors, *Advances in Neural Information Processing Systems 16*. MIT Press, Cambridge, MA.

Ramesh, V. and M. Murty, 1999. Off-line signature verification using genetically optimized weighted features. *Pattern Recognition*, 32:217–233.

Rigoll, G. and A. Kosmala, 1998. A systematic comparison between on-line and off-line methods for signature verification with hidden Markov models. *International Conference on Pattern Recognition*, volume 2, pages 1755–1757.

Rivard, D., 2010. Multi-feature approach for writer-independent offline signature verification. Master's thesis, Ecole de Technologie Superieure, Montreal, Canada.

Rubinstein, Y. and T. Hastie, 1997. Discriminative vs informative learning. *Third International Conference on Knowledge Discovery and Data Mining*, pages 49–53.

Rumelhart, D., G. Hinton, and R. William, 1986. *Learning Internal Representations by Error Propagation*, volume 1. MIT Press.

Sabourin, R. and J. Drouhard, 1992. Off-line signature verification using directional PDF and neural networks. *International Conference on Pattern Recognition*, pages 321–325.

Sabourin, R. and G. Genest, 1994. An extended-shadow-code based approach for off-line signature verification. i. evaluation of the bar mask definition. *12th International Conference on Pattern Recognition*, volume 2, pages 450–453.

Sabourin, R. and G. Genest, 1995. An extended-shadow-code based approach for off-line signature verification. ii. evaluation of several multi-classifier combination strategies. *International Conference on Document Analysis and Recognition*, 1:197.

Sabourin, R., M. Cheriet, and G. Genest, 1993. An extended-shadow-code based approach for off-line signature verification. *Second International Conference on Document Analysis and Recognition*, pages 1–5.

Sabourin, R., G. Genest, and F. Prêteux, 1996. Pattern spectrum as a local shape factor for off-line signature verification. *13th International Conference on Pattern Recognition*, volume 3, pages 43–48.

Sabourin, R., J. Drouhard, and E. Wah, 1997a. Shape matrices as a mixed shape factor for off-line signature verification. *Fourth International Conference on Document Analysis and Recognition*, volume 2, pages 661–665.

Sabourin, R., G. Genest, and F. Prêteux, 1997b. Off-line signature verification by local granulometric size distributions. *IEEE Transactions on Pattern Analysis and Machine Intelligence*, 19(9):976–988.

Sansone, C. and M. Vento, 2000. Signature verification: Increasing performance by a multi-stage system. *Pattern Analysis and Applications*, 3:169–181.

Santos, C., E. Justino, F. Bortolozzi, and R. Sabourin, 2004. An off-line signature verification method based on the questioned document expert's approach and a neural network classifier. *International Workshop on Frontiers in Handwriting Recognition*, pages 498–502.

Scholkopf, B., J. Platt, J. Taylor, A. Smola, and R. Williamson, 2001. Estimating the support of a high dimensional distribution. *Neural Computation*, 13:1443–1471.

Scott, M., M. Niranjan, and R. Prager, 1998. Realisable classifiers: improving operating performance on variable cost problems. *British Machine Vision Conference*.

Senol, C. and T. Yildirim, 2005. Signature verification using conic section function neural network. *20th International Symposium on Computer and Information Sciences*, pages 524–532.

Srihari, S., A. Xu, and M. Kalera, 2004. Learning strategies and classification methods for off-line signature verification. *Ninth International Workshop on Frontiers in Handwriting Recognition*, pages 161–166.

Tang, Y., Y. Tao, and E. Lam, May 2002. New method for feature extraction based on fractal behavior. *Pattern Recognition*, 35(5):1071–1081.

Tax, D., 2001. *One-class Classification*. PhD thesis, TU Delft, Nederland.

Tortorella, F., 2005. A roc-based reject rule for dichotomizers. *Pattern Recognition Letters*, 26:167–180.

Tumer, K. and J. Ghosh, 1996. Analysis of decision boundaries in linearly combined neural classifiers. *Pattern Recognition*, 29(2):341 – 348.

Ulas, A., M. Semerci, O. Yildiz, and E. Alpaydin, 2009. Incremental construction of classifier and discriminant ensembles. *Information Sciences*, 179(9):1298–1318.

Vapnik, V., editor, 1999. *The Nature of Statistical Learning Theory*. Springer-Verlag, New York, 2nd edition.

Vargas, J., M. Ferrer, C. Travieso, and J. Alonso, 2007. Off-line handwritten signature gpds-960 corpus. *International Conference on Document Analysis and Recognition*, pages 764–768.

Vargas, J., M. Ferrer, C. Travieso, and J. Alonso, 2008. Off-line signature verification based on high pressure polar distribution. *11th International Conference on Frontiers in Handwriting Recognition*, pages 373–378.

Vargas, J., M. Ferrer, C. Travieso, and J. Alonso, 2011. Off-line signature verification based on grey level information using texture features. *Pattern Recognition*, pages 375–385.

Vélez, J., Á. Sánchez, and A. Moreno, 2003. Robust off-line signature verification using compression networks and positional cuttings. *IEEE Workshop on Neural Networks for Signal Processing*, pages 627–636.

Wayman, J., A. Jain, D. Maltoni, and D. Maio, editors, 2005. *Biometric Systems: Technology, Design and Performance Evaluation*. Springer, New York.

Wen-Ming, Z., L. Shao-Fa, and Z. Xian-Gui, 2004. A hybrid scheme for off-line chinese signature verification. *IEEE Conference on Cybernetics and Intelligent Systems*, volume 2, pages 1402–1405.

Wilkinson, T. and J. Goodman, 1990. Slope histogram detection of forged handwritten signatures. *International Society for Optical Engineering*, pages 293–304.

Xiao, X. and G. Leedham, May 2002. Signature verification using a modified bayesian network. *Pattern Recognition*, 35(5):983–995.

Xuhua, Y., T. Furuhashi, K. Obata, and Y. Uchikawa, 1996. Selection of features for signature verification using the genetic algorithm. *Computers & Industrial Engineering*, 30(4): 1037–1045.

Ye, X., W. Hou, and W. Feng, 2005. Off-line handwritten signature verification with inflections feature. *IEEE International Conference on Mechatronics and Automation*, volume 2, pages 787–792.

You, X., B. Fang, Z. He, and Y. Tang, 2005. Similarity measurement for off-line signature verification. *International Conference on Intelligent Computing*, pages 272–281.